SPAWAR
Systems Center
PACIFIC

TECHNICAL REPORT 3015
July 2016

Calibration of Linked Hydrodynamic and Water Quality Model for Santa Margarita Lagoon

Final Report

Pei-Fang Wang
Chuck Katz
Ripan Barua
SSC Pacific

James Martin
Mississippi State University

Tim Wool
U.S. EPA Region 4
Water Management Division

SSC Pacific
San Diego, CA 92152-5001

TECHNICAL REPORT 3015
July 2016

Calibration of Linked Hydrodynamic and Water Quality Model for Santa Margarita Lagoon

Final Report

Pei-Fang Wang
Chuck Katz
Ripan Barua
SSC Pacific

James Martin
Mississippi State University

Tim Wool
U.S. EPA Region 4
Water Management Division

SSC Pacific
San Diego, CA 92152-5001

SSC Pacific
San Diego, California 92152-5001

K. J. Rothenhaus, CAPT, USN
Commanding Officer

C. A. Keeney
Executive Director

ADMINISTRATIVE INFORMATION

The work described in this report was performed for Environmental Security, Marine Corps Base Camp Pendleton, San Diego, CA, by the Environmental Sciences Branch (Code 71750) of the Advanced Systems and Applied Sciences Division (Code 71700), Space and Naval Warfare Systems Center Pacific (SSC Pacific), San Diego, CA. Further support was provided by Mississippi State University, Mississippi State, MS, and U.S. EPA Region 4, Water Management Division, Atlanta, GA.

Released by
P. J. Earley, Head
Environmental Sciences Branch

Under authority of
A. J. Ramirez, Head
Advanced Systems & Applied
Sciences Division

ACKNOWLEDGMENT

We are grateful to Mr. Kyle Cook of Environmental Security at Marine Corps Base Camp Pendleton for his support of this applied research project and the wide-ranging technical work required to understand water quality in the lagoon. We thank the Santa Margarita River Nutrient Initiative Group and members of the technical review team for their support, feedback, guidance as well as patience throughout the study. Finally, this work could not have been completed without the tireless efforts of Dr. Martha Sutula of the Southern California Coastal Water Research Project. Dr. Sutula not only helped to frame the application of the model with the stakeholders but also helped to make several key technical decisions.

SB

EXECUTIVE SUMMARY

The Santa Margarita Lagoon (SML) is a water body that forms where the Santa Margarita River and its tributaries meet the Pacific Ocean. The lagoon and lower part of the river are within Marine Corps Base Camp Pendleton (Camp Pendleton). The Regional Water Quality Control Board, San Diego listed the lagoon as an impaired waterbody for eutrophication with excessive nutrients and issued an Investigative Order (R9-2006-076) in 2007 to evaluate the extent of impairment. A watershed stakeholder group, including Camp Pendleton, was established to develop and implement a water quality monitoring effort to evaluate the impairment in 2008. Those data along with measurements made by the Southern California Coastal Water Research Project (SCCWRP) in 2009 provided the first relatively comprehensive evaluation of water quality in the lagoon.

Camp Pendleton along with the stakeholder group's concurrence took a proactive effort in the assessment of impairment by funding the development and calibration of a linked hydrodynamic and water quality numeric model for the lagoon. The linked models aim to provide a predictive tool to assess the lagoon water quality under changing conditions and thereby aid in more effective management decisions to best maintain good water quality.

For the linked models, the Environmental Fluid Dynamics Code (EFDC) hydrodynamic model was selected and linked with the Water Quality Analysis Simulation Program–Eutrophication (WASP-Eutro) both currently supported by the U.S. Environmental Protection Agency (USEPA). Calibration of EFDC was conducted first, followed by calibration of the linked EFDC+WASP-Eutro models. The latest versions of both models were provided by USEPA for use in this project. The calibration was conducted for the 2008–2009 period, during which comprehensive stakeholder datasets were available for model comparison. The calibration of the EFDC model was to ensure that the simulated water surface elevation, salinity, and temperature are in agreement with the corresponding data measured throughout the lagoon during the 2008 and 2009 monitoring period. The key elements of the WASP-Eutro model calibration were to ensure that model correctly simulated lagoon water concentrations and benthic fluxes of nitrogen, phosphorous, and dissolved oxygen, as well as macroalgal biomass.

EFDC Calibration is a three-dimensional numerical model that balances water pressure gradient while allowing water density and water surface elevation to change accordingly with turbulence-averaged equations. The model's physical domain ranged from the ocean beach boundary to the head of tide approximately 3.7 km upstream. Imagery from Google Earth™ was used to generate the numerical outline of the lagoon boundary while a bathymetric survey conducted by Space and Naval Warfare Systems Center Pacific (SSC Pacific) in 2013 was used to determine water depths referenced to mean sea level. The bathymetry data from 2013 was assumed to represent the bathymetry for 2008 and 2009.

Lagoon hydrodynamics is primarily governed by upstream freshwater sources and tidal exchange with the ocean. The salinity and temperatures data measured at Del Mar by Scripps Institution of Oceanography, along with tide height data measured at La Jolla by the National Oceanic and Atmospheric Administration (NOAA) were applied to the model ocean boundary. Salinity, temperature, and freshwater flow data from the U.S. Coast Guard (USGS) gage station at Temecula (Number 11044000) were applied to the model upper boundary. Additionally, hourly climatological datasets for solar insolation, air temperature, humidity, wind speed and direction, barometric pressure, rainfall rate, evapotranspiration rate, and cloud cover were acquired from the air field at Camp Pendleton, NOAA's Quality Controlled Local Climatological Data archive, and from

California's Irrigation Management Information System data for Temecula, CA, and applied as model inputs.

The initial calibration did not accurately simulate the measured water surface elevation and salinity data measured during the period. This fact revealed two key processes that had to be considered with more investigation: the varying sand berm height at the mouth and the total freshwater flow to the lagoon.

Evaluation of the water surface measurement datasets showed daily low water depths in the lagoon were increasing at a rate of ~0.5 m from the winter into the summer and fall, reflecting the increasing berm height during the period. This change was accounted for in the model by applying an empirical change to the depth of the grid cell at the mouth to match the daily low water depth dataset for both 2008 and 2009. The model calibration using the empirical berm height change resulted in a highly accurate simulation in water surface elevation, agreeing within 8 cm of observations. The model was compared to the mean daily minimum, mean daily mean, and mean daily maximum elevations and matched to within 233%, 98.5%, and 98.5%, respectively in 2008 and to within 97.2%, 96%, and 96%, respectively for 2009. The 233% over prediction of the mean daily minimum in 2008 was within 8 cm of the measured value of 6 cm, both relatively small values.

The magnitude of the changing semidiurnal salinity signal, in particular for low salinity, in the lagoon could not be initially matched by the model. This addition implied that there had to be an additional amount of freshwater coming into the lagoon that was not measured at the USGS gauge.) An evaluation of simulated freshwater inflow from a watershed model developed by Tetra Tech, Inc. for the Regional Board could not account for the additional freshwater. The stakeholder technical group was aware that groundwater upstream of the lagoon domain was a potential source of freshwater that might explain both the model-lagoon data mismatch and the lack of observation of the flow made at the USGS gage. The output of a groundwater model developed for Camp Pendleton by Stetson Engineers, Inc. was added as a source of freshwater to the lagoon. This improved the accuracy of the model such that the model vs. observed salinity data matched the daily minimum and maximum range 88.6% of the time in 2008 and 90.2% of the time in 2009.

The final hydrodynamic model calibration metric for calibration was for lagoon temperature, and was simulated by including solar radiation as an additional source of heat for the entire lagoon water. The model output under predicted the measured daily mean temperature of the lagoon by about 10%. Overall, the three key hydrodynamic parameters, including water surface elevation, salinity, and temperature were simulated by the EFDC model with adequate accuracy. The calibration highlighted and revealed key physical processes that were not originally implemented in the standard EFDC model nor necessarily understood at the start of the effort. In particular, the requirement of freshwater from an upper watershed groundwater source to the lagoon had considerable implications for the water quality calibration process.

Linked WASP-Eutro Calibration (WASP) is a water quality model that simulates the water quality response of aquatic systems to natural phenomena as well as to anthropogenic pollutants. The most recent model of WASP-Eutro (7.5x) simulates the dynamic cycles of nutrients, planktonic and macroalgae, and dissolved oxygen in both the water column and in the sediments (diagenesis).WASP-Eutro was linked to the calibrated EFDC model using the same boundaries and grid. The hydrodynamic model output data for each segment including water volume, current velocity, salinity, and temperature were used to drive the transport and water quality kinetics in WASP-Eutro.

WASP-Eutro was used to simulate water concentrations of nitrogen species: inorganic ammonia, nitrite and nitrate, dissolved and particulate organic nitrogen, and total nitrogen; phosphorous species: inorganic phosphate, dissolved and particulate organic phosphorous, total phosphorous; and dissolved oxygen. It was also used to simulate sediment fluxes between the sediment and water column of the same nitrogen and phosphorous species as well as oxygen. Finally, the model was used to simulate the growth of plankton and macroalgae.

As described earlier, the hydrodynamic model calibration process, in particular the need to introduce a watershed groundwater source of freshwater to balance salt in the lagoon, highlighted limitations in our knowledge of the lagoon system. The calibration of the water quality model exposed additional gaps in our knowledge with the result of requiring more iterations and professional judgement adjustments in optimizing the model-measurement comparisons. The calibration process was also challenged by the lack of fully concurrent field data and in some cases their high variability. In particular, a localized ground water source from the historic agricultural fields above the northern shore by the Highway 5 (HWY 5) Bridge was found entering the lagoon and quantified between 2010 and 2014. This source, measured outside the model time domain, was found to be a potentially important source of nutrients to the lower lagoon. A nutrient load from the groundwater source entering in from the upper watershed also had to be assigned by calibration because of a lack of measurements.

Another gap identified by the calibration process was found when attempting to match discrete field measurements of macroalgal biomass made along the intertidal shoreline with a model that did not allow for the development of an intertidal condition (generation of tide flats) and one that had a grid spatial resolution that was considerably larger than the size of these discretized and heterogeneous measurements. The grid size also appeared to play a role in a mismatch between water column nutrients measured in the very shallow shoreline near to the groundwater entry point from the agricultural field with model results. These issues were painstakingly evaluated and iteratively adjusted to provide an optimized model calibration output that best matched observations.

Water column nutrient model results were evaluated against field measurements at the HWY 5 and Stuart Mesa Bridge locations, the axial transect sites, and at the mouth. On average, total nitrogen, inorganic nitrogen, and nitrate predicted by the model were within 8% (over prediction) of the field dataset. The model also simulated the temporal trends observed in the lagoon, decreasing from relatively high levels in winter to considerably lower levels in summer and fall during the dry season. The concentration data were well matched to the upper lagoon location and to the transect data (within 10%) but was poorly matched to the concentrations measured at the HWY 5 Bridge location. The model under predicted the measured concentrations of inorganic nitrogen by over a factor of 10: 2.7 mg/L (model) vs. 27 to 37 mg/L (measurement). As mentioned previously, the mismatch at this location appeared to be explained by the localized groundwater flowing in near to the site, the shallow water sampling in the vicinity of that input, and the potential that there was an unmeasured but previously observed surface water flow to the lagoon at the same location by the North County Transit District.

On average, total and inorganic phosphorous predicted by the model were within 15% of the field dataset. The model also simulated the temporal trends observed in the lagoon, increasing from winter into summer and fall (opposite to the trend in nitrogen). The model also simulated the increasing spatial trend in the data showing a relatively even distribution over the lagoon in winter and then an increasing trend up the lagoon in summer and fall. Unlike the nitrogen results, the model phosphorous concentration data were well matched to all three observation points to within 15%. The better match of the model to the observed data at the HWY 5 location suggest that the groundwater sources of phosphorous there were relatively low.

Water column dissolved oxygen model results were evaluated against the continuous field measurements made in 2009 at the HWY 5 Bridge. Overall, the model could only match the mean and daily minimum night time concentrations in the lagoon, with 26.6% and 20.5% for the dissolved oxygen less than 5 mg/L for the model prediction and field data, respectively. The model could capture the diurnal variation, but over-predicted the peak daytime concentrations, a result of the model not accounting for oxygen flux across the seawater surface interface. Considerable effort was applied to calibrating the model to meet the observed oxygen data, including adjusting the boundary conditions and the feedback mechanisms of the interaction of macroalgae growth, death, and benthic flux. The final model calibration, while unable to simulate the peak values correctly, did provide a good match to the low nighttime dissolved oxygen values that are a potential key metric under consideration for assessing impairment of the lagoon.

The benthic flux of nutrients and oxygen generated in the calibrated model were evaluated against the field measurements made at two field locations. The field data were highly variable compared with the model results for the four index periods. The model correctly simulated the flux direction (into or out of the sediments) for both inorganic nitrogen and phosphorous during both periods. The model over predicted the nitrogen flux by a factor of four and the phosphorous flux by a factor of five to eight, noting that large variances were associated with the field data with magnitudes larger or equivalent to the difference of mean model and data. The benthic dissolved oxygen field data were even more variable than the nutrient data. The model matched the oxygen flux direction but over-predicted the magnitude by a factor of four.

The calibrated model results for macroalgal biomass were evaluated against average conditions throughout the estuary and specifically at the two field measurement locations at the HWY 5 and Stuart Mesa Bridge locations. The model correctly simulated the growth of macroalgae from the zero values observed in the winter months to peaks of macroalgal biomass observed during late summer, though the model generated peak production about one to two months earlier than observations. The model generated an average biomass in the estuary of 82 g-dw/m^2 compared to the measured value 72 g-dw/m^2, during the period of April to November 2008 and 2009. The comparison at the lower lagoon site near the HWY 5 Bridge generally showed agreement with observation except during the late summer when the model result (179 g-dw/m^2) was under-predicted compared with the observed value of 238 g-dw/m^2 algae. The mismatch at this site is comparable to the mismatch observed in the nutrients and can be potentially explained by growth stimulated by the localized groundwater source flowing in near to the site and that the model grid size is 90 times larger than the spatial extent of the discrete measurement along the shoreline. The model/data comparison for the macroalgal biomass at the upper lagoon location (Segment 2) was within 27%, with averaged values of 60.2 g-dw/m^2 and 44.3 g-dw/m^2 for the model and field data, respectively, during the period of June 1 to November 3 for 2008 and 2009.

Macroalgae biomass is under consideration as a key metric for assessing impairment of the lagoon. Because of its importance, considerable efforts were made to assess the processes of macroalgal growth that might provide insight into the factors for the mismatch. Light limitation, particularly along the intertidal shoreline, was found to be a key process that controls production. The adjustment of light, shelf-shading of plants, and the model minimum water depth set at the shoreline were all adjusted to provide the best match to the observed data. A higher spatial resolution grid, allowing drying of the intertidal zone at low tide, and/or providing measures of subtidal macroalgae biomass would all potentially lead to a better model simulation result to the macroalgal datasets.

For this study, we have identified multiple sources of uncertainties and data gaps. For example, the p-load obtained by calibration could be attributed to the uncertainty associated with watershed groundwater load or benthic flux (or other sources) between the Stuart Mesa Bridge and the model upstream boundary. However, no existing data could support either assumed sources. Despite these uncertainties in the data and the model, the overall calibration of the linked EFDC WASP-Eutro models provided a sufficiently reasonable match to field datasets collected between 2008 and 2009. The model should be able to simulate and compare the relative water quality responses among different scenarios, such as load reduction and effect of different benthic flux scenarios and others. To fully characterize and evaluate model performance, a sensitivity analysis should be conducted. In this analysis, key processes that govern the dynamics of the water quality parameters can be identified, which should help design and plan load management scenarios.

CONTENTS

Figures

Tables

ACRONYMS

cms	Cubic meters per second
DO	Dissolved Oxygen
EFDC	Environmental Fluid Dynamic Code (a 3-D hydrodynamic model)\
g-dw/m^2	Grams-dry weight per square-meter for macroalgal biomass
HSPF	Hydrological Simulation Program Fortran
HWY 5	Highway 5
MCAS	Marine Corps Air Station (MCAS)
ME	Mass Emission station
MLLW	Mean Lower Low Water
MSL	Mean Sea Level
NOAA	National Oceanic and Atmospheric Administration
POC	Particulate Organic Phosphorous
ppt	Parts Per Thousands
PON	Particulate Organic Nitrogen
RRB	Railroad Bridge
SDRWQCB	San Diego Regional Water Quality Control Board
SCCWRP	Southern California Coastal Water Research Program
SIO	Scripps Institute of Oceanography
SML	Santa Margarita Lagoon
SMR	Santa Margarita River
SOD	Sediment Oxygen Demand
SSC Pacific	Space and Naval Warfare Systems Center Pacific
Stdev	Standard Deviation
TMDL	Total Maximum Daily Load
USEPA	United States Environmental Protection Agency
USGS	United State Geological Survey
WASP	Water Analysis Simulation Program (USEPA's water quality model)
WSE	Water Surface Elevation

1. INTRODUCTION

The Santa Margarita Lagoon (SML) is a waterbody that forms where the Santa Margarita River (SMR) and its tributaries meet the Pacific Ocean. The lagoon and the lower part of the river are within Camp Pendleton boundaries. The San Diego Regional Water Quality Control Board (SDRWQCB) listed the SML as impaired for eutrophication and issued an Investigative Order (R9-2006-076) in 2007 to evaluate the extent of impairment. A watershed stakeholder group, including Camp Pendleton, was established to evaluate the impairment, which was completed during a relatively comprehensive field sampling effort between 2008 and 2009. Initial investigations under the order led the stakeholders and SDRWQCB to identify additional investigations that would further evaluate the SML condition and support the development of a total maximum daily load (TMDL), if needed for the SML.

Camp Pendleton along with the stakeholder group's concurrence took a proactive effort in the assessment of impairment by funding the development and calibration of a linked hydrodynamic and water quality numeric model for the lagoon. The linked models aim to provide a predictive tool to assess the lagoon water quality under changing conditions and thereby to aid in more effective management decisions to best maintain good water quality. The modeling work was performed by Dr. Pei Fang Wang and scientific staff from the Energy and Environmental Sciences Group of the Space and Naval Warfare Systems Center Pacific (SSC Pacific) in collaboration with Dr. James Martin of Mississippi State University and Mr. Tim Wool of the U.S. Environmental Protection Agency (USEPA) Region IV. The technical work, starting in late 2011 was further guided and evaluated by a group of stakeholder technical staff led by Dr. Martha Sutula of the Southern California Coastal Water Research Project (SCCWRP).

A key element for developing a TMDL is the need to accurately predict the response of the system to changes in watershed loadings. In coastal lagoons such as SML, analysis of this response requires the use of a calibrated and validated hydrodynamic and eutrophication model. The stakeholder group identified development of this modeling capability for SML as a top priority effort, including implementation of the model and additional monitoring to calibrate and validate the model. The modeling effort requires a methodical and iterative development and assessment process including development of appropriate input parameters, modification and testing of computer code for site specific applications, and iterative testing and manipulation to assure acceptable agreement with measured and expected conditions. Following USEPA's TMDL study approach (USEPA, 1997), the stakeholders and the SDRWQCB selected and specified the integrated hydrodynamic and water quality modeling system EFDC+WASP-Eutro for application in this study. Following this guidance, we have conducted an evaluation of the use of the EFDC hydrodynamic model and then the linked WASP+EFDC water quality model for the SML based on the period of 2008 through 2009.

The Santa Margarita Lagoon is roughly 3.7 km in length from the mouth where it opens to the Pacific Ocean to the head of tide. The lagoon has variable widths, with a maximum width of ~400 m in its western end and narrows to between 60 and 20 m across for the inland two-thirds of its length. The water body is very shallow, averaging ~1 m with a maximum depth of ~5.4 m, based on the bathymetry data surveyed by SSC Pacific in 2013. Maximum depths were found around the support piling for the two bridges spanning the lagoon: the HWY 5 Bridge about 1 km from the mouth and the Stuart Mesa Bridge about 2 km from the mouth. The lagoon is usually tidally connected to the ocean through its opening at the mouth. Historical data show the lagoon closes completely and is segregated from the ocean about 25% of the time. The data also show that tidal flow through the mouth generally decreases during the summer months as the beach berm height builds from wave and beach sand dynamics, compounded by lower freshwater flows. The summer dry season, typically

from late April through late October, is also a period when algal biomass dominated by macroalgae tend to grow the most. Excessive growth of macroalgae can be a consequence of excessive nutrients that were identified by the regional board as a cause for impairment, which led to the investigative order in 2007.

For the linked models, the Environmental Fluid Dynamics Code (EFDC) hydrodynamic model was selected and linked with the Water Quality Analysis Simulation Program–Eutrophication (WASP-Eutro), both currently supported by the USEPA. Calibration of EFDC was conducted first, followed by calibration of the linked EFDC+WASP-Eutro models. The latest versions of both models were provided by USEPA for use in this project. The calibration was conducted for the 2008-2009 period, during which comprehensive stakeholder datasets were available for model comparison. The calibration of the EFDC model was used to ensure that the simulated water surface elevation, salinity, and temperature are in agreement with the corresponding data measured throughout the lagoon during the 2008 and 2009 monitoring period. The key elements of the WASP-Eutro model calibration were to ensure that model correctly simulated lagoon water concentrations and benthic fluxes of nitrogen, phosphorous, and dissolved oxygen, as well as macroalgal biomass.

The overall model calibration was optimized by iteratively applying known inputs, evaluating results with available data, and then adjusting parameters using best professional judgement to provide simulation results that best matched the measured datasets. An iterative approach is standard practice in modeling but in this case was particularly important to generate accurate outcomes for this highly dynamic system. Going through the calibration process revealed limitations in a priori knowledge of some key processes occurring in the lagoon as well as limitations in the measured data. Although the overall model calibration described below was considered successful, variations and uncertainties in both the measured and modeled parameters must be taken into consideration when implementing it for management decisions.

2. HYDRODYNAMIC MODEL CALIBRATION AND VALIDATION

The modeling methodology is described below for the 2008–2009 application of EFDC for SML. The methodology addresses a general description of the model, along with the development of required inputs and boundary conditions. These requirements include acquisition and compilation of bathymetry, atmospheric conditions, ocean boundary conditions, and upstream boundary conditions including river and groundwater flows and loadings.

2.1 MODEL DESCRIPTION

The hydrodynamic model Environmental Fluid Dynamics Code (EFDC) was selected to model the hydrodynamics and water quality transport for SML. Its governing hydrodynamic equations are three-dimensional (i.e., it addresses water movement up and down stream, vertically in the water column, and horizontally across the channel). The model balances water pressure while allowing water density and water surface elevation (WSE) to change with turbulence-averaged equations. It is a three-dimensional sigma-coordinate model, meaning that there are a constant number of layers throughout the model domain each with a specified percentage of total depth and thus, the thickness of those layers changes with WSE (Tetra Tech, 2002). EFDC has been used extensively throughout the United States with applications including the Los Angeles Harbor/San Pedro Bay, Dominguez Channel and the Loma Alta Slough.

There are many versions of the EFDC model, and not all of these versions are suitable for this study. To address this issue, we acquired an updated version of EFDC source code from USEPA Region IV, Atlanta, GA, in July 2010, which has been configured correctly for linking the hydrodynamic model output with the water quality model, WASP. We set up the model by generation of a model grid, specifications of model inputs and boundary conditions, model test and diagnostic runs, and model calibration.

WASP Version 7.4 (Water Quality Analysis Simulation Program V7.4) has been applied broadly throughout the United States for water quality modeling and was recently used to simulate the transport and fate of nutrients in nearby Loma Alta Slough. In these applications, hydrodynamic output from the EFDC model, including water surface elevations and velocity field for each of the model cells, is stored at every pre-selected time step into a binary file (e.g., SML.hyd). This hydrodynamic output file will then be linked to USEPA's water quality model, WASP, which uses the same model grid configuration as that for EFDC (Figure 2-1). The EFDC hydrodynamic model output file (SML.hyd) supplies the hydrodynamic information to drive the transport of the water quality parameters such as nutrients, in the lagoon.

The modeling assumptions for this conceptual model, as depicted in Figure 2-1, are summarized as follows:

1) Assumptions for the hydrodynamic model (EFDC) are discussed in Section 2.2 Model Inputs and Boundary Conditions and in Section 2.3 Model Set Up and Development
2) Assumption for the linked water quality model (WASP) are discussed in Section 3.1 and Section 3.2
3) Assumptions for the external loads and associated uncertainties of WASP are discussed in the Figure 3-31 under Uncertainties in Eutrophication Modeling
4) For the eutrophication model, settling and deposition rate was assumed to be a constant for the entire lagoon over the simulation period.

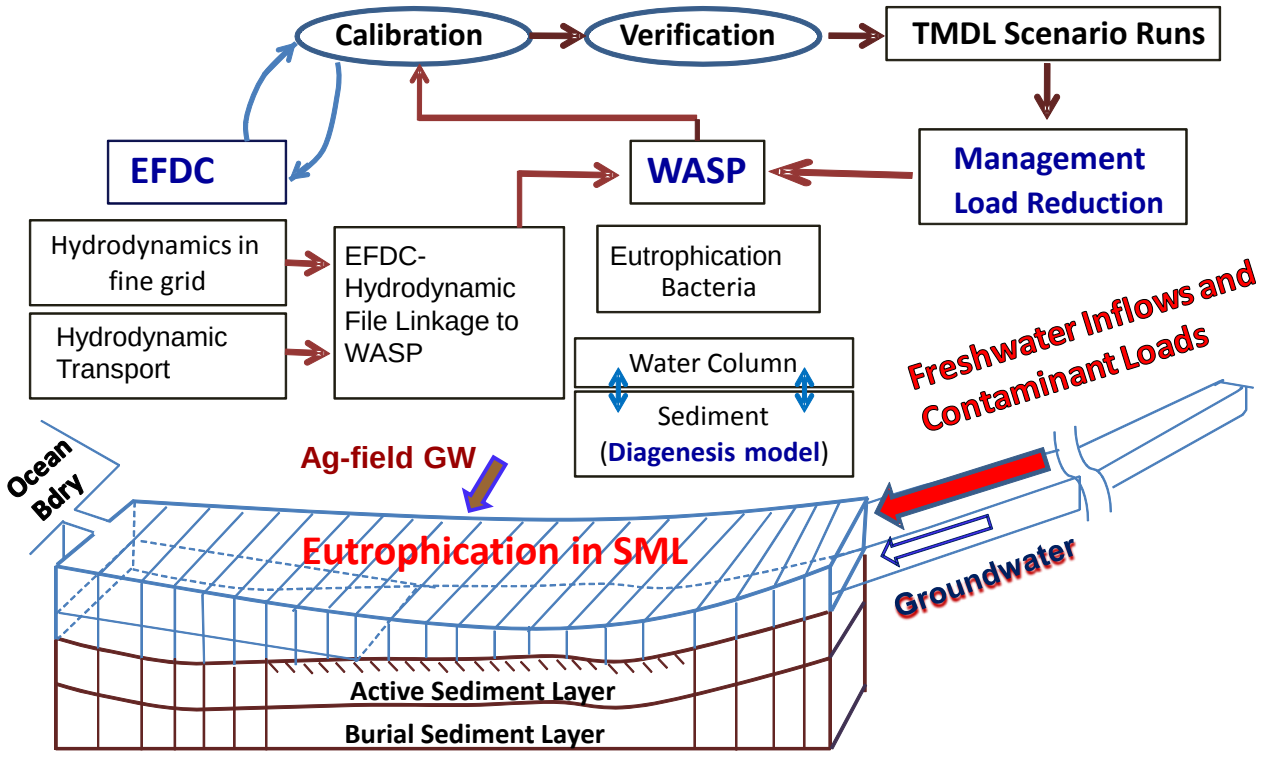

Figure 2-1. Conceptual model of the linked hydrodynamic model (EFDC) and water quality model (WASP).

2.2 MODEL INPUTS AND BOUNDARY CONDITIONS

Hydrodynamics and water quality in SML are governed by the interactions of freshwater inflows, including both surface water and groundwater from the surrounding land-based sources and upstream boundary with saltwater from the downstream ocean boundary. Freshwater inflows and nutrient loads from the watershed are measured at two USGS gauge stations, including gage height and flow rate at the Ysidora station (USGS Station #11046000) and water temperature and salinity at the Temecula station (USGS Station #11044000).

2.2.1 Bathymetry

A survey was conducted by SSC Pacific from February to March 2013 to measure bathymetry in the study area of the SML. The bathymetry was mapped using a high-resolution, single-beam-depth sounder mounted on a small unmanned boat that was remotely controlled for its navigation through the shallow-water domain of the lagoon. Acoustic soundings were sent through the water column to the bottom. Based on the time lag between the emitting and the returning signals from reflection of the bottom, water depths were measured. A total of 197808 water depth data were recorded in the surveyed water domain (Figure 2-2).

The majority of the SML is shallow, with depths less than 1–2 m. Just below and in the vicinity of RRB and the Stuart Mesa Bridge, scouring causes the water to be deeper with depths reaching ~3–5 m. Depths in the rest of the lagoon are generally less than 2 m, and depths in the lower lagoon (Figure 2-2), midway between ocean sand berm to the RRB, are generally less than 1 m. The bathymetry survey data was used to generate the model grid files for the EFDC model, since this

2013 bathymetry data is the most complete (covering the entire lagoon domain) and most recent (to 2008–2009) data available.

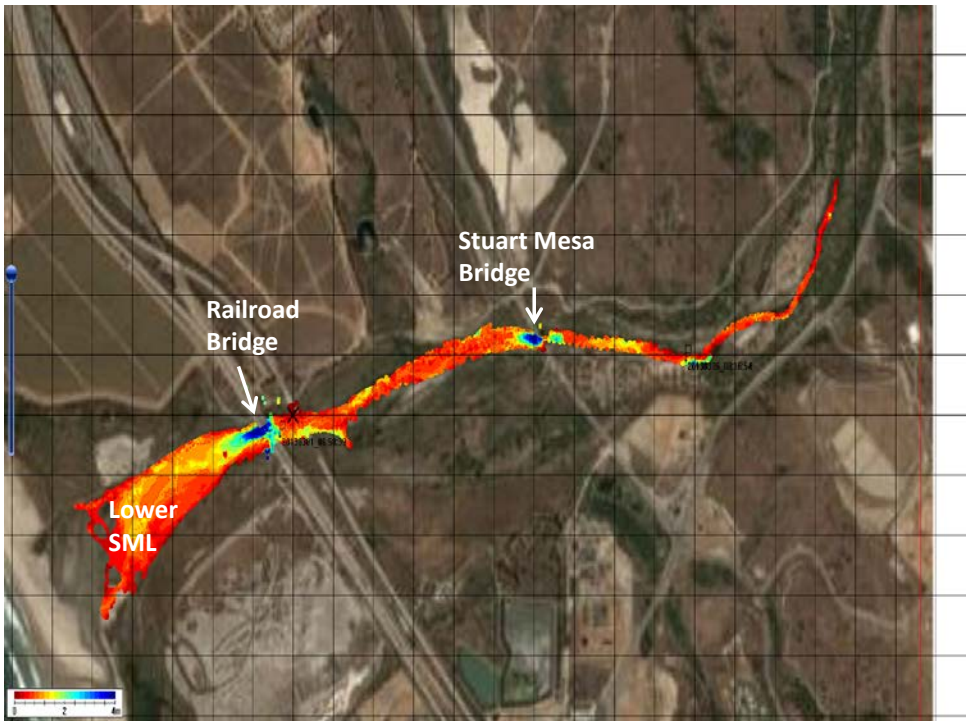

Figure 2-2. Measured bathymetry contours (relative to MSL) from SSC Pacific Survey (February to March 2013).

2.2.2 Atmospheric Conditions

EFDC simulates water surface elevations, currents, salinity, and temperature of the lagoon water. Dynamics of the salinity of the lagoon water results from the interactions of freshwater inflows from the upstream watershed and the ocean saline water through the ocean boundary. Similarly, temperature variations result from the interactions from the upstream and ocean boundary flows and as well as from heat exchange between the lagoon water and the atmosphere. Therefore, EFDC requires two additional input files to account for the effects of air/water heat exchange to the water temperature: the atmospheric loading file, aser.inp, and the wind speed/direction file, wser.inp.

Preparation of weather input files (aser.inp and wser.inp) and ocean boundary conditions were created from archived data sets hosted by the National Oceanic and Atmospheric Administration (NOAA) and the California Office of Water Use Efficiency. Specifically, quality-controlled datasets for 2008 and 2009 from the MCAS Camp Pendleton airport weather station were obtained from the NOAA Quality Controlled Local Climatological Data (QCLCD) archive. Datasets were also obtained from the California Irrigation Management Information System (CIMIS) database for the Temecula station for the same calendar years. Data was also collected from NOAA's National Data Buoy Center for the station designated as "Oceanside offshore". The locations of the stations reporting the accessed data are shown in Figure 2-3.

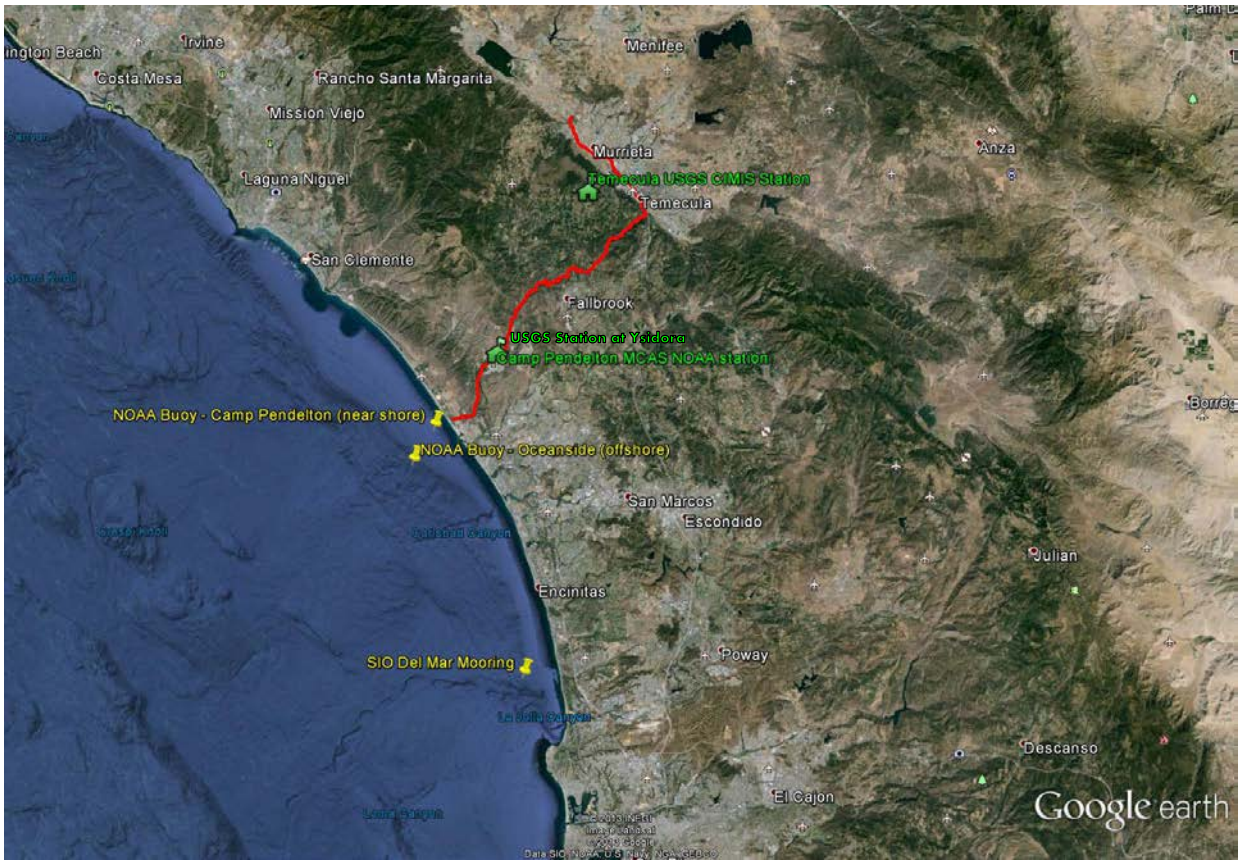

Figure 2-3. Locations of data source for creating EFDC atmospheric and wind input files.

Each input file was created to represent hourly conditions in the watershed. Specific data needed by the EFDC model were barometric pressure (mbar), dry bulb temperature (°C), relative humidity, rainfall rate (m/s), evapotranspiration rate (m/s), net solar shortwave radiation ($J/m^2/s$), cloud cover, wind speed (m/s), and wind direction. Data from the Marine Corps Air Station (MCAS) Camp Pendleton were used to provide barometric pressure, temperature, relative humidity, rainfall, cloud cover, wind speed, and wind direction. Evaporation estimates and solar radiation measurements were obtained from the CIMIS dataset originating from Temecula. Ocean temperature data recorded from the buoy at Oceanside was used to build a data file representing the boundary condition at the ocean.

Both the datasets from the MCAS Camp Pendleton and Temecula, CA, had sufficient data to complete an hourly record for 2008 and 2009. However, there were small gaps in the dataset that were missing. For gaps of data spanning 6 hours or less, the missing data were estimated by linear interpolation between data points immediately before and after the gap. For gaps longer than 6 hours, values were estimated by using data from the previous day for the time period corresponding to the gap.

2.2.3 Oceanic Conditions

The oceanic WSE was needed to drive the simulation of tidal circulation within the lagoon. Tide gauge data for tidal conditions in the immediate vicinity of the lagoon entrance were lacking. NOAA's tide records at La Jolla (http://NOAA-tide.gov) provided tide data closest to the study area and were used for setting up the ocean boundary condition for the study. In addition, scattered surf and tide data (high and low tides) at Oceanside were available and were compared with NOAA's La

Jolla tide gauge data and revealed that, while there is a slight phase lag of about 15 min between La Jolla and Oceanside, the magnitudes of high and low tides are very close at these two locations. Therefore, NOAA's tidal records at La Jolla for 2008–2009 were used for this study.

Figure 2-4 shows the tidal height time series at La Jolla for Jan 1-15, 2008, which covers a 2-week period for the Spring/Neap tidal cycle. Tidal range at La Jolla is about 2 m, dominated by M2 (tidal period of 12.42 hours) and K1 (tidal period of 23.92 hours). The ocean tides function as the driving force to mix ocean water with the lagoon water so long as the lagoon entrance remains open to the ocean.

Figure 2-4. Ocean tidal height at La Jolla (2 weeks: January 1, 2008 to January 16, 2008) covering the spring/neap tidal cycle.

Like the oceanic WSE boundary, Scripps Institute of Oceanography (SIO) measured salinity, temperature and dissolved oxygen (DO) in the nearshore of Del Mar. Temperature and salinity data are necessary to define conditions at the model oceanic boundary and salinity and temperature data measured by SIO at Del Mar were used as the ocean boundary conditions. Figure 2-5 shows the time series of temperature measured at three ocean sites, including NOAA Oceanside offshore, NOAA Camp
Pendleton nearshore, and SIO at Del Mar. Data at Del Mar includes both surface and 5-m depth data. Figure 2-6 shows that salinity of the nearshore ocean water remained at a relatively constant value ranging between 33.3 and 33.5 ppt for most of the year. During January to February 2008, ocean salinity was reduced as low as 31–32 ppt for a brief period after relatively large storm events.

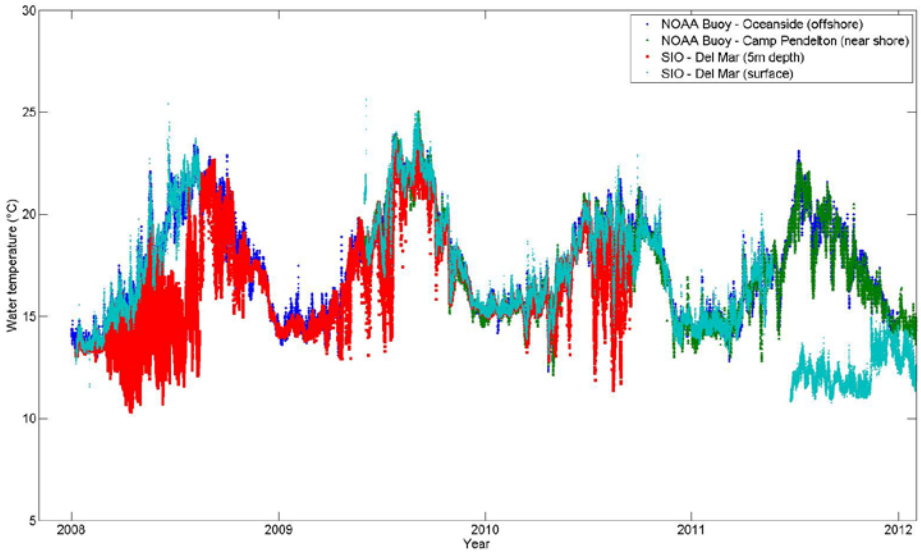

Figure 2-5. Ocean temperature measured offshore by NOAA and SIO (data provided by SIO).

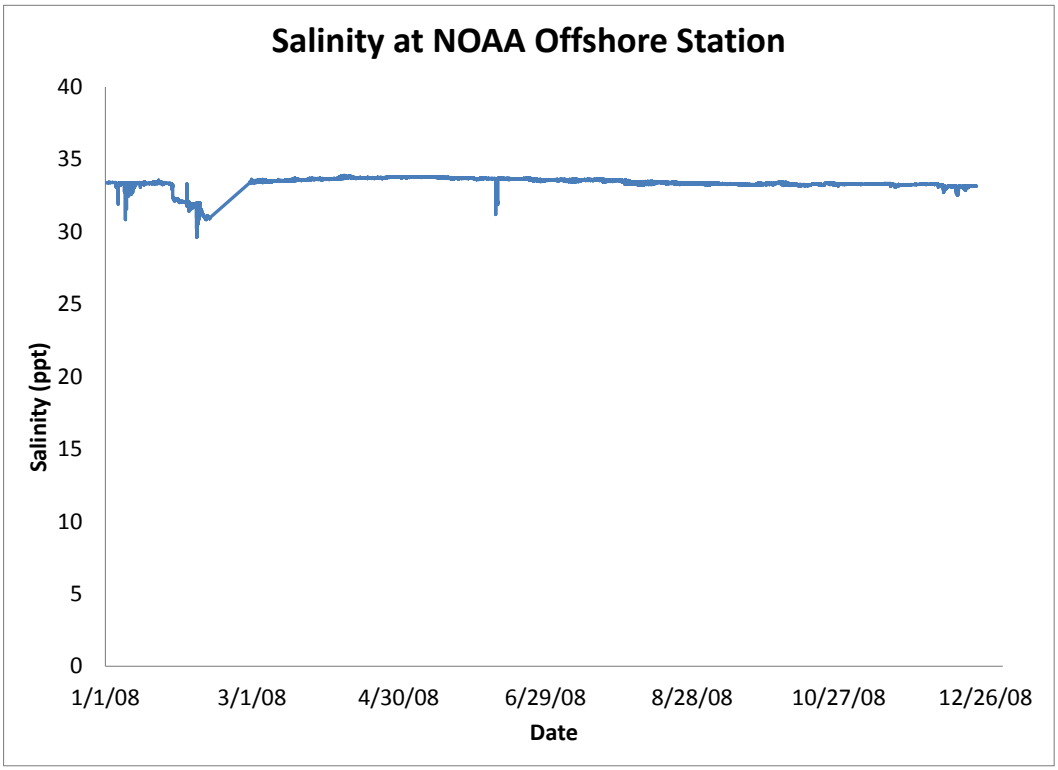

Figure 2-6. Salinity at NOAA offshore site for 2008.

2.2.4 Upstream Boundary Loads

Freshwater and nutrients from the upstream watershed constitute the major loads to the lagoon water. The EFDC model requires flow of freshwater and associated salinity and temperature from the upstream boundary. In Section 2.3 we discuss the development of the model inputs for the freshwater inflows, and upstream salinity and temperature conditions.

The USGS gauge station measures freshwater discharge at Ysidora (11046000), and river salinity and temperature at Temecula (11044000) (Figure 2-3). Therefore, the salinity and temperature data and the freshwater discharge data were measured at two different locations. We used these two datasets for the upstream boundary conditions, since no better data were available.

Figure 2-7 shows the time series of salinity and temperature measured at Temecula for 2008–2009. Several temperature data were missing during different times of the 2-year period. The summer/winter temperature cycles were reflected in the time series. Water salinity was relatively constant (~0.4 ppt) throughout the year. The temperature and salinity data were assigned to freshwater discharge data as the upstream boundary conditions for EFDC.

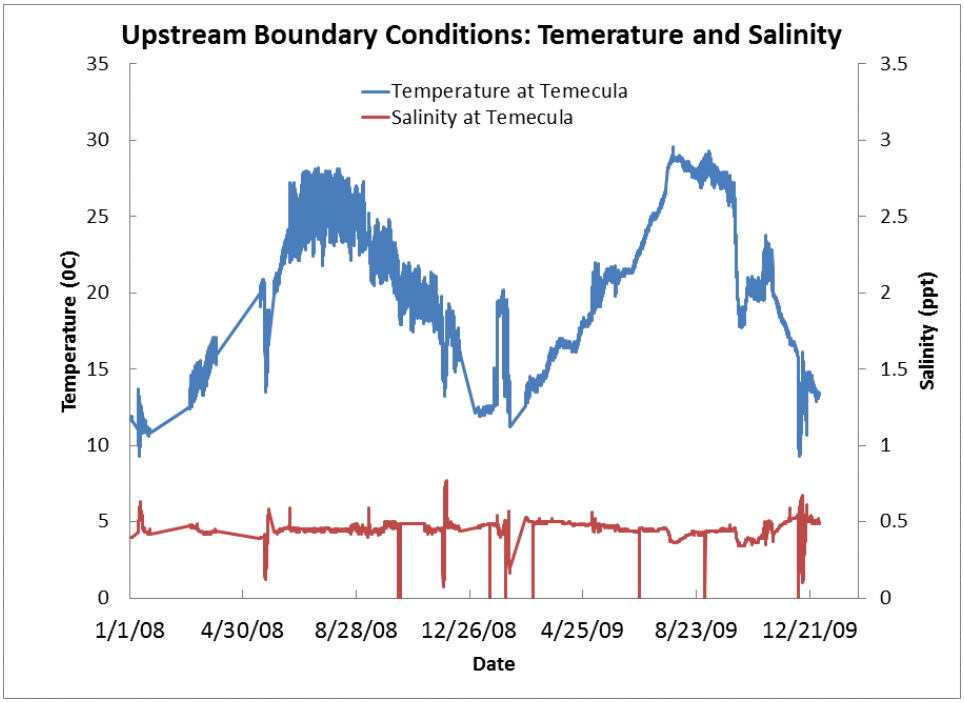

Figure 2-7. Upstream boundary conditions for temperature and salinity at USGS Temecula station (11044000).

2.2.5 Freshwater Inputs

The Santa Margarita River provides the major source of freshwater discharge to the SML primarily during the wet season from roughly October to May. The wet season generally starts from October to December when the first storm flushes the lagoon. Water flow from these early storms usually results in the widening and/or deepening of the lagoon entrance and can result in re-opening the mouth after it has become completely closed (during the dry period). The more open condition allows for a more active interaction and mixing within the lagoon between freshwater from the upstream watershed and salt water from the ocean. At the peak of the wet season, the lagoon is generally kept open and exchange of the lagoon water and ocean water is active. As the rainy season winds down and ceases

around the end of May, the sand at the ocean boundary can accumulate and increase in height resulting in reduced exchange of lagoon water with the ocean. In the middle of the dry season, riverine freshwater flow is minimal and ground water flow to the lagoon, although small, becomes the primary freshwater source to the lagoon.

Groundwater inputs are small in comparison to the river flows during the wet season, but may become relatively important during the dry summer season when the river flows are minimal. The importance of groundwater to salinity of the lagoon water during the dry season was confirmed during this model calibration study.

Five sources of freshwater river flow data or upstream modeling results were available for the SML hydrodynamic and transport model:

1. USGS gauge station at Ysidora (USGS Station Number:11046000)
2. Hydrological Simulation Program Fortran (HSPF)-simulated freshwater flow rates provided by Tetra Tech Inc. through SCCWRP
3. Simulated freshwater flow rate by Stetson's groundwater model provided by Camp Pendleton through SCCWRP
4. Simulated groundwater flow rate by Stetson's groundwater model provided by Camp Pendleton through SCCWRP
5. Calibrated flow rate

The USGS gauge measured surface river discharge at Ysidora. HSPF model-simulated freshwater flow rates were provided by Tetra Tech. Stetson's groundwater model simulated both freshwater surface flow and groundwater flow to the lagoon. The groundwater flow rate from Stetson's model are the only groundwater inflow estimates (measured or modeled) available. In the model result section, Stetson's modeled groundwater flow results were added to each of the freshwater flow datasets, including USGS, HSPF- and Stetson-simulated surface flow for model calibration.

Section 2.4 demonstrates that the EFDC simulated salinity using freshwater flow rates from the USGS gauge, HSPF model, and Stetson's groundwater model were in agreement with measured values, except during the non-rainy days of the wet season (January to April 2008 and 2009) throughout the 2-year simulation period. As a result, further calibration of the freshwater flow rates was conducted. In this calibration, an extra small amount of additional freshwater flow rate (0.0–0.7 cms) was added to the Stetson+GW flow rate during the non-rainy days of the wet season. With the calibrated flows, simulated salinities compare well with the measurements, in particular, during the non-rainy days of the wet season. Further discussion about the calibrated flow is made in Section 4.

Figure 2-8 shows upstream river freshwater flow rates for the USGS, HSPF, and Stetson data and modeled flow, as well as the groundwater flow rate estimate from Stetson for 2008. Overall, the river flow rates from the USGS gauge data and the Stetson model are in close agreement, whereas the HSPF-model results during the storm events have peak flows that are significantly higher than the USGS data and Stetson model results. Groundwater flow rate estimates from the Stetson model range between 0.01 and 0.25 cms, and were generally in the range of 0.01 to 0.1 cms during the dry season. This small flow rate from groundwater during the dry season was found to be important to match the EFDC model simulated salinity to the measured values during the dry seasons. Figure 2-9 shows the total freshwater flow rates resulting from the addition of the Stetson modeled groundwater flow rate to the USGS measured river flow, the HSPF-simulated river flow, and the Stetson modeled river flow, respectively. Figure 2-10 and Figure 2-11 show the corresponding surface and groundwater flow rates and the combined flow rates, respectively, for 2009.

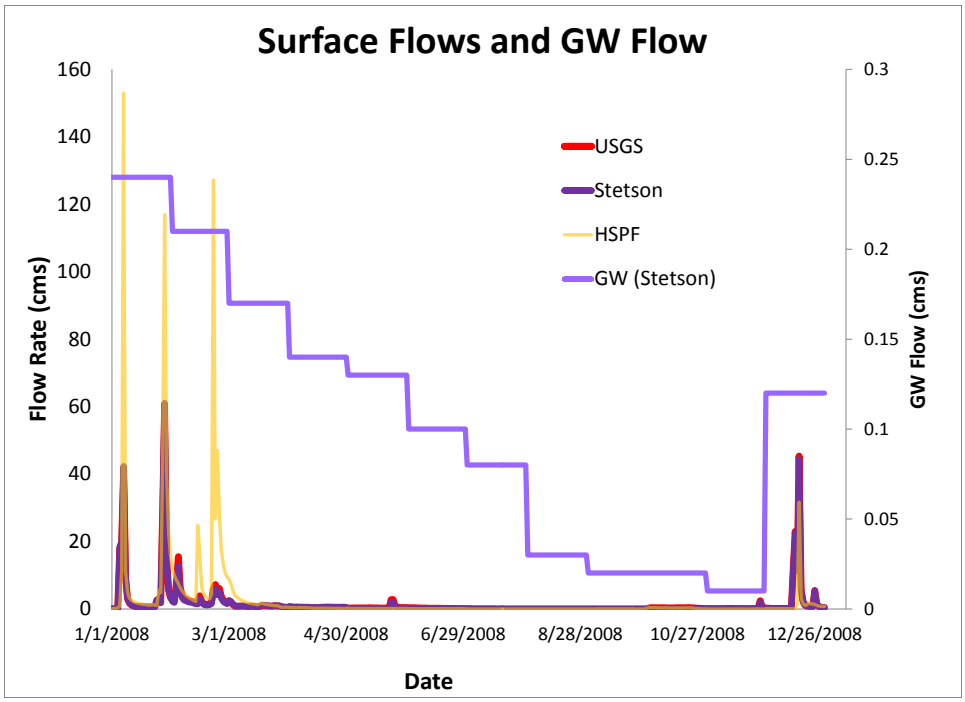

Figure 2-8. Riverine surface flows from the USGS gauge at Ysidora, the Stetson model and the HSPF model, and groundwater flow from the Stetson model for 2008.

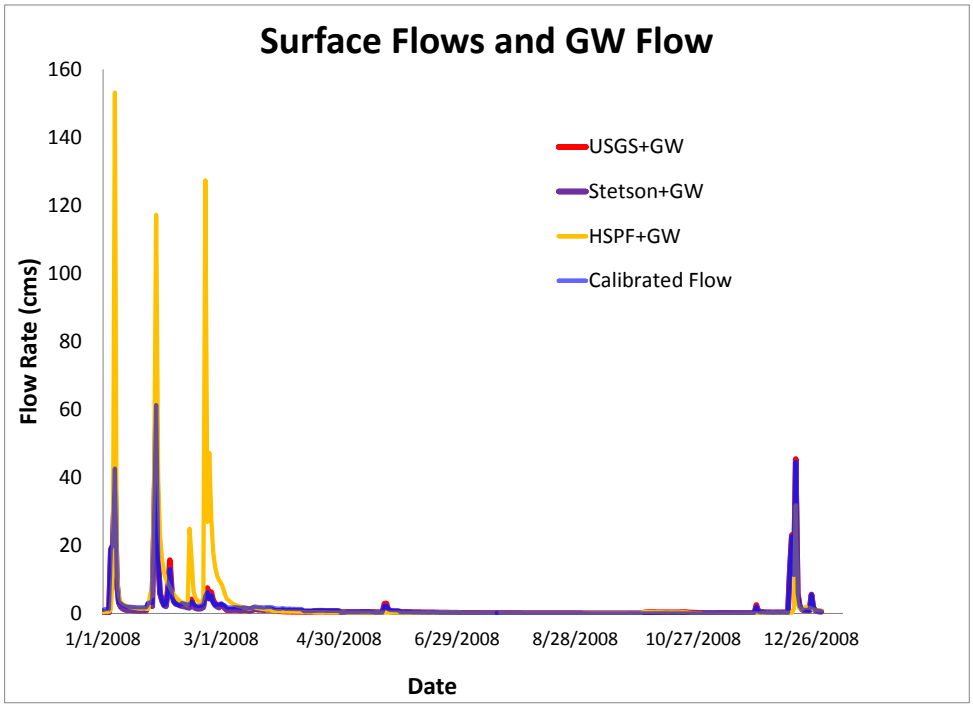

Figure 2-9. Combined flow (river flow + GW flow) resulting from the addition of the Stetson modeled GW for to the USGS measure river flow, the Stetson model river flow, and the HSPF modeled flow, along with the calibrated flow results for 2008.

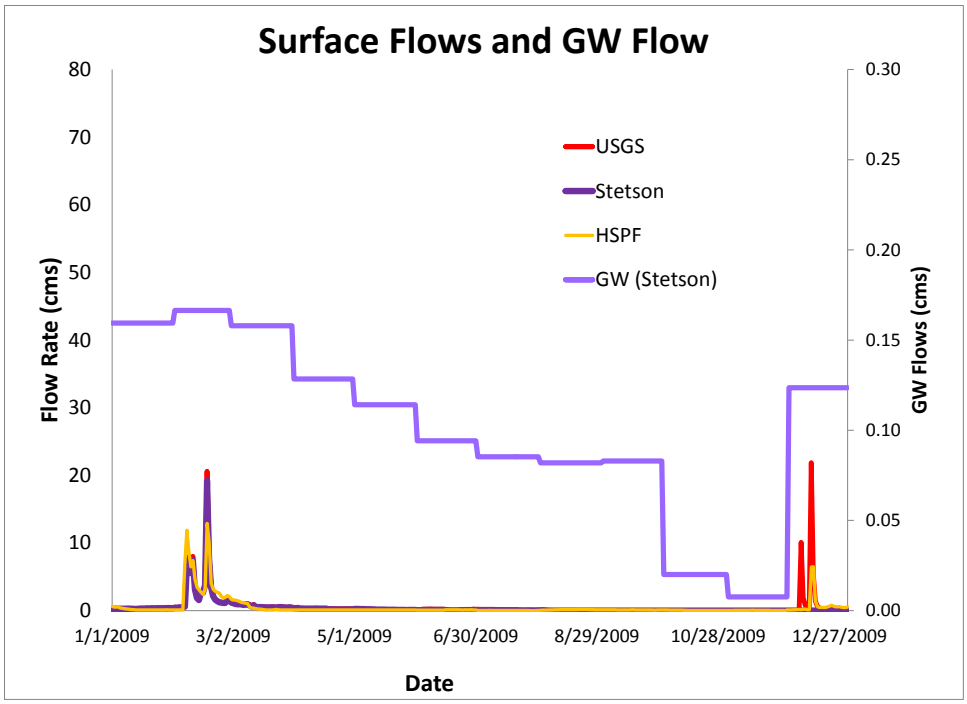

Figure 2-10. Riverine surface flows from USGS gauge at Ysidora, model data by Stetson's and HSPF models, and groundwater flow by Stetson's model for 2009.

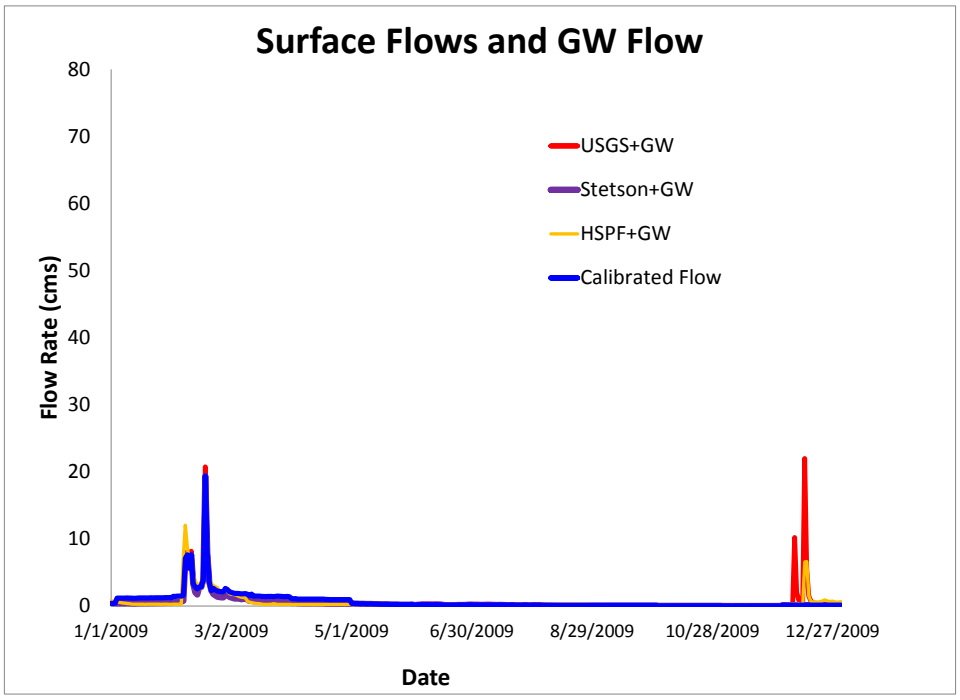

Figure 2-11. Combined flow (river flow + GW flow) resulting from the addition of the Stetson modeled GW for to the USGS measure river flow, the Stetson model river flow, and the HSPF modeled flow, along with the calibrated flow results for 2009.

2.3 MODEL SETUP AND DEVELOPMENT

2.3.1 Grid Generation

The EFDC model grid was generated based on the measured bathymetric data (Figure 2-12). A main channel extends from the ocean boundary of the lagoon eastward to the upstream boundary of the study area at the Santa Margarita River. From the upstream boundary to the RRB, the lagoon is narrow and channelized, and therefore, one model segment was adequate for resolution across the river. Downstream from the RRB the lagoon becomes wider and multiple model segments were generated to resolve the lateral topographic variations across the lagoon. The grid for the lower lagoon was shallow, with a channel connecting the ocean through the sand berm at the mouth (Figure 2-12).

Water depth for each grid cell was obtained by interpolation of the bathymetric survey data (Figure 2-2). Each cell was assigned a constant bottom depth. Following the bathymetry data, interpolated model water depths at the RRB and the SMB model cells were the deepest, 3.4 and 3.1 m (averaged over each model cell), respectively. Grid depths for the rest of the lagoon were less than 2 m, and were less than 1 m in the lower lagoon.

The physical domain was simulated with 182 horizontal grid cells ranging in size from 12 m x 84 m (upstream) to 88 m x 127 m (lower lagoon). Across the lagoon width, the grid ranged from 1 cell in the upper and middle portion of the lagoon to 2–3 cells near the HWY 5 Bridge and to up to 8 cells in the shallow lower lagoon near the mouth. The lagoon water was connected to the ocean through one grid cell representing the sand berm at the mouth. There were 138 grid cells (17 along the axis) from the mouth to the HWY 5 Bridge, 27 grid cells (16 along the axis) from the Railroad Bridge to the Stuart Mesa Bridge, and 17 single grid cells along the axis to the head of tide. The water depth used for each grid cell was averaged from the bathymetric referenced to mean sea level. The three-dimensional, sigma-coordinate grid used three vertical layers evenly divided in the water column.

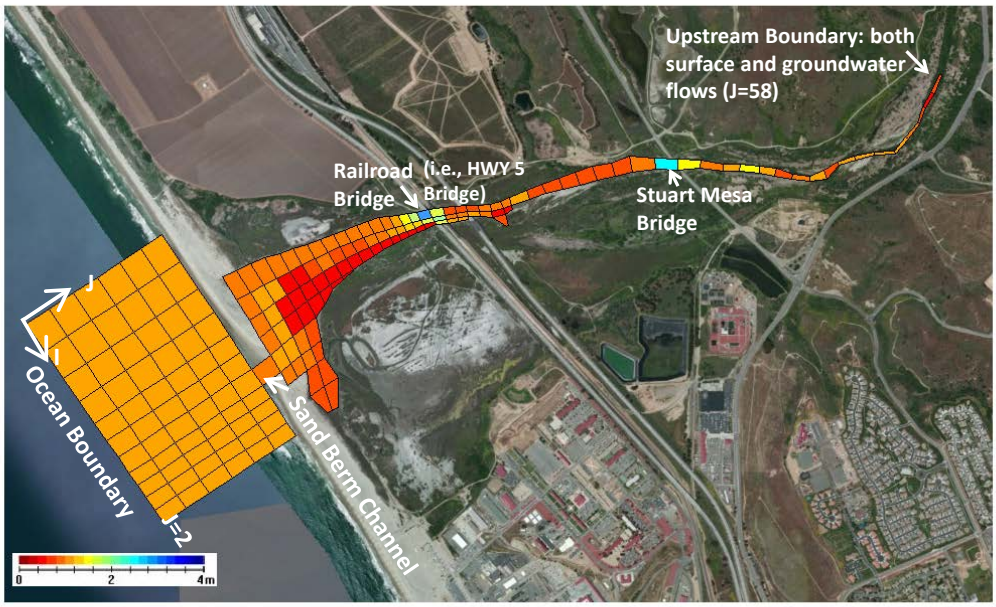

Figure 2-12. The EFDC model grid with bathymetry for the Santa Margarita Lagoon (Railroad Bridge and HWY 5 Bridge are the same location).

2.3.2 Boundary Conditions

There are two boundaries for the model grid, the upstream boundary at the head of tide and the downstream ocean boundary. The upstream boundary (Segment J=58, Figure 2-12) receives freshwater inflows and nutrient loads from the watershed. The four freshwater discharges described above were used as boundary conditions for 2008–2009. The downstream boundary connects the lagoon and the ocean. The NOAA ocean tide data measured at La Jolla were adjusted for relevance to MSL prior to use at this boundary.

Salinity and temperature data measured at the USGS gauge station at Temecula (2008–2009) were used as the upstream boundary condition for the simulation of these two water quality parameters. The downstream boundary conditions at the ocean were assigned with the data measured nearshore at Del Mar by SIO throughout the simulation periods. Meteorological data measured at the two stations near the study area were used as the boundary condition between the water surface and the atmosphere for the heat exchange between the air and the lagoon water and the model input files for the boundary conditions described above. The locations of the data used for the boundary conditions are shown in Table 2-1.

Table 2-1. Model input data and files for the boundary conditions.

Location	Upstream Boundary	Ocean Boundary	Atmospheric Boundary
Freshwater Inflows	1) USGS Gauge Station at Ysidora 2) HSPF-simulated flow at model upstream boundary 3) Stetson-Model-simulated flow (both surface water and groundwater) at model upstream boundary 4) Calibrated flow (to be explained in the next section)		Evaporation data at CIMIS Station at Temecula
Salinity	0.4 ppt (USGS Ysidora Station) upstream Salinity as output from Stetson's GW model	33.2-33.6 ppt (NOAA offshore)	
Temperature and Dissolved Oxygen	USGS Gauge Station at Temecula	1) NOAA offshore Oceanside station 2) SIO Del Mar Station	1) NOAA Station at Camp Pendleton 2) CIMIS Station at Temecula
Ocean tide		NOAA tide gauge at La Jolla	

2.4 MODEL CALIBRATION AND VALIDATION

Model calibration compared model output to measurements made in the lagoon. The first comparison was between measured and modeled water surface elevation (water depth) at the USGS RRB Station for the 2-year period of 2008–2009. Next, the measured and simulated temperature and salinity at the same site were compared.

2.4.1 Water Surface Elevation

Water surface elevation is an important characteristic of the lagoon that dictates the volume of water in the lagoon at any specific time. It is a hydrodynamic property governed by the interaction between the ocean water and freshwater inflow in the lagoon. Comparison of modeled versus measured water surface elevation provides a basis for validating that the volume of water is accurately predicted by the model, which is a good indicator that the model is correctly simulating the hydrodynamics of the lagoon.

A key consideration in evaluation of the WSE in the lagoon is the degree of closure of the lagoon entrance at the ocean boundary. During 2008–2009, the lagoon entrance was never completely closed. Over time, the sand berm grew and flow was reduced, but exchange of ocean and lagoon water was never completely blocked by the sand berm. This is reflected by the water depth data measured at the USGS RRB station. Measured water depths show that water surface elevation at the RRB is affected by the tidal action throughout the 2-year simulation period. The daily maxima of the WSE are in sync with the daily maxima of ocean tide, while the daily minima of the WSE vary over time as a function of the changing sand berm height. The dynamics of sand berm height is governed by complex processes involving nearshore sediment transport, beach evolution, lagoon sediment transport, and storm-driven flow events. Simulation of these complex processes is beyond the scope of the current study, and instead we used the daily minima of the measured water depths at RRB as an empirical estimate of the sand berm height. The EFDC model code was modified to use the empirical time series of the sand berm height at the grid location closest to the lagoon entrance (cell 8,8). Model simulations were conducted with the empirical sand berm heights and results compared with the measured water surface elevation.

Figure 2-13 and Figure 2-14 show comparisons between simulated and measured water surface elevations at RRB for 2008 and 2009, respectively. Overall, simulated water surface elevations are very close to the measured values throughout the 2-year periods. Missing measured daily minimum data exist for May to April 2009, and linear interpolation was conducted to fill the gap.

Table 2-2 shows the quantitative comparison between the model and measurements. Mean daily mean is the average of daily means over the simulation period and are predicted to be 0.64 and 0.63 m, whereas measured values are 0.65 and 0.66 m for 2008 and 2009, respectively. Similar accuracy levels are obtained for the validation of daily minima and daily maxima.

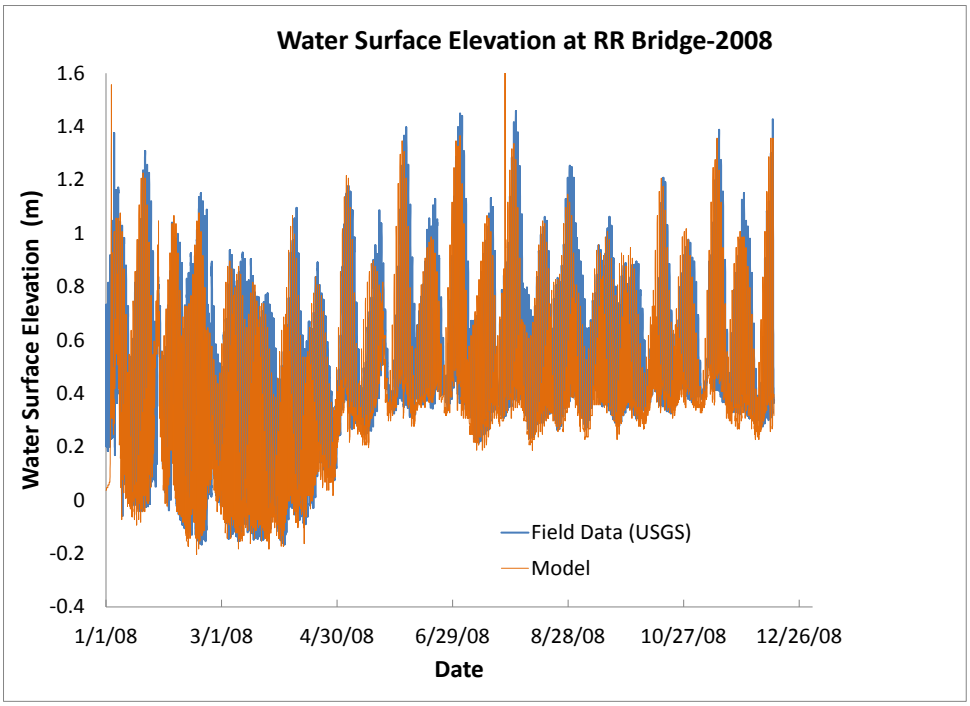

Figure 2-13. Simulated and measured WSE at RRB for 2008.

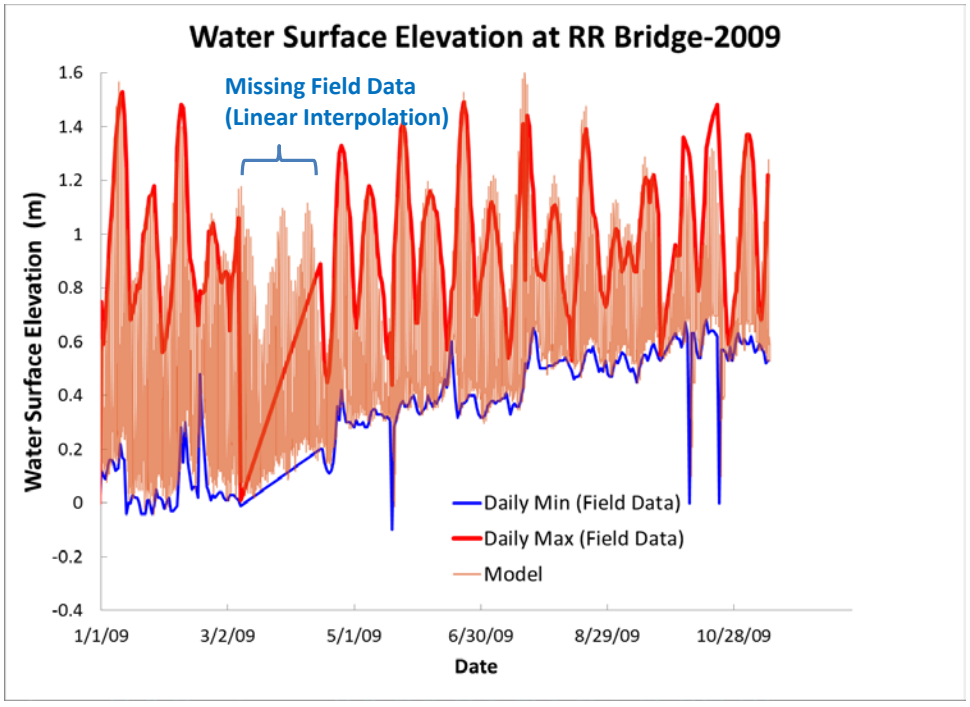

Figure 2-14. Simulated and measured WSE at RRB for 2009.

Table 2-2. Model-data comparison of the WSE at RRB for 2008 and 2009.

	Water Surface Elevation at Railroad Bridge		
2008	Mean Daily Min (m)	Mean Daily Mean (m)	Mean Daily Max (m)
Field Data	0.06	0.65	1.29
Model	0.14	0.64	1.27
Difference	-0.08(-233)%	0.01 (1.5%)	0.02 (1.6%)
2009	Mean Daily Min (m)	Mean Daily Mean (m)	Mean Daily Max (m)
Field Data	0.35	0.66	0.98
Model	0.34	0.63	1.02
Difference	0.01 (2.8%)	0.03 (4.5%)	-0.04 (-4.1%)

Through proper setup of the model and boundary conditions, and modification of the EFDC code to incorporate the sand berm height, we were successful in providing good simulations of the lagoon WSE as validated by comparison to the 2008–2009 USGS data at RRB. Note, however, that because the model relies on empirical estimates of the sand berm height, predictions of future conditions may have limitations and uncertainties associated with the assumed conditions at the lagoon entrance.

2.4.2 Salinity and Temperature

Similar to typical coastal waters and estuaries in Southern California, salinity of the lagoon water is highly sensitive and responsive to the tidal interactions with the ocean and freshwater inputs from the watershed because these water bodies are characterized by energetic tidal exchange of ocean saline water and intermittent riverine freshwater pulses across shallow, low-volume lagoon systems. As a result, effects from the dynamic exchange between the ocean and the lagoon water are fast and responsive, which makes it challenging to simulate salinity to the accuracy level that is required to describe the dynamic characteristics of the transport and mixing between the ocean water and freshwater.

As discussed in Section 2.2.5, four historical freshwater discharge estimates were available for the period of interest, including the USGS gauge data, HSPF-model and Stetson-model estimates for surface water flow, and the Stetson-model groundwater flow estimates. These datasets were categorized into two subsets: surface water discharge only, and the combined surface and groundwater discharge. In addition, we developed another estimate of freshwater discharge from the EFDC model calibration for salinity. Therefore, in the analysis of lagoon salinity we will discuss model results from the following freshwater discharge estimates:

1. Surface water discharge only for USGS data, HSPF model and Stetson model
2. Combined surface water discharge with groundwater discharge (estimated by Stetson model)
3. Calibrated freshwater discharge data (obtained from model calibration for salinity)

The location of the USGS salinity and temperature sensor at the RRB was at a fixed height. Because the EFDC model uses the sigma-grid that divides the water column into the same

proportions among the three layer (0.33, 0.33, 0.33 for surface, middle, and bottom layer) with the dynamic fluctuation of the WSE, primarily driven by tides, the relative location of the sensor fluctuates during tidal changes (see Figure 2-15). During flood tide, WSE increases and the relative location of the sensor is in the middle or bottom layer. During the ebb tide, WSE decreases and the relative location of the sensor is in the middle or surface layer. Therefore, when compared with measurements, model data of the surface and bottom layers are used during ebb and flood tide, respectively.

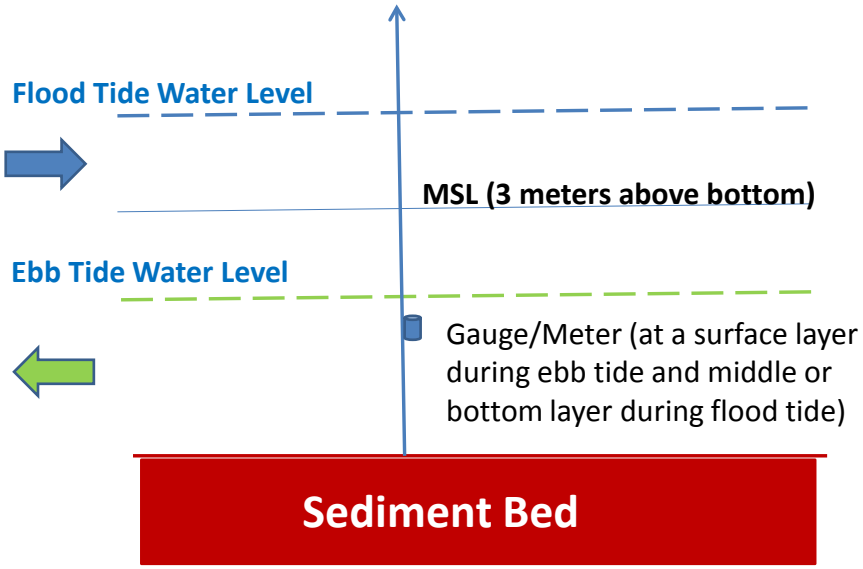

Figure 2-15. Change of layer location for the USGS salinity and temperature sensor during high and low tides.

Figure 2-16 shows EFDC-simulated salinity versus measured salinity at the RRB for the scenario with only the surface freshwater discharge measured at the USGS Ysidora station as the upstream boundary condition. Figure 2-17 shows the corresponding comparison with the combined surface freshwater discharge based on the USGS data added to the groundwater discharge estimated from the Stetson model as the upstream boundary condition. The comparisons indicate that during storm events with high freshwater discharge, the simulated and measured salinities compare fairly well, with fluctuation between the high value of 33–34 ppt and the lower value of 1–2 ppt. However, during non-rainy days in the wet season (December to May), EFDC-simulated salinities (in green) were high (15–25 ppt) in comparison to the measured range (2–15 ppt; in blue). This difference between simulated and measured salinities during the non-rainy days in the wet season persisted for the combined surface and groundwater discharge condition as well (Figure 2-17), indicating that the addition of groundwater does not significantly improve the agreement between modeled and measured salinity during the wet season. However, addition of the groundwater freshwater discharge does help to improve predicted salinity during the dry season (July to October). Without the addition of groundwater discharge (Figure 2-16), simulated salinity during the dry season remained at the 33–34 ppt range, which is very close to the ocean boundary condition salinity value, whereas the measured salinity ranged between 28–34 ppt during the period. With the addition of groundwater discharge (Figure 2-17), simulated salinities were reduced to the range of 27–34 ppt, comparable to the 28–34 ppt range of the measurements. In addition, simulated salinity during the period shows no saline water/freshwater tidal fluctuations if no groundwater discharge is added. With the addition of groundwater discharge, simulated salinities show fluctuations from tide/freshwater effects with a

magnitude comparable to that of the measured values. Therefore, although small in magnitude, groundwater during the dry season appears to be an important source of freshwater in the lagoon, which is reflected by the measured salinity during these periods.

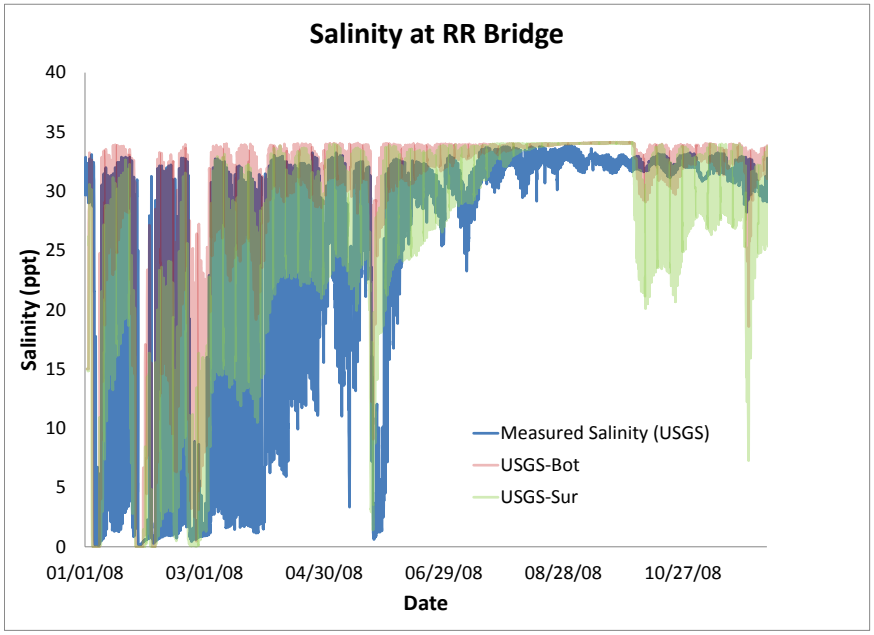

Figure 2-16. Simulated and measured salinity at the RRB for surface water discharge based on the USGS gauge at Ysidora for 2008. The modeled salinities were generated for both the surface (sur) and bottom (bot) layer.

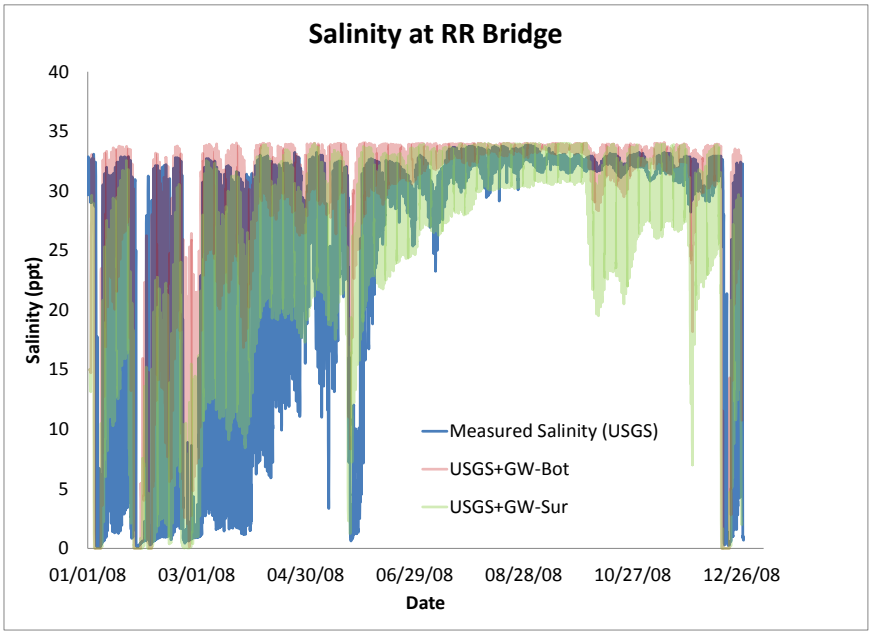

Figure 2-17. Simulated and measured salinity at the RRB for combined surface water (USGS-Ysidora) and groundwater discharge (Stetson model) for 2008. The modeled salinities were generated for both the surface (sur) and bottom (bot) layer.

Figure 2-18 and Figure 2-19 show the corresponding results using the Stetson model discharges as the upstream boundary condition and Figure 2-20 and Figure 2-21 show the corresponding results using the HSPF-model discharges at the upstream boundary. While simulated salinities from the three freshwater flow rates (USGS gauge, HSPF model, and Stetson model) compare well with the measurements during the storms with both simulated and measured salinities reduced to 0–2 ppt, there are mismatches between model and data. In particular, model-simulated salinities during the non-rainy days of wet season (January to April) were higher than measured values with a difference ranging between 5–10 ppt. Such model-data mismatches occur in late January and March to April 2008 (Figure 2-17, Figure 2-19 and Figure 2-21). In comparison, simulated salinity using freshwater flow from Stetson's model (surface + groundwater) matches with measurements slightly better than using from the USGS gauge flow, and both are much better than the results using freshwater flow from HSPF's model (Figure 2-17, Figure 2-19 and Figure 2-21).

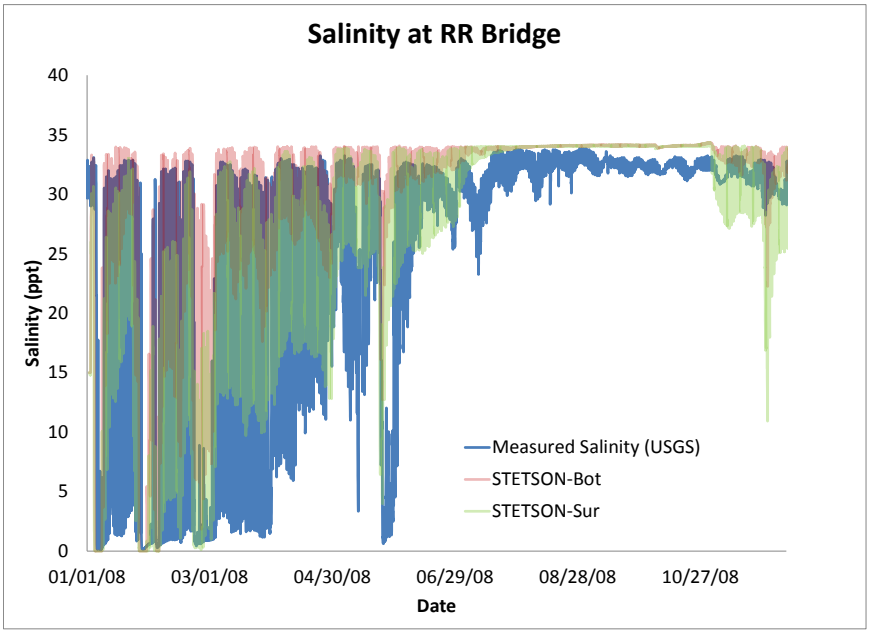

Figure 2-18. Simulated and measured salinity data at the RRB for surface water (Stetson-model) for 2008. The modeled salinities were generated for both the surface (sur) and bottom (bot) layer.

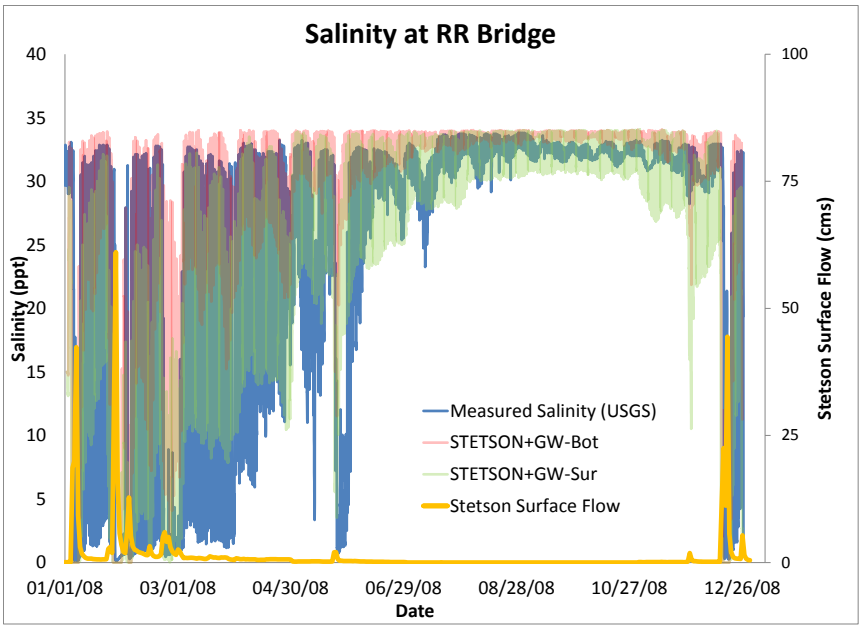

Figure 2-19. Simulated and measured salinity data at the RRB for combined surface water (Stetson model) and groundwater discharge (Stetson model) for 2008. The modeled salinities were generated for both the surface (sur) and bottom (bot) layer.

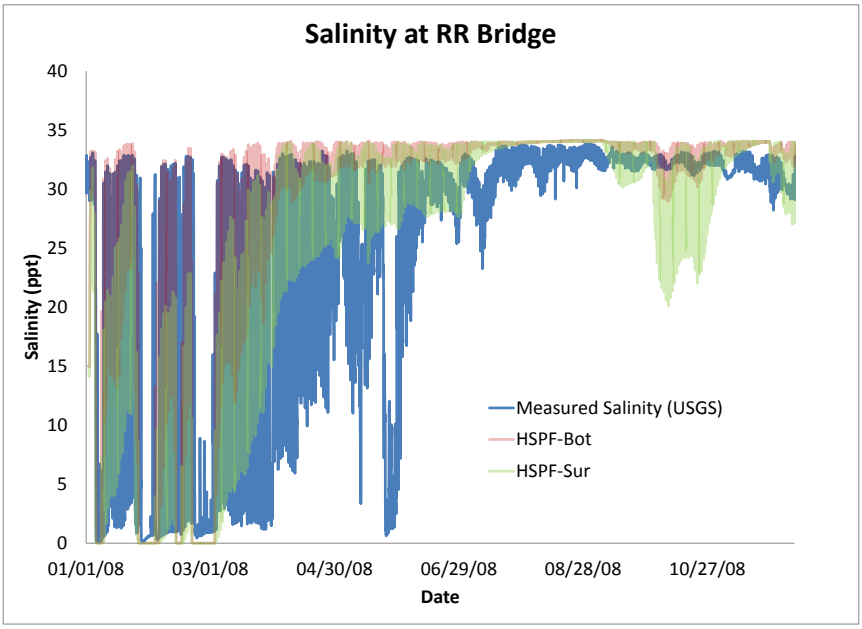

Figure 2-20. Simulated and measured salinity data at the RRB for surface water (HSPF model) discharge for 2008. The modeled salinities were generated for both the surface (sur) and bottom (bot) layer.

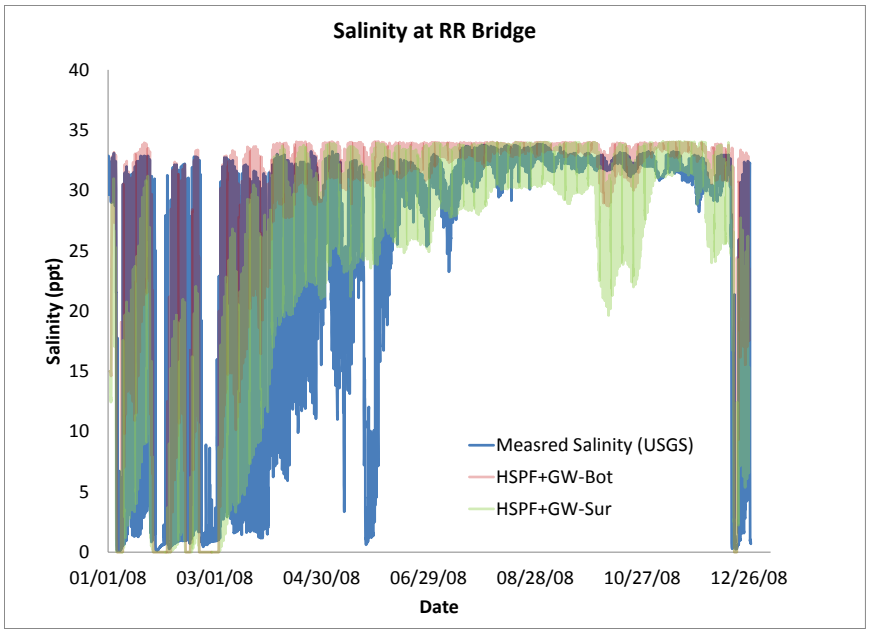

Figure 2-21. Simulated and measured salinity data at the RRB for combined surface water (HSPF model) and groundwater (Stetson model) discharge for 2008. The modeled salinities were generated for both the surface (sur) and bottom (bot) layer.

Based on the over-prediction of salinity levels in the lagoon during non-rainy days in the wet season, we attempted to empirically calibrate the model upstream boundary condition by adjusting these flows. Figure 2-22 shows the results obtained by calibrating the upstream freshwater discharge to provide improved correspondence with lagoon salinities. The upstream boundary flow was calibrated by incrementally increasing the amount of freshwater discharge to the Stetson-model discharge condition during the non-rainy days in the wet season while leaving the dry season discharges unchanged. As a result of the empirical calibration, simulated salinity during the wet season is substantially improved in comparison to the measured salinity. To achieve a best fit to the salinity data the non-rainy day flow had to be increased over the Stetson model condition by 0.1 to 0.9 cms. However, one should remember that these higher flows during the non-rainy day wet season condition are not supported by any of the existing USGS data or watershed modeling results and are purely an empirical adjustment to try to improve the lagoon model response based on the measured salinities in the lagoon. Alternative explanations that could also explain these differences include inadequate simulation of exchange at the ocean boundary (i.e., the exchange is not as efficient as EFDC predicts) or higher freshwater retention within the lagoon than is predicted by the EFDC model.

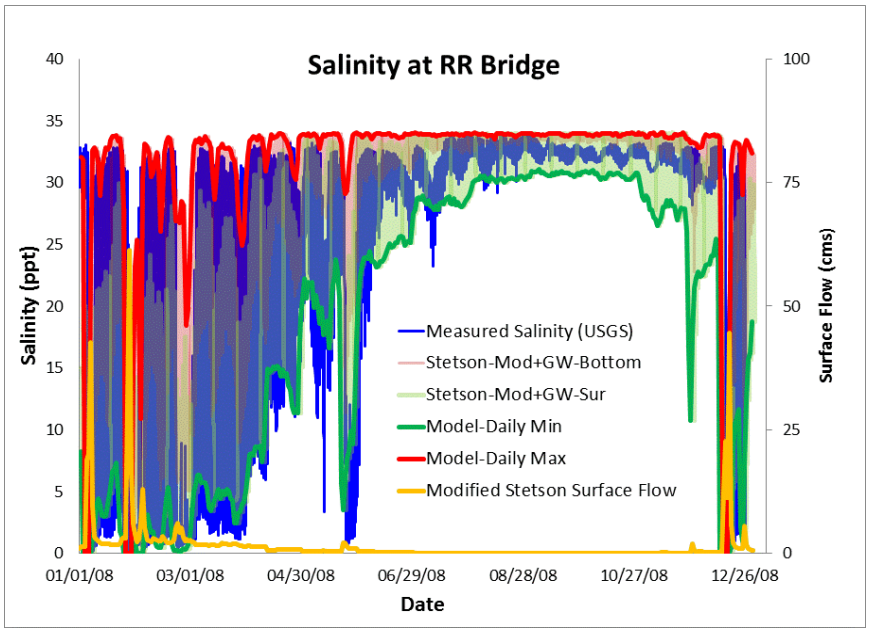

Figure 2-22. Simulated and measured salinity data at the RRB for the empirically calibrated upstream flow for 2008.

Figure 2-23, Figure 2-24, and Figure 2-25 show the similar comparisons between the simulated and the measured salinity for 2009 for the scenarios with combined surface water and groundwater for USGS-gauge discharge, Stetson-model discharge, and HSPF-model discharge, respectively. Figure 2-26 shows the corresponding results for the empirically calibrated flow. The results with the empirically calibrated flow for 2009 show improvement between model and data, similar to the improvement for the 2008 scenario.

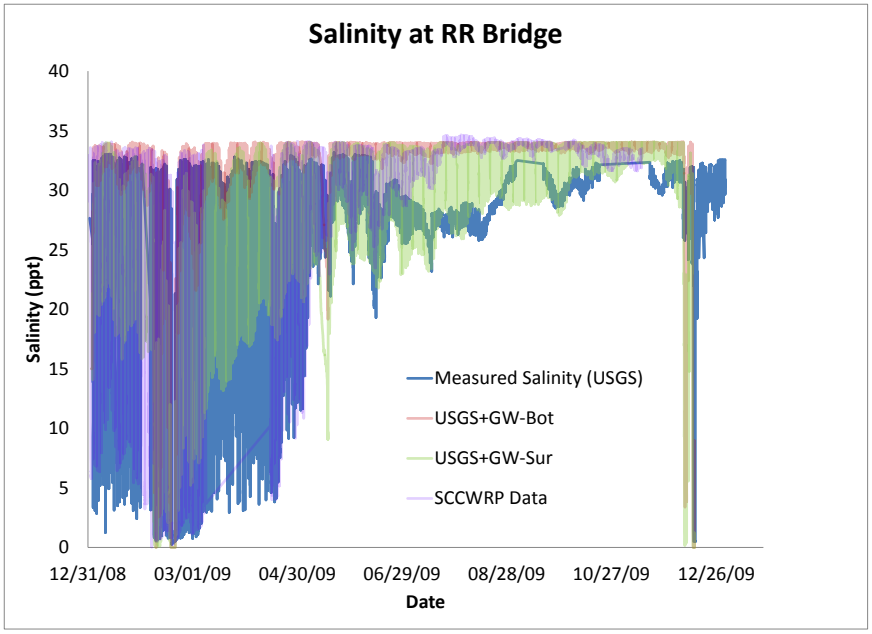

Figure 2-23. Simulated and measured salinity data at the RRB for combined surface water (USGS gauge) and groundwater discharge (Stetson model) for 2009.

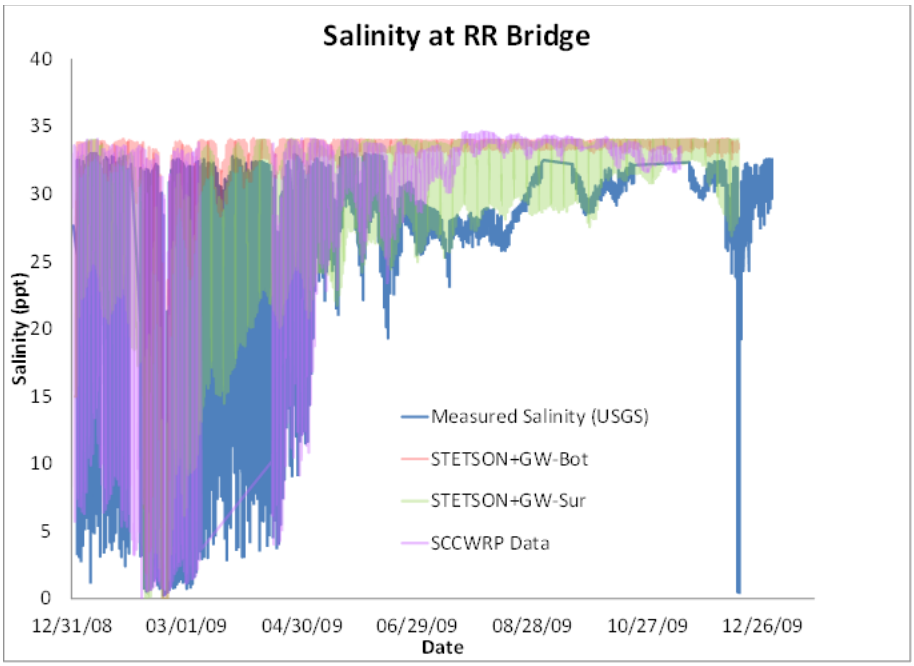

Figure 2-24. Simulated and measured salinity data at the RRB for combined surface water (Stetson model) and groundwater discharge (Stetson model) for 2009.

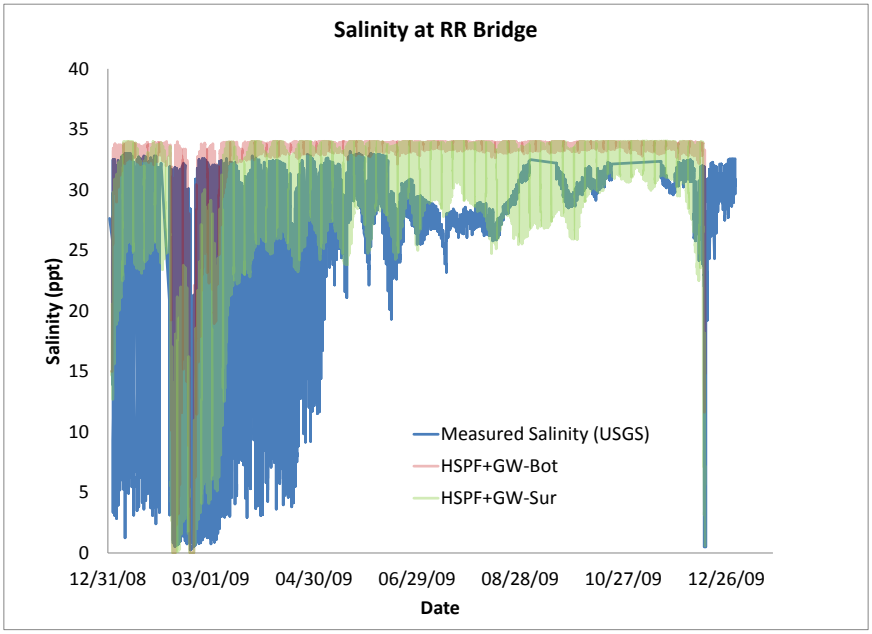

Figure 2-25. Simulated and measured salinity data at the RRB for combined surface water (HSPF model) and groundwater discharge (Stetson model) for 2009.

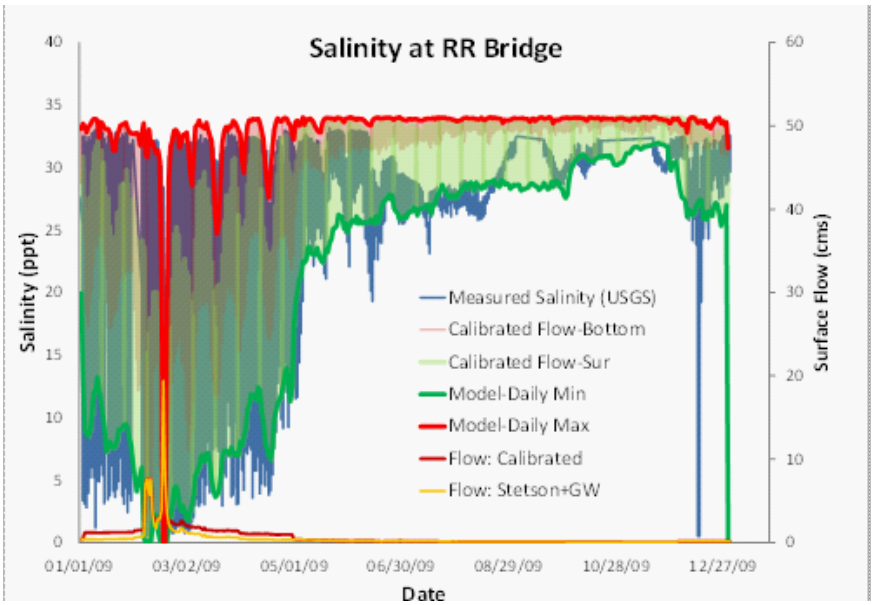

Figure 2-26. Simulated and measured salinity data at the RRB for calibrated flow discharge for 2009.

Table 2-3 shows a summary of the quantitative comparisons between model and measurement results for salinity for 2008 and 2009. Addition of groundwater to the three sets of surface freshwater improved the salinity during the dry season. Overall, out of the three original discharge datasets, scenarios with the USGS gauge discharge and Stetson model discharge produce the best model-data comparison, which is followed by the scenario with HSPF-model discharge. However, results of the scenarios with the calibrated flows provide the best match to the data, matching between ~60 to 90% of the data. The primary improvement occurs during the non-rainy days of the wet season, when the surface water discharges were adjusted upward with a small amount flow rate. From a physical interpretation, this small amount of flow rate could be from ungauged surface water flow, or groundwater discharges.

Table 2-3. Comparison of simulated and measured salinity at the RRB for 2008 and 2009.

Model	Is Measured Salinity Within Simulated Daily Min-Max Range?			
	2008		2009	
	Yes (match %)	No (mismatch %)	Yes (match %)	No (mismatch %)
USGS+GW	66.2	33.8	69.0	31.0
HSPF+GW	64.4	35.6	54.22	45.8
Stetson+GW	76.5	23.5	64.1	35.9
Calibrated Flow	88.6	11.4	90.2	9.8

Figure 2-27 and Figure 2-28 show comparisons between the calibrated flow discharge rate and the three sets of combined discharge rates, including USGS-gauge discharge, Stetson-model discharge and the HSPF-model discharge for 2008 and 2009, respectively. The empirically calibrated flow discharge is based on the combined surface and groundwater discharges from the Stetson model. Therefore, as shown in Figure 2-27and Figure 2-28, calibrated flows match well with the Stetson

flow discharge for most of the periods, except during the non-rainy days of the wet season when a small amount of additional flow is required to improve the relationship.

Figure 2-29 shows added flows (calibrated) based on combined surface and groundwater flow from Stetson's model for 2008. It shows that flows were added during the non-rainy days (post storms). No added flow was needed during the dry season (May to October). Calibration results suggest that groundwater, or possibly ungauged surface water, after storms may have higher retention capacity than the estimated groundwater flow predicted by Stetson's model. Such a conclusion is based on model calibration by matching salinity between the model and the data. Further investigation is needed to improve our understanding and quantification of groundwater flow characteristics in the region.

Figure 2-30 shows the model-data comparison of temperature at the RRB for 2008–2009. Simulated temperature compares well with the measured values. The model captures both the diurnal and seasonal trends and fluctuation magnitudes in the data The simulations appear to do a good job in representing the complex balance of the upstream and ocean boundaries, the heat exchange through the water–air interface and the hydrodynamic transport and mixing of the lagoon water, all of which influence the measured temperatures in the lagoon. Similar to salinity results, predicted temperature in the water column exhibits stratification between the upper and lower water layers. Temperature in the bottom layer is about 0 to 5 °C lower than that in the surface layer. Simulated temperature in the surface layer also fluctuates on a diurnal cycle with amplitudes larger than those in the bottom layer, reflecting heating and cooling during the daylight and night time through the surface layer.

In EFDC, heat from solar radiation enters into the lagoon water either to the surface layer or to the entire water column (user's option). When solar heat enters into the surface layer, heat exchange with the lower water column occurs through the hydrodynamic vertical mixing. Results in Figure 2-30 are for solar radiation only to the surface layer. Results of distributing solar radiation to the entire water column are similar to those of Figure 2-30, only with smaller diurnal fluctuation temperature amplitudes for the radiation over the water column.

Both simulated and measured temperatures exhibit diurnal fluctuations, water temperature reaching maxima and minima during midday and nighttime, respectively. Daily means, daily minima, and daily maxima of water temperature were extracted and compared between the model and field data. Figure 2-31 shows model-data correlation for daily-mean temperature at the RRB for 2008–2009. Compared with field data, model results under-predicted daily mean temperatures by ~10%. From Figure 2-32, note that amplitudes of diurnal fluctuations (daily maxima minus daily minima) for both model and field data were larger than the 10% deviation between the model and the data of daily mean temperature. These differences are shown in Figure 2-32.

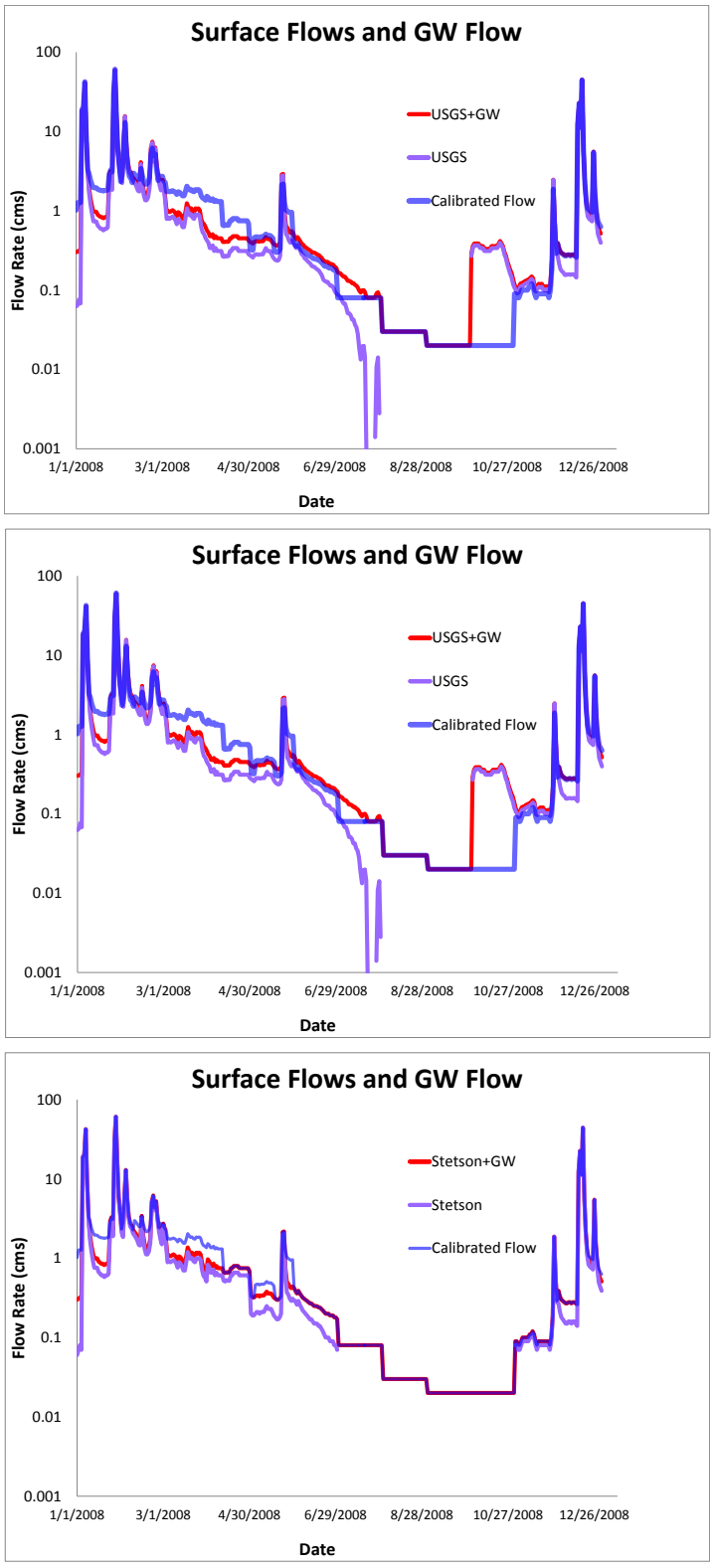

Figure 2-27. Comparisons of calibrated flow and the combined USGS flow (top), Stetson (middle) and HSPF (bottom) for 2008.

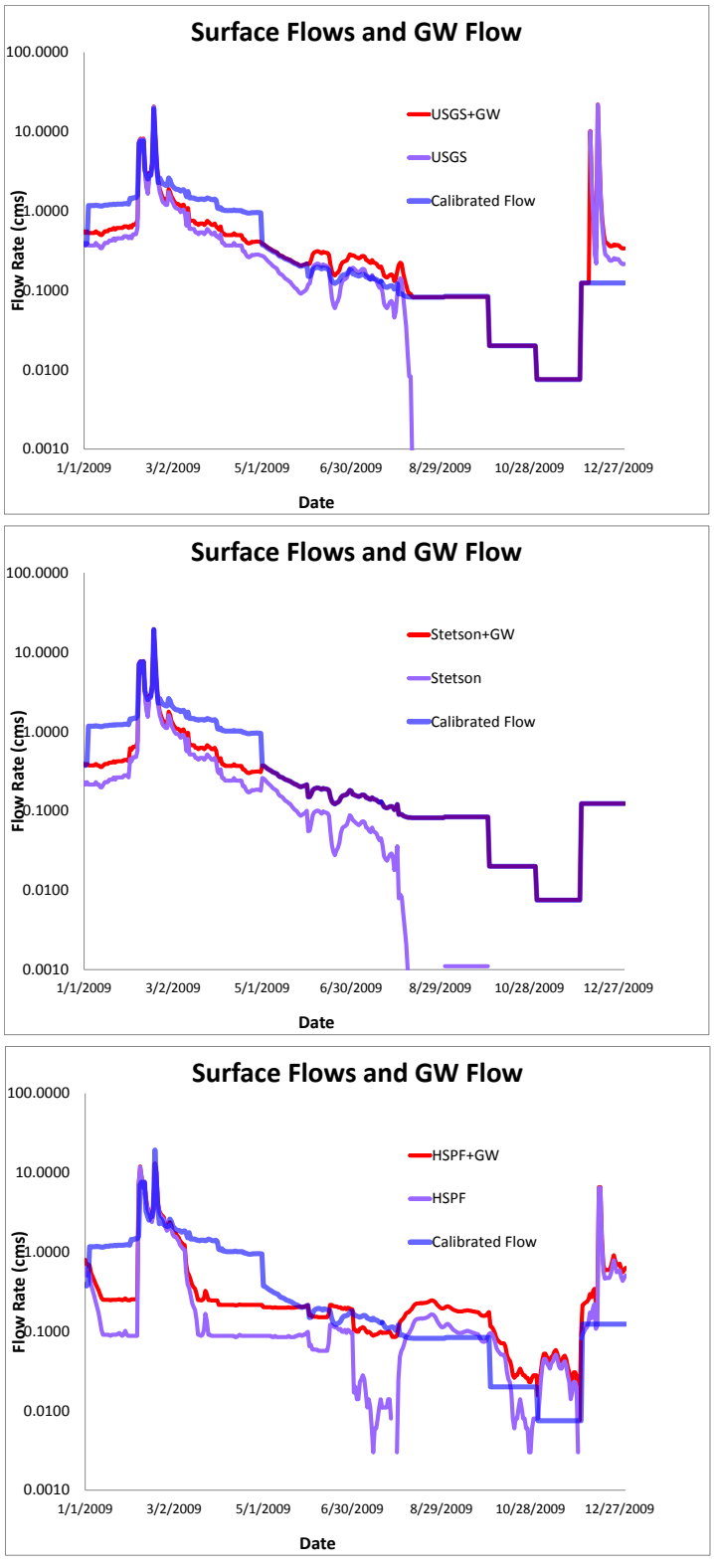

Figure 2-28. Comparisons of calibrated flow and the combined USGS flow (top), Stetson (middle) and HSPF (bottom) for 2009.

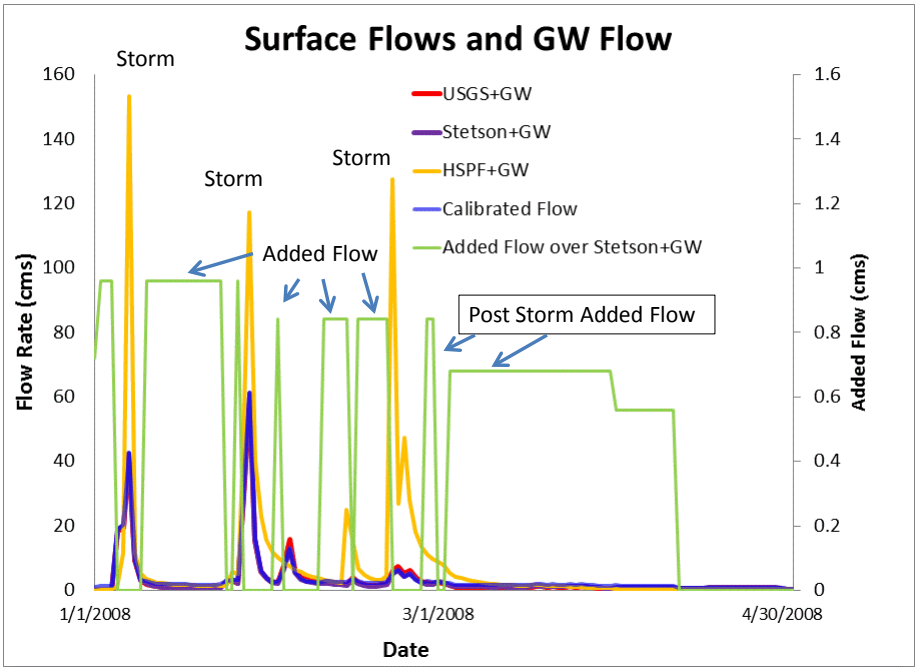

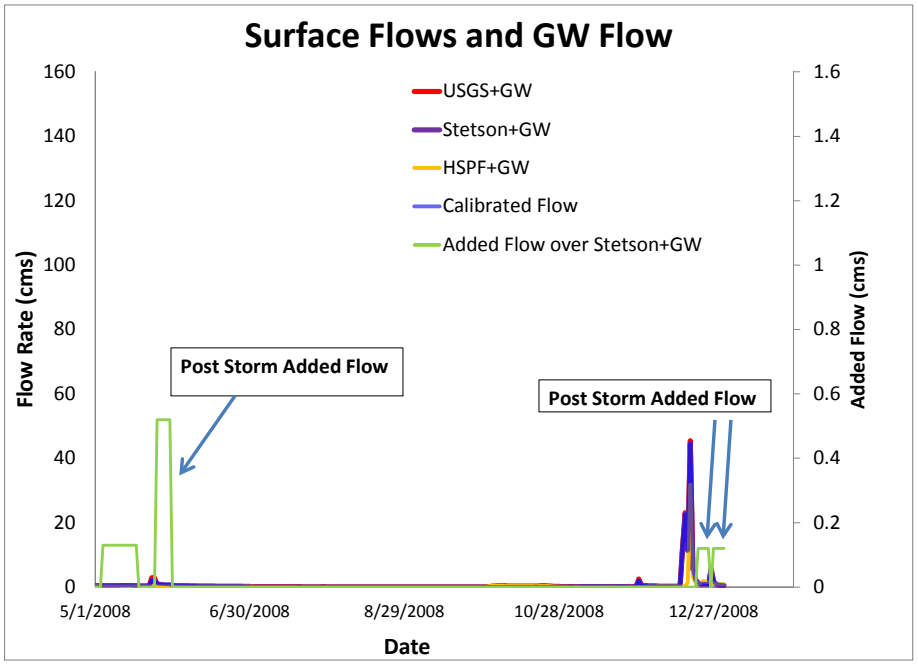

Figure 2-29. Added flow during non-rainy days (post storms) of wet season (above) vs. dry season (below). Added flow is based on Stetson flow (surface water + groundwater).

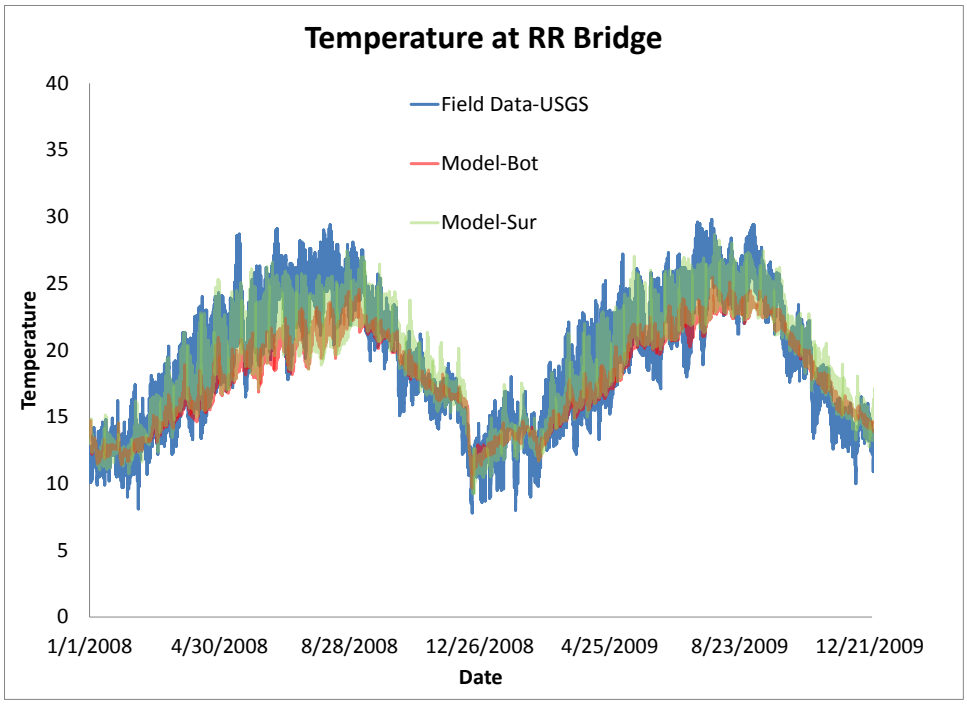

Figure 2-30. Simulated and measured water temperature at the RRB for 2008–2009. The modeled temperature was generated for both the surface (sur) and bottom (bot) layer.

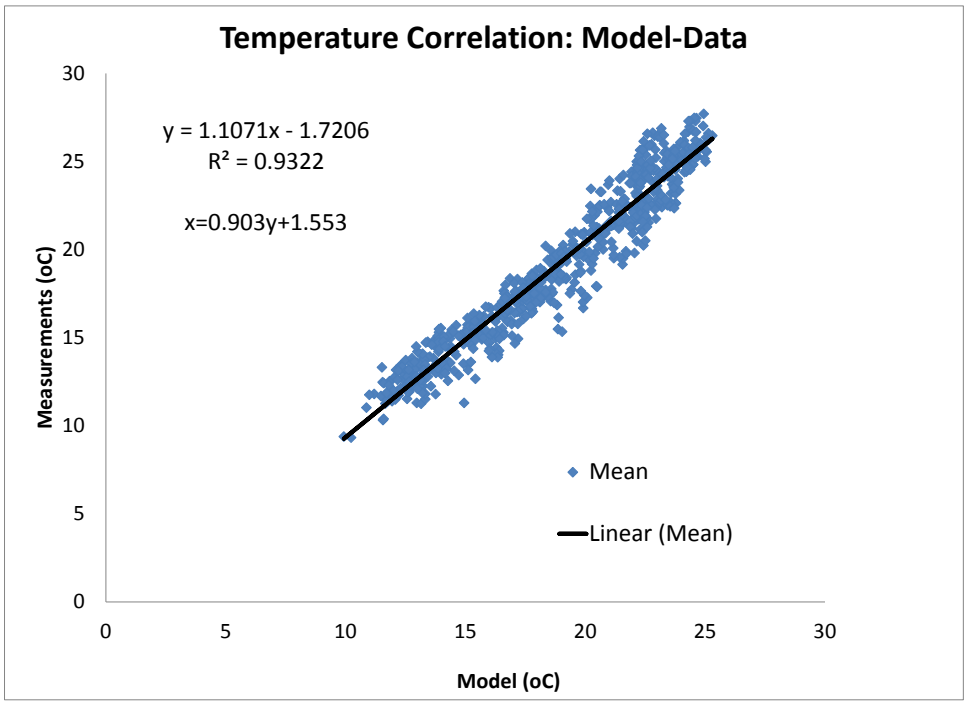

Figure 2-31. Model-data comparison and correlation for daily-mean temperature at RRB, 2008–2009.

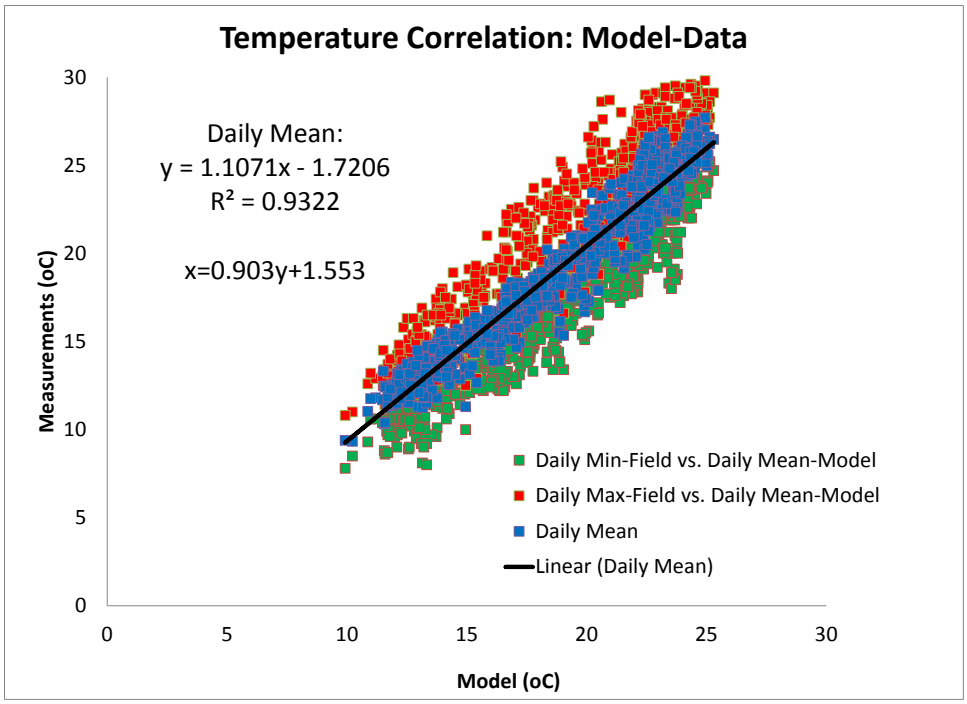

Figure 2-32. Model-data comparison between daily mean (model-x-axis) and daily minima and daily maxima (field data-y-axis), scattering of daily minima and maxima is larger than the scattering daily mean temperature between model and data.

3. ESTUARY EUTROPHICATION MODEL CALIBRATION AND VALIDATION

This section summarizes the development, calibration, and validation of the estuary eutrophication model for the SML. This summary includes identification and description of the data that were utilized for the model, as well as the approach that was followed for constructing, calibrating, and verifying the model for the SML. This portion of the model calibration focused on simulating nutrient loading and cycling and its effects on algal biomass production and dissolved oxygen (DO).

WASP is a water quality model that simulates the water quality response of aquatic systems to natural phenomena as well as to anthropogenic pollutants. WASP-Eutro simulates the biogeochemical processes of aquatic plant growth and their response to nutrients (nitrogen and phosphorous). These general processes include the mass loading and cycling of nutrients in the water body as they are taken up in aquatic plants (algae) as they grow during photosynthesis, and are released back into the water column or sediments when the plants die. It also includes the generation of DO during photosynthesis as well as its depletion in the absence of light as a result of plant respiration and from the degradation of the plants by bacteria once they die. The most recent model of WASP-Eutro (7.5x) simulates the dynamic cycles of nutrients, planktonic and macroalgae, and dissolved oxygen in both the water column and in the sediments (diagenesis).

WASP-Eutro was linked to the calibrated EFDC model using the same boundaries and grid. The hydrodynamic model output data for each segment including water volume, current velocity, salinity, and temperature were used to drive the transport and water quality kinetics in WASP-Eutro. The hydrodynamic model, run at a time step of four seconds was used to generate an input file to WASP-Eutro run with a time step of 120 seconds. To make the model reach a steady state, for the water column and the sediment bed, the model was run for a 3-year span simulating 2007 (repeating the 2008 input dataset), 2008, and 2009. The output of this 3-year run was used as the initial steady state conditions. The model runs for 2007, 2008, and 2009 were then repeated using these initial conditions to generate the final outputs that were used for comparison to field data.

WASP-Eutro was used to simulate water concentrations of nitrogen species: inorganic ammonia, nitrite, and nitrate, dissolved and particulate organic nitrogen, and total nitrogen; phosphorous species: inorganic phosphate, dissolved and particulate organic phosphorous, and total phosphorous and dissolved oxygen. It was also used to simulate sediment fluxes between the sediment and water column of the same nitrogen and phosphorous species as well as oxygen. Finally, the model was used to simulate the growth of plankton and macroalgae.

3.1 METHODS

3.1.1 Data Sources

3.1.1.1 Inputs

As discussed in Section 2, freshwater in the SML originates from multiple sources, including the surface water inflows, and groundwater. Watershed runoff from the upstream boundary was the major surface freshwater inflow to the lagoon. Flow data measured at the USGS station in Ysidora was used as the freshwater inflow from the upstream model boundary. Groundwater flow from the upstream was based on the Stetson Inc. groundwater model. Another source of groundwater near the RRB was also discovered and quantified in 2010 by SSC Pacific, The source of this groundwater was from long-term watering of an agricultural field on the bluff above the lagoon. The field was allowed to go fallow in 2010 and is no longer watered. Though this source of groundwater was not a

significant source of freshwater flow, its location and associated magnitude of nutrients were identified as potentially important to lagoon water quality. The calibrated freshwater inflow data were used to drive the water quality model simulation for the period between 2007 and 2009, with the first year of the modeling designed to stabilize the simulation. Model results were then compared to the field data collected during 2008 and 2009

In support of the SDRWQCB Investigative Order for Santa Margarita Lagoon and other 303(d)-listed estuaries, field data were collected by CDM Federal Programs Corporation for the stakeholders and by SCCWRP through the 2008 and 2009 timeframe. The field datasets included a suite of surface water measurements collected at three fixed stations: Segment 1 near the Railroad Bridge, Segment 2 just downstream of the Stuart Mesa Bridge, the Ocean Inlet station, and the 12 axial transect stations from the mouth to the Stuart Mesa Bridge during four index periods in 2008. Nutrients were also collected during three storm events from a station at the Basilone Bridge upstream of the lagoon. The nutrient measurements included total and dissolved nitrogen, nitrate, nitrite, ammonia, and particulate nitrogen, total and dissolved phosphorous, inorganic phosphorous and particulate phosphorous. Nutrient loads from the watershed were calculated my multiplying concentrations by the freshwater discharge. Groundwater nutrient loads were processed in a similar manner. The watershed groundwater nutrient load was based on concentrations and discharge predicted by the Stetson's groundwater model. The groundwater nutrient load derived the agricultural field adjacent to the lagoon was based on concentrations and discharge measured by SSC Pacific in 2010. These nutrient loads were assigned as boundary conditions for the receiving water quality model of the lagoon.

3.1.1.2 Lagoon Continuous Water Quality Data

Continuous water quality data collected by CDM in 2009 were deemed unusable by the stakeholders because of calibration and other sensor errors. Instead, the continuous water quality data collected by SCCWRP including salinity, temperature, and DO were used. These data were collected using in situ instruments in near bottom lagoon water near the RRB site (Segment 1 station) between January 1, 2009, and November 13, 2009. The temperature and salinity data were used for the hydrodynamic model calibration.

3.1.1.3 Lagoon Nutrients and Eutrophication

The concentrations of the total and dissolved inorganic nitrogen and phosphorous within the lagoon during the three wet weather events and four dry weather index periods were taken from CDM Federal Programs Corporation (2009) (Table 3-1).

Macroalgal biomass was collected at the three intertidal locations shown in Figure 3-1 during the four index periods by SCCWRP (McLaughlin et al., 2013). Benthic fluxes of nutrients and oxygen were collected from two mid-channel stations shown in Figure 3-1 during the four index periods also by SCCWRP. Model-simulated concentrations of nutrients were compared with the measured values at the 15 surface water sampling locations (Figure 3-1) for 2008. Model/data comparisons were also conducted for DO at Segment 1 for 2009 and macroalgal biomass at Segment 1 for 2008–2009 and at Segment 2 for 2008.

Two supplemental data sources were also used to improve our modeling studies in the lagoon. Dissolved oxygen concentrations were measured at the Del Mar Pier by the Scripps Institute of Oceanography and were used as the oceanic boundary condition for 2008. Dissolved oxygen data was measured by the USGS station at Temecula and later modified by calibration as the boundary condition at the model upstream boundary.

Table 3-1. Summary of the data collection for eutrophication in Santa Margarita Lagoon by time period, types of sampling event, organization.

Period	Event	Organization	Date
Continuous Monitoring	Water Quality Monitoring	CDM	1/1/08-10/21/08
Index Period 1	Ambient Sampling	CDM	1/30-2/1/08, 2/6-2/8/08
	Transect Sampling	CDM	2/7/08
	Benthic Chamber Study	SCCWRP	1/10/08
	Pore Water Peeper Deployment	SCCWRP	1/7-1/21/08
	Sediment Core	SCCWRP	1/21/08
	Macroalgae Monitoring	UCLA	1/7-1/21/08
Index Period 2	Ambient Sampling	CDM	3/24-3/26/08, 3/31-4/2/08,
	Transect Sampling	CDM	3/27/08
	Benthic Chamber Study	SCCWRP	3/20/08
	Pore Water Peeper Deployment	SCCWRP	3/18-4/3/08
	Sediment Core	SCCWRP	4/3/08
	Macroalgae Monitoring	UCLA	3/18-4/3/08
Index Period 3	Ambient Sampling	CDM	7/21-7/23/08, 7/28-7/30/08
	Transect Sampling	CDM	7/24/08
	Benthic Chamber Study	SCCWRP	7/7/08
	Pore Water Peeper Deployment	SCCWRP	7/3-7/23/08
	Sediment Core	SCCWRP	7/23/08
	Macroalgae Monitoring	UCLA	7/3-7/23/08
Index Period 4	Ambient Sampling	CDM	9/23-9/25/08, 9/29-10/1/08
	Transect Sampling	CDM	9/25/08
	Benthic Chamber Study	SCCWRP	9/15/08
	Pore Water Peeper Deployment	SCCWRP	9/12-9/29/08
	Sediment Core	SCCWRP	9/29/08
	Macroalgae Monitoring	UCLA	9/12-9/29/08
Agriculture Field	Groundwater seepage and N-P Load	SSC Pacific	6/8-6/9/2010 4/10-4/12/2012 10/21-10/23/2013

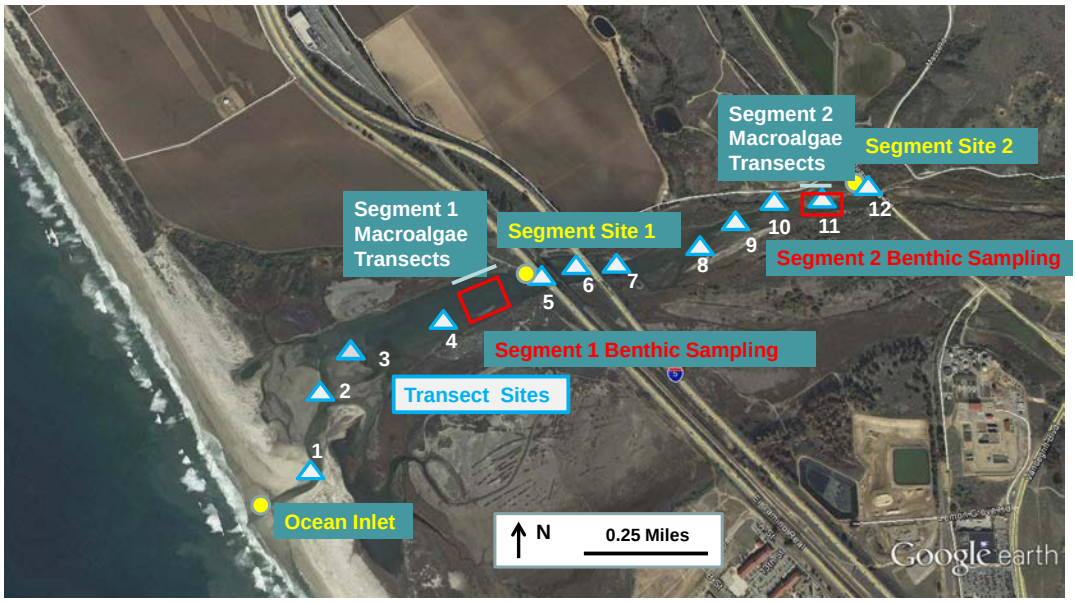

Figure 3-1. Locations of in-lagoon data collected during 2008 (Table 3-1).

3.1.2 Model Development

The USEPA's Water Analysis Simulation Program (WASP) is the recommended USEPA standard model for dynamic water quality analysis and is supported and updated by the U.S. EPA Center for Exposure Assessment Modeling in Athens, GA, and Region IV in Atlanta, GA. The WASP 7.5X model, developed by Dr. James Martin of the Mississippi State University and Tim Wool of USEPA Region IV, has the most updated version of macroalgae biomass dynamics, the sediment diagenesis module, and the advanced eutrophication module. Eight variables are simulated in the model, including ammonia, nitrate and nitrite, organic nitrogen, orthophosphate, organic phosphorous, carbonaceous biological oxygen demand, dissolved oxygen, and three species of aquatic plants that include phytoplankton, periphyton, and macroalgal biomass (Figure 3-2). These variables and the associated processes constitute four interacting systems, including the aquatic plant kinetics, the nitrogen cycle, the phosphorous cycle, and DO.

The EFDC hydrodynamic model was run every 4 sec during 2007–2009. The hydrodynamic and transport results of each model segment, which include water volume, current velocity, salinity, and temperature, were stored at every 60 sec as the hydrodynamic output file, resulting in a file size of 3.5 GB. The hydrodynamic output file that was linked within the WASP7.5X water quality model was used to drive the transport and water quality kinetics for the simulation of 2007–2009. The sand berm, which controlled the opening/closure of the inlet, varied during each of the 3-year period. The hydrodynamic information included in the hydrodynamic output file was carried into the transport process for the water quality parameters.

To make the model reach a steady state for the water column and the sediment bed, we conducted the model simulations with the following procedures. First, we set up the model and conducted the model simulation of 2007, 2008, and 2009. The model inputs for 2007, including the hydrodynamics and the nutrient loads, were generated by repeating the loads from 2008. Model simulations were conducted from a quiescent state for two consecutive 3-year simulation periods (6 years) to let the water column deposited nutrients in the sediment, reach a steady state. The steady-state sediment nutrient contents (output from the sediment diagenesis module), including the in-organic nitrogen and phosphorous, were assigned as the initial sediment condition for the new 3-year simulations.

Model output of nutrient concentrations were compared with measured data for 2008 and DO for 2009 and macroalgal biomass for 2008 and 2009.

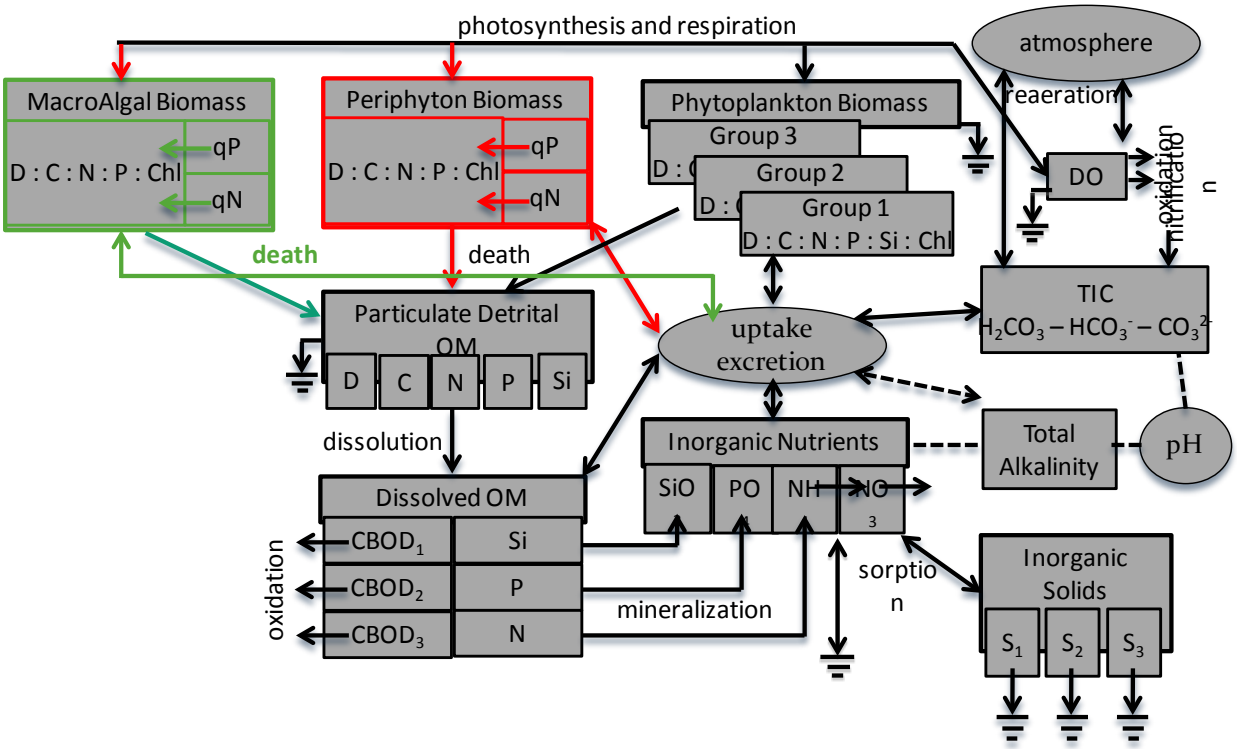

Figure 3-2. Processes and state variables simulated in the WASP 7.5X model.

The sediment diagenesis module implemented in WASP was based on the work by DiToro, Pauin, Subburamu, and Gruber (1990) (Figure 3-3). The researchers observed that in freshwater systems sediment oxygen demand (SOD) is not linearly proportional to the deposition of organic material, but varies with the square root of the deposited load. Deposited organic material is broken down in anaerobic sediments into methane and ammonia. This decomposition process is often referred to as "diagenesis." The subsequent oxidation of methane and ammonia in the aerobic layer is responsible for sediment oxygen demand. DiToro, et al. (1990) also showed that the square root variation of SOD with load followed from the finding that methane's solubility in pore water is limited; when the concentration of methane exceeds its solubility, methane gas is formed and bubbles through the water column to the surface. The methane that escapes to the surface was assumed to be not oxidized, accounting for the fact that SOD is not linearly proportional to the load of deposited material.

In the DiToro, et al. sediment oxygen demand model, sediment oxygen demand is predicted by modeling the transport and oxidation of methane (CH_4) and ammonia (NH_3), which are produced by the bacterial decomposition, or "diagenesis," of the reactive portions of particulate organic carbon (POC) and particulate organic nitrogen (PON) in the sediment (the reader is referred to the original article by DiToro et al. [1990] for a complete discussion of model processes and equation derivations). In this model, carbon and nitrogen diagenesis are assumed to occur at uniform rates in a homogenous layer of the sediment of constant depth, termed the "active layer." An active depth of H = 0.15 m was selected for the sediment diagenesis module. In the active layer the concentrations of POC material and PON material can be modeled by a simple first-order decay processes.

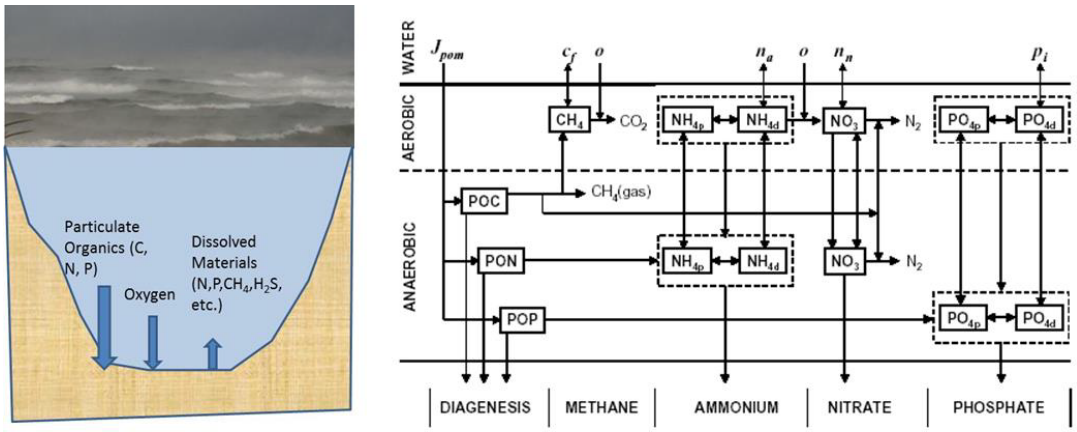

Figure 3-3. Processes and state variables simulated in the sediment diagenesis module.

Output of the sediment diagenesis includes sediment fluxes of ammonia-N, nitrate-N, methane, orthophosphate, and sediment oxygen demand. These benthic fluxes are therefore potential sources of nutrients back into the water column that can further support algal biomass production.

WASP 7.5X uses the same model grid as that for EFDC with the same boundary loading cells. Water quality loads measured at the Basilone Bridge station were assigned at the upstream boundary for the WASP 7.5X model. Figure 3-4 and Figure 3-5 show the time series of the loads of four nitrogen variables, including ammonia, nitrate, dissolved organic nitrogen and particulate nitrogen, and two major phosphorous variables, including inorganic-P and particulate-P, respectively. The loading data were processed as daily loads based on the raw data measured at the ME station. Figure 3-6 shows the groundwater nutrient loads of nitrogen and phosphorous from the watershed and the agricultural field. Groundwater nitrogen load from the watershed was based on the groundwater model by Stetson, Inc. Groundwater nitrogen and phosphorous loads from the agricultural field were adjusted (calibrated) based on the data measured by SSC Pacific in 2010, which were used for 2008–2009 simulations. Phosphorous load from the groundwater of the watershed was obtained by calibration.

3.2 RESULTS AND DISCUSSION OF EUTROPHICATION MODEL

Simulations were conducted during January 1, 2007, and December 23, 2009. Simulated time series were produced for nutrient concentrations, DO, and macroalgal biomass. Model/data comparisons were conducted for nitrate, inorganic nitrogen and total nitrogen, inorganic phosphorous, and total phosphorous for 2008, dissolved oxygen for 2009, and macroalgal biomass for 2008–2009. Model-predicted fluxes of DO, inorganic nitrogen, and inorganic phosphorous were also compared with measured data.

Table 3-2 through Table 3-6 contain the names and values of the parameters for the kinetics of nutrients, sediment diagenesis, light, macroalgae, and phytoplankton used in the water quality model.

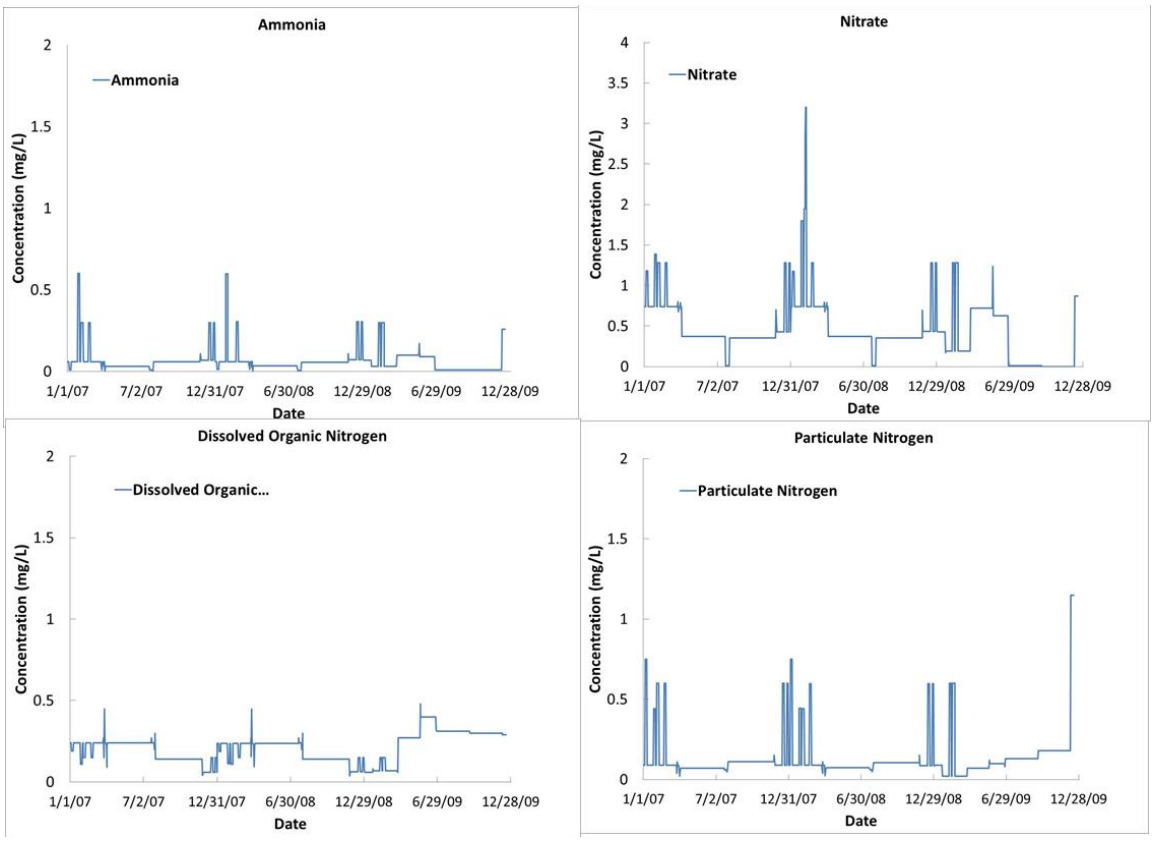

Figure 3-4. Loading concentrations of nitrogen loads of ammonia, nitrate, dissolved organic nitrogen and particulate-N measured at ME station.

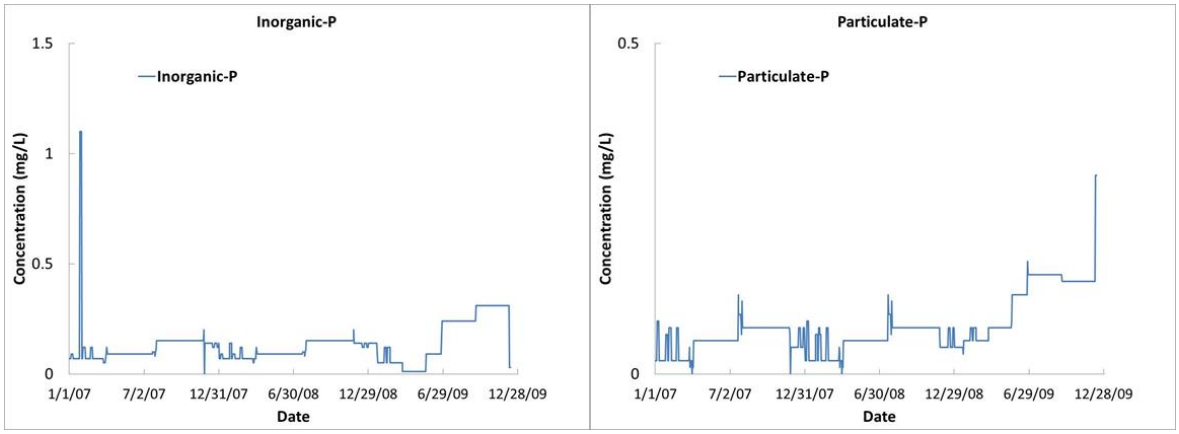

Figure 3-5. Loading concentrations of phosphorous loads of inorganic-P and particulate-P measured at ME station.

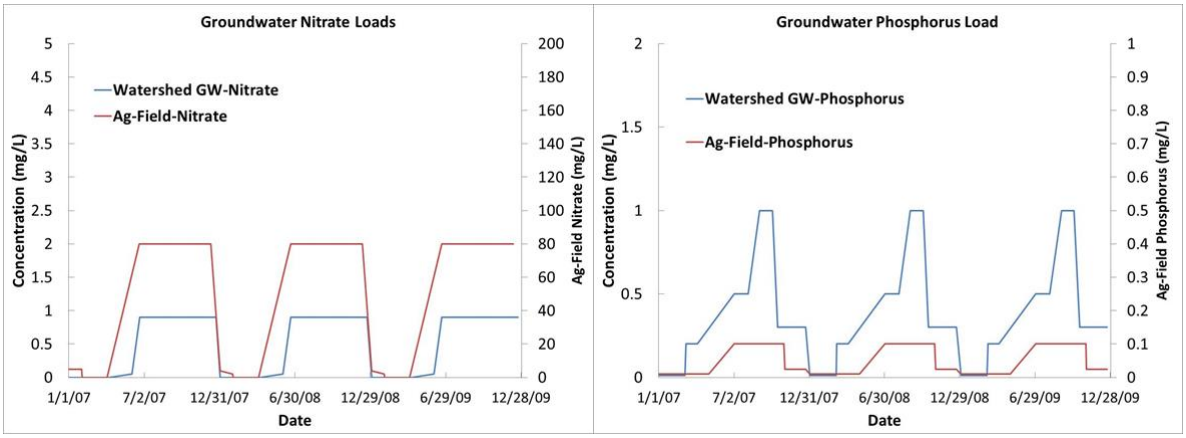

Figure 3-6. Loading concentrations of nitrogen loads (left) and phosphorous loads (right) from groundwater from the watershed and the agricultural field (Ag-Field).

Table 3-2. WASP model parameters and values for nutrient kinetics.

Nutrients	Values
Nitrification rate constant @20 ^{o}C (1/day)	0.08
Nitrification temperature coefficient	1.08
Half saturation constant for nitrification oxygen limit (mg O_2/L)	2.0
Denitrification rate constant @20 ^{o}C (1/day)	0.09
Denitrification temperature coefficient	1.04
Half saturation constant for denitrification oxygen limit (mg O_2/L)	0
Detritus dissolution rate (1/day)	0.3
Temperature correction for detritus dissolution	1.04
Dissolved organic nitrogen mineralization rate constant @20 ^{o}C (1/day)	0.1
Dissolved organic nitrogen mineralization temperature coefficient	1.07
Dissolved organic phosphorous mineralization rate constant @20 ^{o}C (1/day)	0.27
Dissolved organic phosphorous mineralization temperature coefficient	1.07
CBOD(1) decay rate constant @20 ^{o}C (1/day)	0.2
CBOD(1) decay rate temperature correction coefficient	1.04
CBOD(1) half saturation oxygen limit (mg O_2/L)	0.5
Fraction of detritus dissolution to CBOD(1)	1.0
Reaeration option (sums wind and hydraulic Ka	1.0
Calculation reaeration option (0 = Covar; 2 = Owens; 3 = Churchill; 4 = Tsivoglou)	1.0
Maximum allowable calculate reaeration rate, per day	5.0
Use total depth of water column for reaeration	1.0

Table 3-3. WASP model parameters and values for sediment diagenesis kinetics.

Sediment Diagenesis Processes	Values
Activate Sediment Diagenesis Model (1 = On, 0 = Off)	1
Determines if a steady-state calculation sets initial conditions (1 = No,0 = Yes)	1
1 = Write Restart File (SOD_IC.OUT)	1
Maximum error for testing convergence of the steady-state solute	0.001
Maximum number of iterations of steady-state solution	1000
Salinity concentration (ppt) for determining whether methane or sulfide SOD	1.0
Determines whether fresh or saltwater nitrification/denitrification rates	1
Solids concentration in Layer 1 kg/L	0.5
Solids concentration in Layer 2 kg/L	0.5
Diffusion coefficient between layers 1 and 2 (m^2/day)	0.0025
Temperature coefficient for Dd	1.08
Thickness of active sediment layer cm	0.1
Burial velocity for Layer 2 to inactive sediments (m/day)(0.00000685)	6.85E-06
Diffusion coefficient for particle mixing (m2/day)	6.00E-05
Temperature coefficient for Dp	1.117
Reference POC (O2 EQ. = 0.*2.67) measurement for particle mixing	0.2667
Decay constant for benthic stress (1/day)	0.03
Particle mixing half-saturation constant for oxygen (gO_2/m^3)	4.0
Nitrogen constants: fraction PON to G1	0.65
Fraction PON to G2	0.15
Diagenesis rate for PON G1	0.035
Temperature coefficient for diagenesis of PON G1	1.1
Diagenesis rate for PON G2	0.0018
Temperature coefficient for diagenesis of PON G2	1.15
Diagenesis rate for PON G3	0.0
Temperature coefficient for diagenesis of PON G3	1.17
Freshwater nitrification reaction velocity (m/day)	0.1313
Saltwater nitrification reaction velocity (m/day)	0.1313
Temperature coefficient for nitrification	1.123
Half-saturation coefficient for ammonia in the nitrification reaction (mg/L)	0.728
Half-saturation coefficient for oxygen in the nitrification reaction (mg/L)	0.37
2nd step reaction velocity for nitrification (NO^2 to NO^3) (m/day)	100
Temperature coefficient for second step reaction velocity	1.123
Half-saturation coefficient for oxygen in the second reaction step (mg O^2/L)	0.37
Freshwater denitrification reaction velocity in Layer 1(m/day)	0.1
Saltwater denitrification reaction velocity in Layer 1 (m/day)	0.1

Table 3-3. WASP model parameters and values for sediment diagenesis kinetics. (continued)

Sediment Diagenesis Processes	Values
Temperature coefficient for denitrification	1.08
Denitrification reaction velocity in Layer 2 (m/day)	0.25
Nitrogen partition coefficient (L/kg)	1.0
Phosphorous: Fraction POP to G1	0.65
Phosphorous: Fraction POP to G2	0.2
Diagnesis rate for POP G1	0.035
Temperature coefficient for diagenesis of POP G1	1.1
Diagnesis rate for POP G2	0.0018
Temperature coefficient for diagenesis of POP G2	1.15
Diagnesis rate for POP G3	0.0
Temperature coefficient for diagenesis of POP G3	1.17
Phosphorous partition coefficient in layer 2 (L/kg)	20
Incremental freshwater partition coefficient in Layer 1	20
Incremental saltwater partition coefficient in Layer 1	20
Critical oxygen concentration in Layer 1 incremental phosphate sorption (mgO_2/L)	2
Carbon Constants: Fraction CBODu to G1	0.65
Fraction CBODu to G2	0.2
Diagnesis rate for CBODu G1	0.035
Temperature coefficient for diagenesis of CBODu G1	1.1
Diagnesis rate for CBODu G2	0.0018
Temperature coefficient for diagenesis of CBODu G2	1.15
Diagnesis rate for CBODu G3	0.0
Temperature coefficient for diagenesis of CBODu G3	1.17
Methane oxidation reaction velocity (m/day)	0.7
Temperature coefficient for methane oxidation	1.079
Half-saturation coefficient for oxygen in oxidation of methane (mg/L)	0.37
Reaction velocity for dissolved sulfide oxidation in Layer 1 (m/day)	0.2
Reaction velocity for particulate sulfide oxidation in Layer 1 (m/day)	0.4
Temperature coefficient for sulfide oxidation	1.079
Sulfide oxidation normalization constant (mg/L)	4.0
Sulfide partition coefficient in Layer 1 (L/kg)	100
Sulfide partition coefficient in Layer 2 (L/kg)	100
Algae Constants: Fraction settled algae to G1	0.65
Fraction settled algae to G2	0.2
Dissolution Rate of particulate biogenic silica at 20 ^oC (1/day)	0.5
Temperature Effect on Silica Dissolution	1.1
Silica Saturation Concentration in Porewater (mg si/m^3)	4000.0

Table 3-3. WASP model parameters and values for sediment diagenesis kinetics. (continued)

Sediment Diagenesis Processes	Values
Incremental change (mult) for freshwater in partition coefficient Si as DO	10.0
Partition coefficient between dissolved/sorbed silica in Layer 2	100.0
Critical oxygen concentration for silica sorption	1.0

Table 3-4. WASP model parameters and values for light kinetics.

Light	Values
Light option (1 uses input light; 2 uses calculated diel light)	1
Background light extinction coefficient (1/m)	0.4
Detritus and solids light extinction multiplier	0.3
DOC light extinction multiplier (values below modify global value)	0.05

Table 3-5. WASP model parameters and values for macroalgal kinetics.

Macroalgae	Values
If = 1, then floating forms, transported (QBY, RBY = 0); if = 2, then submersed form	1
Macroalgae transport drag fraction (0 to 1)	1.0
MacroAlgae D:C ratio (mg D/mg C)	4.5
MacroAlgae N:C ratio (mg N/mg C)	0.08
MacroAlgae O_2: C production (mg O_2/mg C)	2.69
Macroalgal self-shading coefficient (m^3m^{-1} g-dw^{-1})	0.02
Macroalgal bed height (m, used if MacAlg_SYS = 2)	0.5
MacroAlgae P: C ratio (mg P/mg C)	0.011
MacroAlgae Chl a: C Ratio (mg Chl/mg C)	0.025
MacroAlgal growth model, 0 = Zero Order; 1 = First Order MacroAlgal Growth Model	1
MacroAlgae maximal growth rate (gDW/m^2-day, or 1/day)	7
If = 1, then use theta formulation; if = 2, then use optimal formulation	2
Temperature coefficient for macroalgal growth	1.07
Optimal temperature for macroalgal growth (^oC)	31.5
Shape parameter for below optimal temperatures for macroalgae	0.02
Shape parameter for above optimal temperatures for macroalgae	0.07
Macroalgal carrying capacity for first-order model (gDW/m^2)	300
Macroalgal respiration rate constant (1/day)	0.23
Temperature coefficient for macroalgal respiration	1.07
Internal nutrient excretion rate constant for macroalgae (1/day)	0.09
Temperature coefficient for macroalgal nutrient excretion	1.07
Macroalgae death rate constant (1/day)	0.05

Table 3-5. WASP model parameters and values for macroalgal kinetics. (continued)

Macroalgae	Values
Temperature coefficient for macroalgal death	1.07
Macroalgal half saturation uptake constant for extracellular phosphorous (mg P/L	0.001
Macroalgal light constant for growth (langleys/day)	1100
Macroalgae ammonia preference (mg N/L)	0.025
Minimum cell quota of internal nitrogen for macroalgal growth (mgN/gDW)	7.2
Minimum cell quota of internal phosphorous for macroalgal growth (mgP/gDW)	1.0
Maximum nitrogen uptake rate for macroalgae (mgN/gDW-day)	720.0
Maximum phosphorous uptake rate for macroalgae (mgP/gDW-day)	50.0
Half saturation uptake constant for macroalgal intracellular nitrogen (mgN/gDW)	9.0
Half saturation uptake constant for macroalgal intracellular phosphorous (mgP/gD)	1.3
Detachment critical shear stress	1.0

Table 3-6. WASP model parameters and values for phytoplankton kinetics.

Phytoplankton	Values
Phytoplankton detritus to carbon ratio for Group 1 (mg D/mg C)	3.5
Phytoplankton nitrogen to carbon ratio for Group 1 (mg N/mg C)	0.15
Phytoplankton phosphorous to carbon ratio for Group (mg P/mg C)	0.009
Phytoplankton carbon to chlorophyll ratio for Group (mg C/mg Chl)	100.0
Phytoplankton maximum growth rate constant @20 ^{o}C for Group 1 (1/day)	1.7
Phytoplankton growth temperature coefficient for Group 1	1.07
Optimal temperature for growth for Group 1 (^{o}C)	25.0
Shape parameter for below optimal temperatures for Group 1	0.02
Shape parameter for above optimal temperatures for Group 1	0.07
Phytoplankton respiration rate constant @20 ^{o}C for Group 1 (1/day)	0.3
Phytoplankton respiration temperature coefficient for Group 1	1.07
Phytoplankton death rate constant (non-zoo predation) for Group 1 (1/day)	0.05
Phytoplankton half-saturation constant for N uptake for Group 1 (mg N/L)	0.01
Phytoplankton half-saturation constant for P uptake for Group 1 (mg P/L)	0.001
Phytoplankton optimal light saturation for Group 1 (Ly/day)	340.0

Results of model/data comparison are quantified with statistics and correlation coefficients for nutrients (nitrogen and phosphorous), dissolved oxygen and macroalgal biomass, and sediment fluxes.

3.2.1 Nitrogen

Nutrient loads enter the study domain from the upstream boundary (ME station) from the surface and groundwater inflow and from the agricultural field groundwater inflow. Upon entering the lagoon, these nutrient loads interact with the macroalgal cycle, sediment diagenesis cycle, and

dissolved oxygen dynamics (Figure 3-1). The in-lagoon nutrient data that were measured during the four index periods and transect surveys during 2008 (Table 3-1) were compared with the model results. Table 3-7 contains the summary of model/data correlation results.

Table 3-7. Summary of mode/data comparison results for nitrate, inorganic-N and total-N for 2008.

Model	Model/Data Correlation		Model/data relative magnitude
	Correlation	R^2	
Nitrate	Model = 0.96*Data+0.057	0.94	Model/data match, no apparent over/under prediction
Inorganic-N	Model = 1.08*data+0.037	0.90	Model over-predicted
Total-N	Model = 1.06*Data+0.250	0.91	Model over-predicted

Figure 3-7 shows the model/data comparison for nitrate among the 12 axial transect stations and the three locations which include Ocean Inlet (Figure 3-1), Segment 2, and Segment 1 during the four index periods of 2008. The one or two data points at each transect station contrasts with the one to eight data points at each of the three fixed sampling stations (stations 13 through 15). Model results and measured data are plotted as bar charts for each station during the four index periods (top in Figure 3-7). The figure shows that, with the exception of Segment 1, predicted nitrate concentrations follow the same trends as those of measured values.

During 2008, in-lagoon nitrate had the highest concentrations during the Index-1 period, followed by the Index-2 period. Nitrate concentrations were lowest during the Index-3 and Index-4 periods. Model/data mismatch at Segment 1 was consistent throughout the four index periods of 2008. For example, a nitrate concentration of ~2 mg/L at Segment 1 was predicted by the model, compared to the measured value of over 10 mg/L for the Index-1 period. For the Index-2 period, the model predicted that a nitrate concentration of 0.5 mg/L, whereas measured data exceeds 7 mg/L at Segment 1. As to be discussed later, such model/data mismatch at Segment 1 is consistent with the results of other water quality parameters. Therefore, results at Segment 1 were excluded for model/data correlation analysis and comparison of spatially averaged concentrations.

For each index period, model/data comparisons were conducted for spatially averaged concentrations over the 14 stations (bottom left of Figure 3-7). A linear correlation was also developed using the model/data for all the 14 stations during 2008 (bottom right of Figure 3-7). Overall, the figure shows close model/data correlation, with a slope of 0.96 for model versus data ($R^2 = 0.94$), with no significant over- or under-prediction by the model.

Figure 3-8 shows the time series of model-simulated concentrations of inorganic-N and the field data measured at the 15 stations during the four index periods of 2008. Overall, the lagoon exhibited responsiveness to varying loads of the wet weather and the dry weather. The figure shows that inorganic-N concentrations reached 0.5–3.0 mg/L during wet weather and was reduced to less than 0.05 mg/L during dry weather. These temporal variations were reflected by both the model results and field data. Most of the 47 field data points measured at the Ocean Inlet compared well with the model results. The overall relative errors were less than 40%, or 0.2 mg/L, except two data points. On April 2 at 4:30 p.m., the model predicted a concentration of 0.27 mg/L, compared with the field data value of 1.15 mg/L. On July 21 at 3:55 p.m., the model predicted a concentration of 0.19 mg/L. whereas the measured field data was 1.59 mg/L (Figure 3-9).

Similar to the model/data mismatch of nitrate concentration at Segment 1, the largest model/data mismatch of inorganic-N concentrations also occurred at Segment 1 during the Index-1 and Index-2

periods, and less for the other two periods. During the first two periods, model results were in the range of less than 2.7 mg/L, whereas multiple measured data had values up to 37 mg/L and 27 mg/L for the Index-1 period and Index-2 period, respectively. Such large magnitudes of model/data mismatch are uncharacteristic of the model/data patterns, which exhibited consistent results for the other 14 stations throughout 2008. Again, results of Segment 1 were excluded from further statistical analysis.

Figure 3-10 shows the linear model/data correlation for inorganic-N concentrations, which has a slope of 1.08 for model versus data ($R^2 = 0.90$), with slight over-prediction by the model toward larger concentrations.

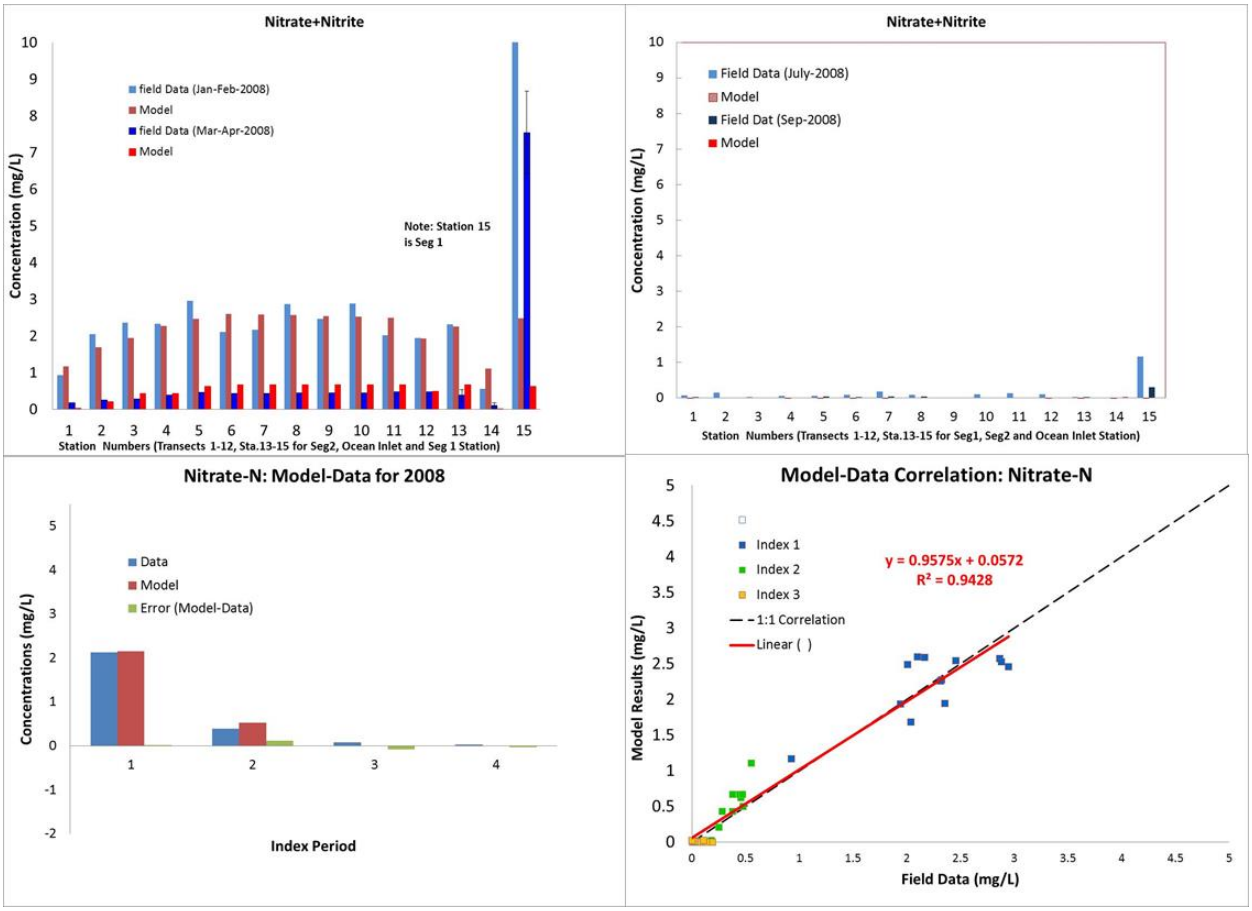

Figure 3-7. Model/data comparison for nitrate concentrations with bar charts at the 15 stations for the four index periods (top), spatially averaged model/data (bottom left) and model/data correlation (number of field data = 56, bottom right).

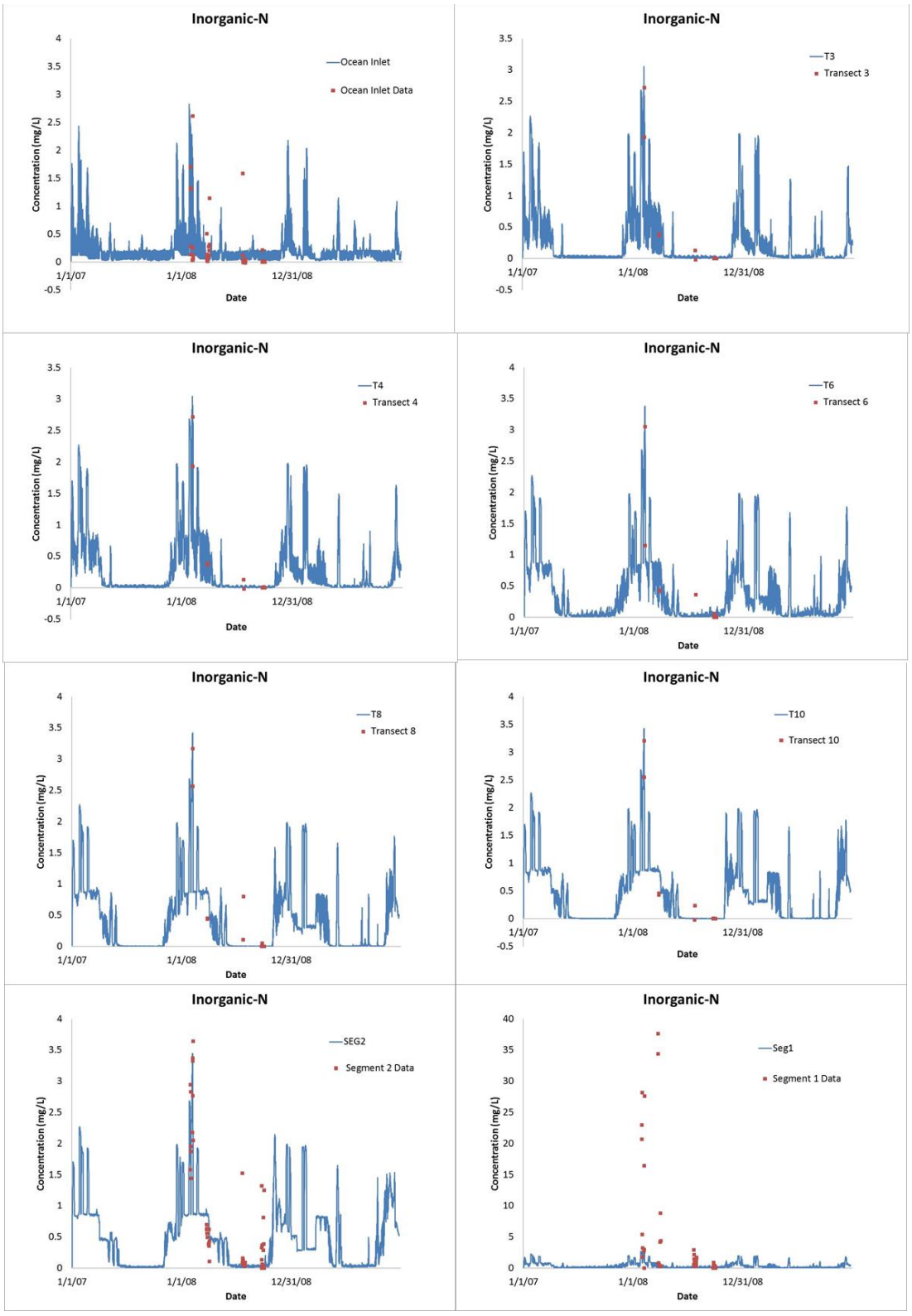

Figure 3-8. Time series of simulated and measured inorganic-N for stations from Ocean Inlet upstream the lagoon to Segment 2 and Segment 1 (bottom right).

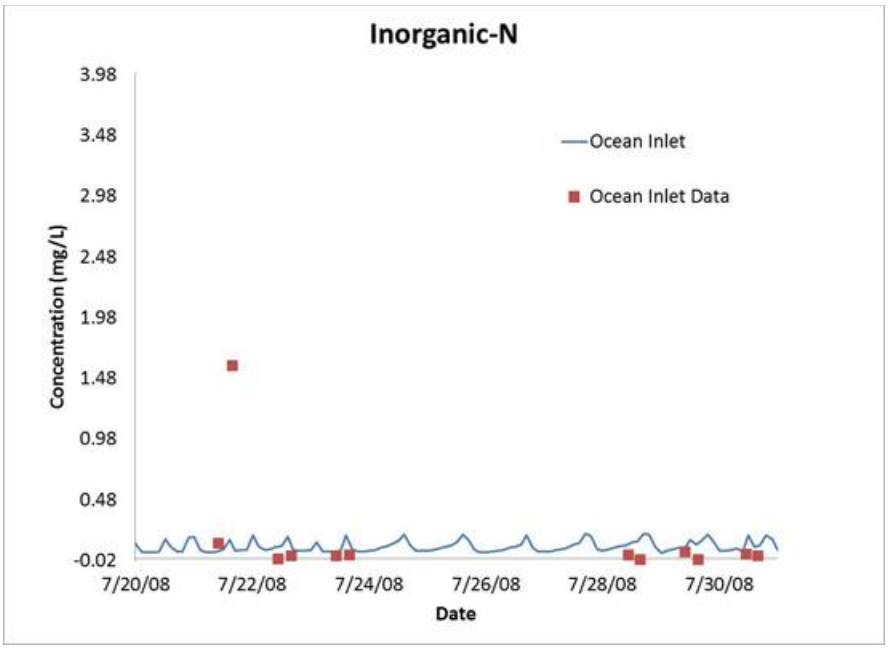

Figure 3-9. Model/data comparison for inorganic-N during the Index-3 period (note the uniquely large value of 1.586 mg/L of field data versus the rest of the data points and model results).

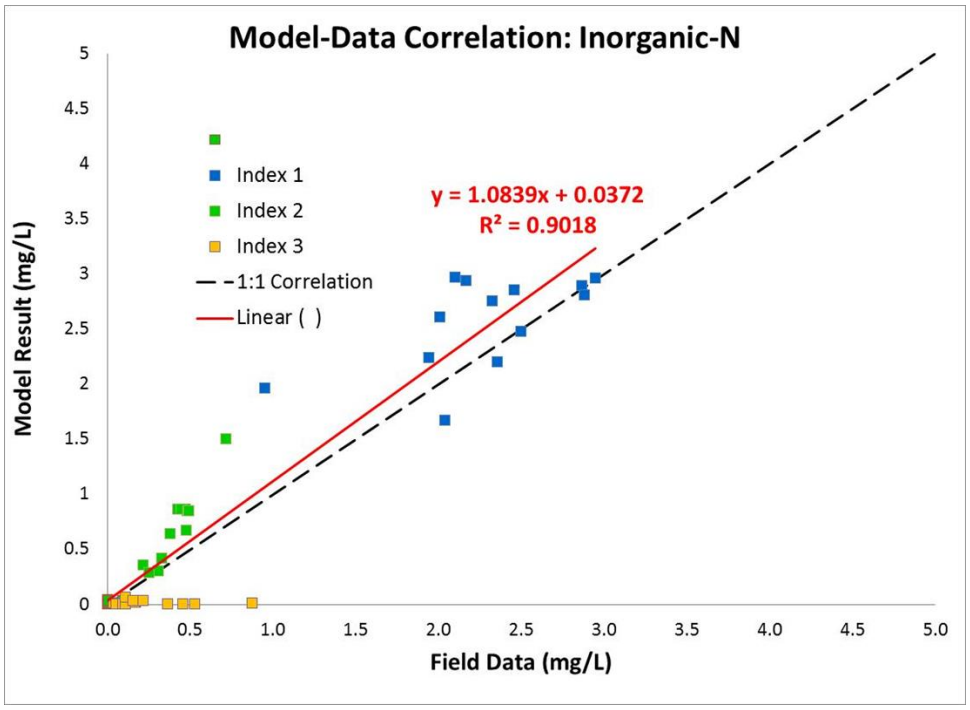

Figure 3-10. Linear model/data correlation for inorganic-N (number of field data = 56).

Figure 3-11 shows model/data comparison for total-N at the 15 stations during the four index periods of 2008. Data at each of the axial transect stations included only one or two data points, whereas each of the three stations (stations 13 through 15) has 1 to 8 data points. The bar-charts show that predicted total-N concentrations followed the same trends as those of measurements, except at Segment 1, which exhibited persistent mismatch between the model and the field data. During 2008,

in-lagoon total-N had the highest concentrations during the Index-1 period, followed by the Index-2 period. Unlike the results of nitrate and in-organic-N, total-N concentrations retained relative low values (less than 1 mg/L), which presumably were in the forms of organic-N during the Index 3 and 4 periods. The model/data mismatch at Segment 1 was consistent throughout the four index periods of 2008, with the model/data mismatch distinctively high during the Index-1 and Index-2 periods. For example, a total-N concentration of ~3.4 mg/L and 1.1 mg/L at Segment 1 were predicted by the model, compared to the measured value of 37.2 mg/L and 7.8 mg/L for Index-1 and Index-2 periods, respectively. As discussed previously, such model/data mismatch was persistent with the results of other nitrogen parameters, including nitrate and inorganic-N. Once again, results of Segment 1were excluded from further statistical analysis. Figure 3-11 also shows the model/data of spatially averaged over the 14 stations for each of the four Index periods (bottom left) and the model/data correlation for all the data at the 14 stations during the four index periods (bottom right).

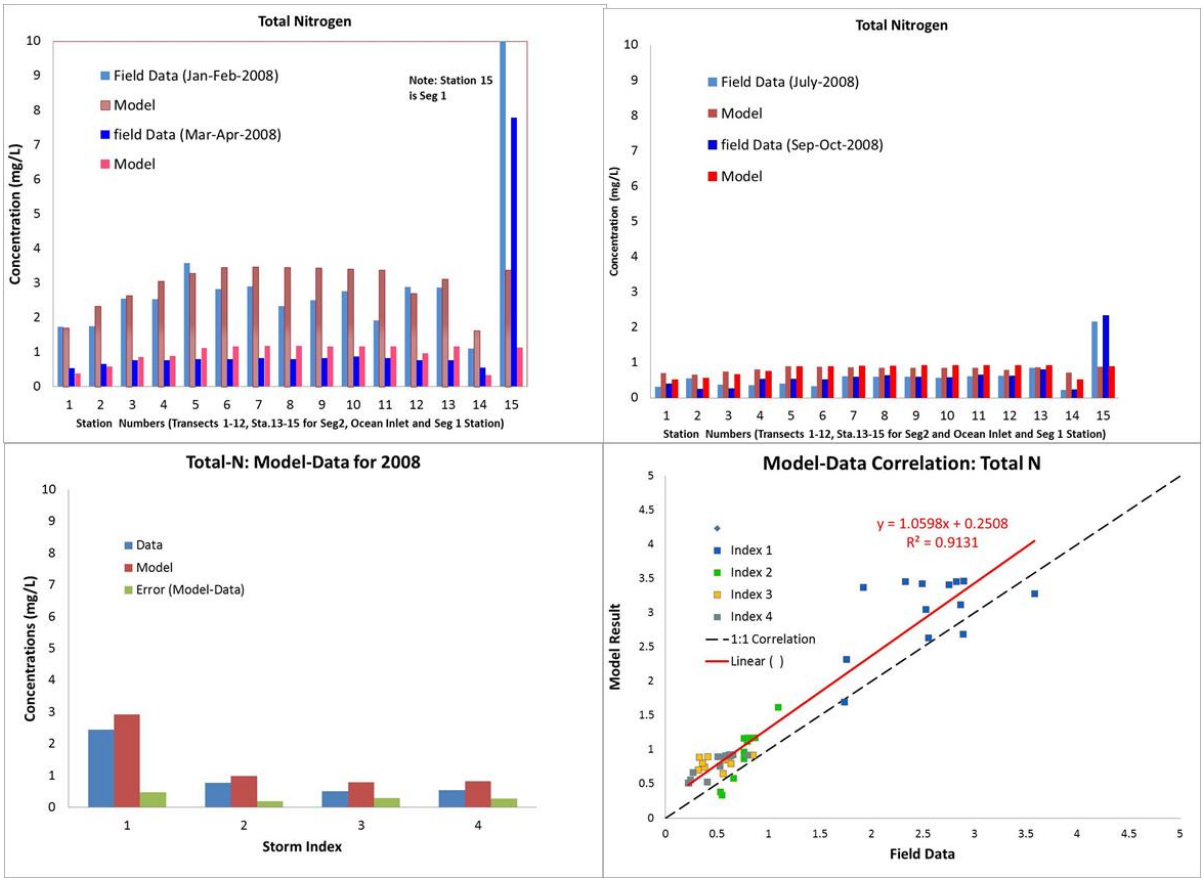

Figure 3-11. Model/data comparison for total-N concentrations with bar charts at the 15 stations for the four index periods (top), spatially averaged model/data (bottom left) and model/data correlation (number of field data = 56, bottom right).

Overall, the figure shows a model/data linear correlation with a slope of 1.06 for model versus data ($R^2 = 0.91$) with over-prediction by the model throughout the concentration ranges. Further discussion can be found later in the report.

3.2.2 Phosphorous

Phosphorous loads entered the lagoon from the upstream boundary (Basilone Bridge Station) as surface and groundwater flow and as groundwater from the agricultural field As boundary conditions, they were identified by the various forms including ortho-phosphorous (inorganic-P), dissolved- and particulate organic-P. Upon entering the lagoon, these nutrient loads interact with the macroalgal cycle, DO dynamics and sediment diagenesis cycle (Figure 3-1). Model results were compared with measured data and Table 3-8 contains summary of the model/data correlation results.

Table 3-8. Summary of mode/data comparison results for inorganic-P and total-P for 2008.

Model	Model/Data Correlation		Model/data relative magnitude
	Correlation	R^2	
Inorganic-P	Model = 0.855*data+0.031	0.76	Model over-predict for [C] < 0.16 mg/L Model under-predict for [C] > 0.16 mg/L
Total-P	Model = 0.69*Data+0.08	0.81	Model over-predict for [C] < 0.24 mg/L Model under-predict for [C] > 0.24 mg/L

Figure 3-12 shows the time series of model-simulated concentrations of inorganic-P and the corresponding field data measured at the 15 surface water stations during the four index periods of 2008. Overall, model results were in agreement with the measurements during both the wet and dry weather throughout the entire lagoon. During spring, January to April, inorganic-P was more evenly distributed over the lagoon, whereas during the summer and fall, July to October, inorganic-P concentrations exhibited an increasing trend from Ocean Inlet toward the upstream segments. In addition, inorganic-P also exhibited an increasing trend from the spring (Index 1 and 2 periods) toward the summer and the fall (Index 3 and 4 periods). These temporal trends of phosphorous were opposite to the trends of nitrogen, including nitrate, inorganic-N and total-N, which exhibited decreasing trends from the spring to the summer and the fall. These two different patterns between nitrogen and phosphorous may have further implication about the loading sources during different times of the year.

At Segment 1, model/data of phosphorous had a better match, in contrast to the model/data mismatch for nitrogen. It is unclear why model/data match at Segment 1 was good for phosphorous, but not for nitrogen. Further studies would be needed to assess this more.

Figure 3-13 shows the model/data linear correlation for inorganic-P with a slope of 0.86 for model versus data ($R^2 = 0.76$). Model results were over-predicted for concentrations less than 0.16 mg/L and under-predicted for concentrations greater than 0.16 mg/L.

Figure 3-14 shows the model/data comparison for total-P, which is similar to that of inorganic-P. Therefore, the discussion and conclusions about the inorganic-P results and the model/data comparison also apply to total-P. Once again, compared to the results of nitrogen, model and data have a closer match at Segment 1 for total-P (and inorganic-P, discussed above). Overall, the figure shows a model/data correlation with a slope of 0.86 for model versus data ($R^2 = 0.76$). Model results are over-predicted for concentration less than 0.24 mg/L and under-predicted for concentrations greater than 0.24 mg/L.

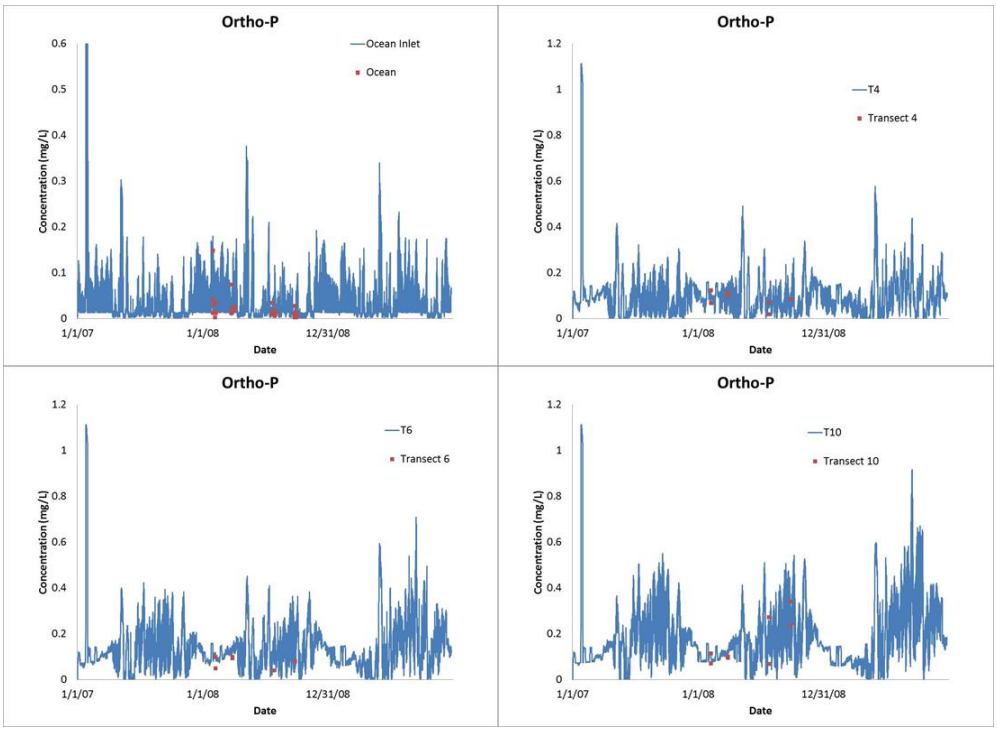

Figure 3-12. Time series of simulated and measured inorganic-P for stations from Ocean Inlet toward upstream of the lagoon.

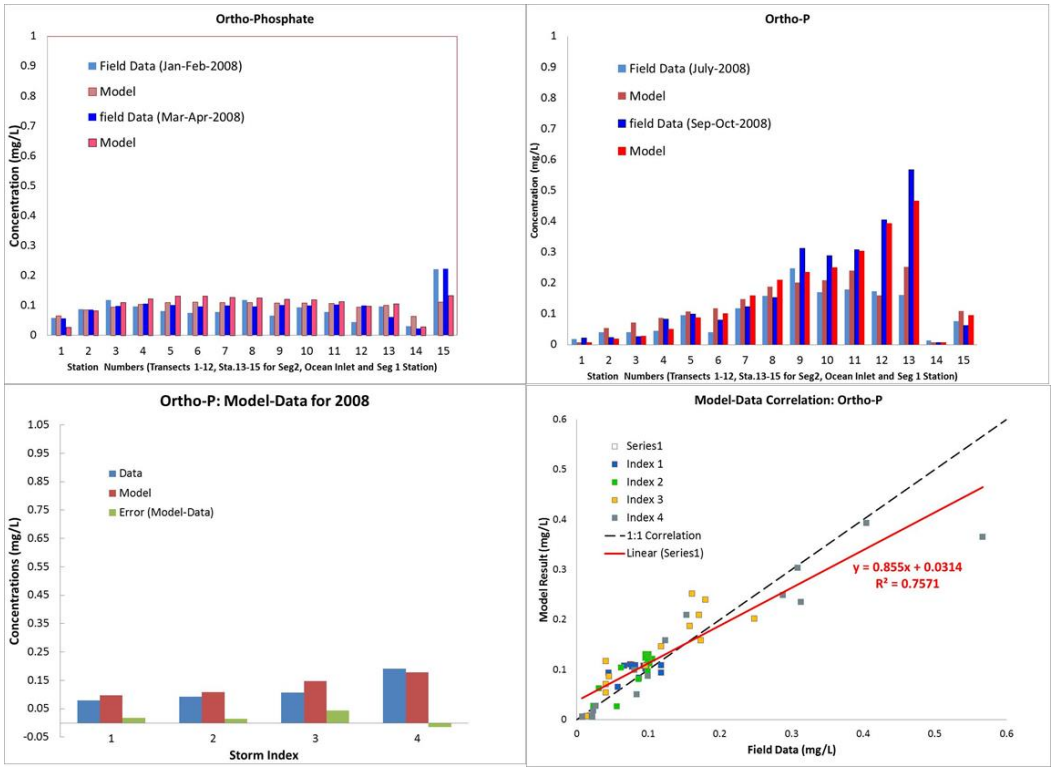

Figure 3-13. Model/data comparison for inorganic-P concentrations with bar charts at the 15 stations for the four index periods (top), spatially averaged model/data (bottom left) and model/data correlation (number of field data = 56, bottom right).

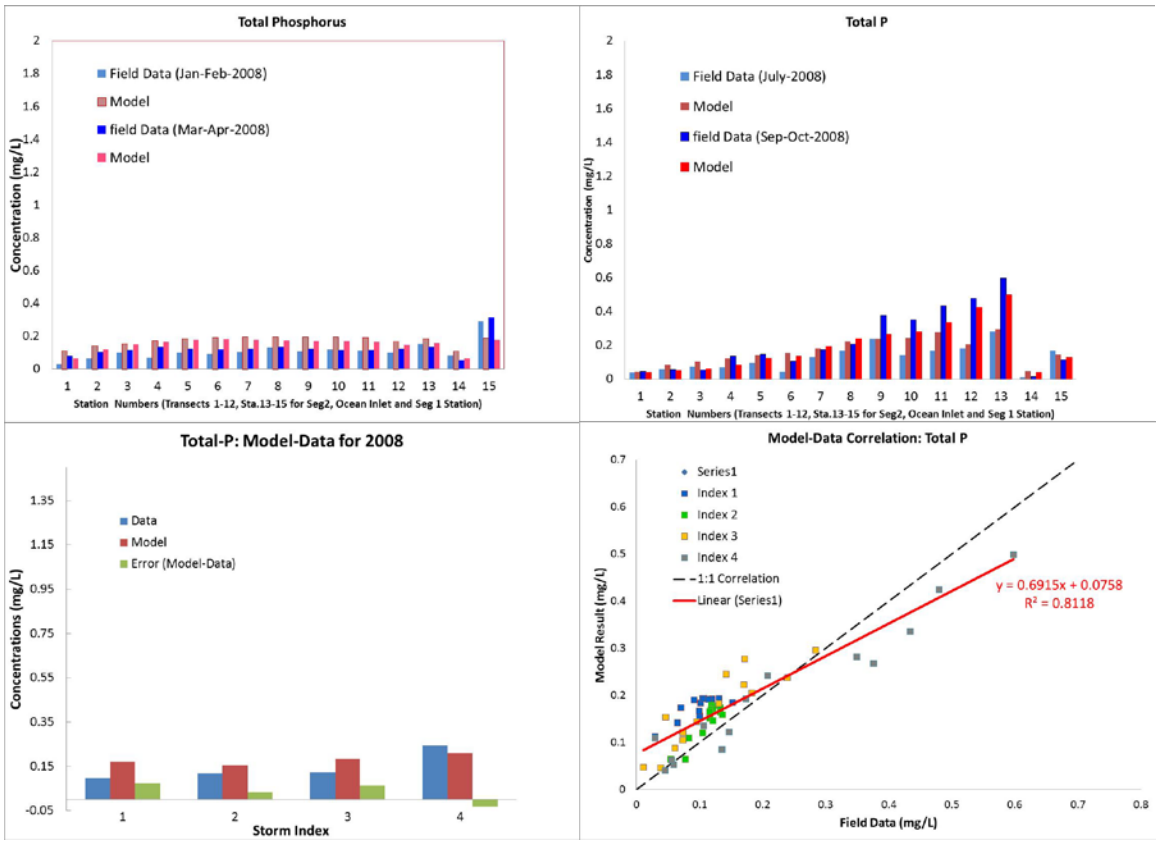

Figure 3-14. Model/data comparison for total-P concentrations with bar charts at the 15 stations for the four index periods (top), spatially averaged model/data (bottom left) and model/data correlation (number of field data=56, bottom right).

3.2.3 Dissolved Oxygen

Overall, the dissolved oxygen simulations show that the model was generally able to capture both the mean daily value as well as the magnitude of the diurnal variation. Table 3-9 shows 273 days over the three periods when the dissolved oxygen sensor successfully collected data: January 1 to March 8, April 14 to September 23, and September 30 to November 13. The model could capture both the mean and diurnal variation during Periods 2 and 3. For Period 1, the model predicted DO concentrations matched only the daily mean value, but produced diurnal variation with amplitudes of 0.5–1.0 mg/L compared to amplitudes of up to 5 mg/L observed in the field data.

Table 3-9. Periods for dissolved oxygen measurement near HWY 5 Bridge for 2009.

Time Period	DO Sensor/Data	Days with Data (Missing Days)
1/1 to 3/8	Yes (Period 1)	67
3/8 to 4/14	No data	(37)
4/14 to 9/23	Yes (Period 2)	162
9/23 to 9/30	No data	(7)
9/30 to 11/13	Yes (Period 3)	44

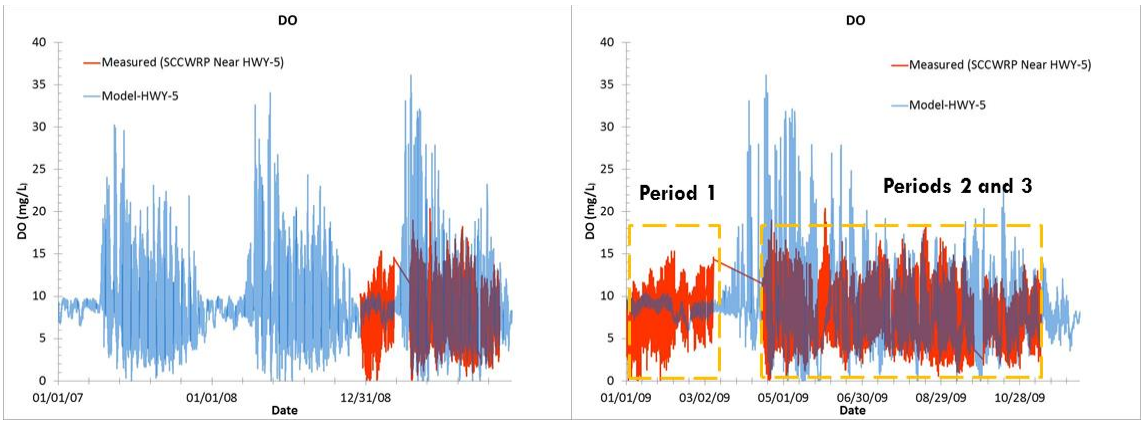

Figure 3-15. Model/data comparison for dissolved oxygen concentrations at Segment 1 (near HWY 5 Bridge) for 2009.

Figure 3-16 and Table 3-10 show the model/data comparison for the cumulative probabilities for DO concentrations. The model predicted an occurrence of DO less than 3 mg/L for 5.9% of the data, compared to 6% measured by the field data. Cumulative probabilities deduced by the model start to diverge and under-predict values from those of the field data as DO concentrations increase above 3 mg/L. For DO concentrations less than 5 mg/L, a potential critical metric, field data have a cumulative probability of 26.6%, whereas the model predicts a probability of 20.5%, an under-prediction.

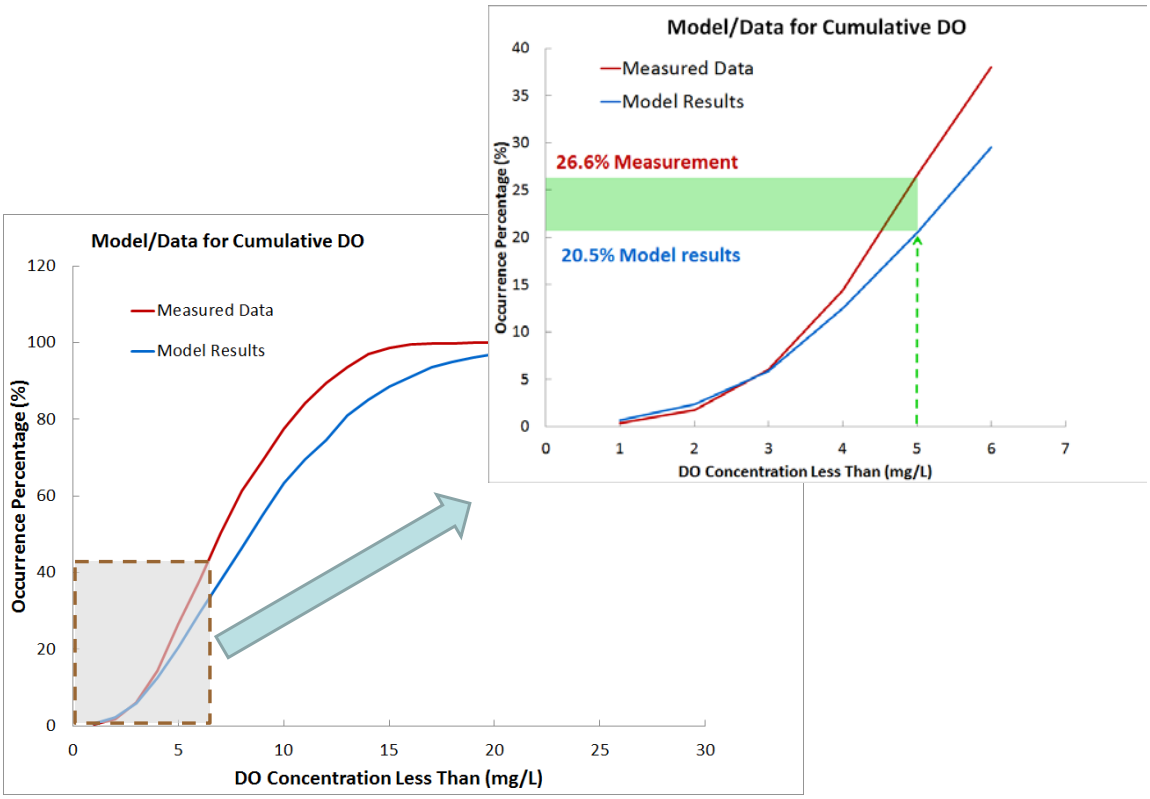

Figure 3-16. Cumulative probabilities of occurrence for simulated and measured dissolved oxygen concentrations.

Table 3-10. Cumulative probabilities of measured and simulated DO.

DO (mg/L) and Less	Field Data (%)	Model Results (%)
1	0.3	0.7
2	1.7	2.3
3	6.0	5.9
4	14.4	12.5
5	26.6	20.5
6	38.0	29.5
7	50.4	38.0
9	69.4	55.2
11	84.3	69.5
13	93.7	81.0
15	98.7	88.6
17	99.8	93.5
20	100	97.0
25	100	99.3

In general, eutrophication of a waterbody is characterized by excessively large amplitude of diurnal variations in dissolved oxygen Such diurnal variation of dissolved oxygen is illustrated by Figure 3-17, which shows the model/data comparison during two 1-month periods, July 26 to August 28 and October 18 to November 14. During daytime, photosynthesis of macroalgae (and other primary producers such as planktonic and benthic algae) produces DO, and the water column can be enriched with oxygen, and during nighttime, respiration of macroalgae becomes a major sink for dissolved oxygen in the water column. When macroalgal biomass is in excess, enrichment in daytime and deficit in nighttime are intensified. While the model results matched the field data for the daily lows (nighttime), the model over-predicted the peak values during daytime. This over-prediction may be because the model has no process that allows oxygen to escape through the water surface to the atmosphere.

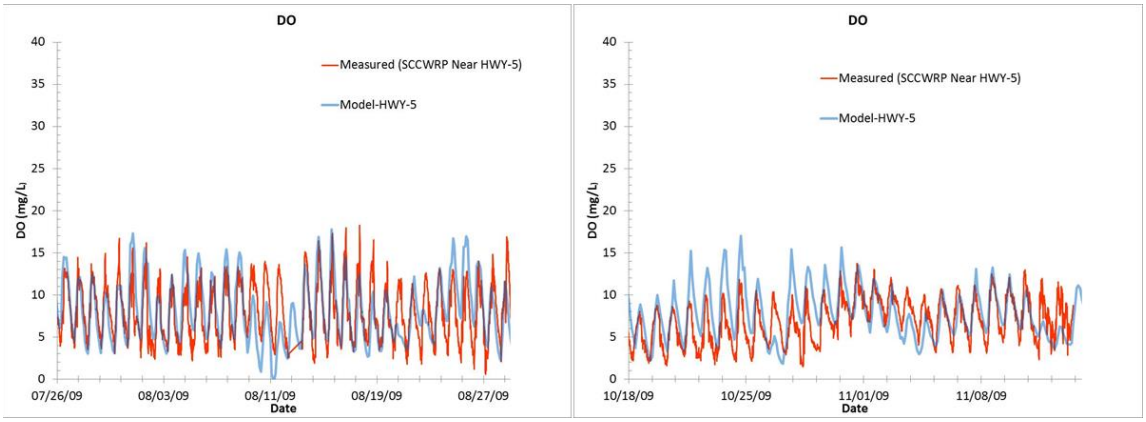

Figure 3-17. Diurnal variation during two 1-month periods for both model and field data.

Dissolved oxygen data collected at the USGS Station in Temecula was used as the upstream boundary condition for the model. The USGS Temecula station is the nearest location with year-long time series data, but it is 17 miles northeast of the upstream boundary of the study site. The stakeholder technical team questioned if it was appropriate to use data from a location so far upstream of the lagoon. We conducted an evaluation and sensitivity analysis of the boundary condition by evaluating more recent stream data collected by SCCWRP and varying the absolute value and the amplitude of the daily oscillation and determined that the differences in the boundary

value had no appreciable effect on the model predictions in the lagoon. After examination of the data it was determined that the choice of the upstream boundary value was less important than the processes occurring locally in the lagoon. This result is important because unlike nutrients that were governed by the watershed loads from the upstream boundary, in-lagoon dissolved oxygen concentration was primarily governed by the local condition.

Figure 3-18 shows the locations near the study domain where dissolved oxygen data were collected. In addition to the USGS data at Temecula, SCCWRP also measured DO with sparse data over the stretch of the Santa Margarita River (SMR1-SMR2) during four periods: January, April, May, and June of 2015. In addition, DO data were also measured at the Fallbrook Public Utility District (FPUD) sump near the city of Fallbrook for 2008.

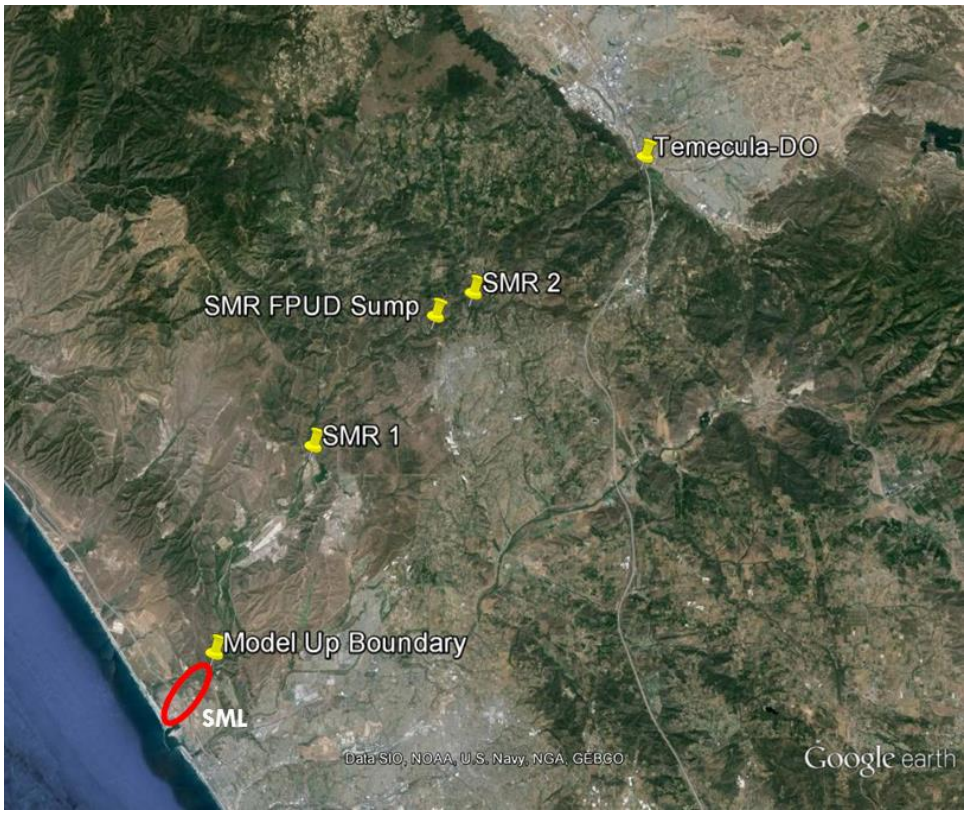

Figure 3-18. Locations of field data of dissolved oxygen, including USGS station at Temecula, Santa Margarita River (SMR1-SMR2), and FPUD sump.

Figure 3-19 shows dissolved oxygen concentrations measured at the FPUD sump compared with the data measured at the USGS Temecula station for 2008. USGS data at Temecula has several periods of missing data and linear interpolations were used to fill the data gaps. One would find it difficult to conclude that these two data sets bear significant similarities. First, the temporal trends of these two datasets show little resemblance with USGS data decreasing from January to March and then increasing sharply in June, followed by a relatively stable value throughout the rest of the year. However, the FPUD data exhibit a slowly decreasing trend from January to May, followed by a slowly increasing trend toward the end of the year. Compared to the USGS data at Temecula, data at the FPUD sump exhibits diurnal oscillations with magnitudes ranging from 5 to 8 mg/L for the daily high/low, which is significant since the FPUD sump is located closer to the model boundary than the Temecula station. These comparison results lead to the following questions: how is the eutrophic

condition (i.e., the dissolved oxygen) further downstream the Santa Margarita River and how should we specify dissolved oxygen at the model boundary, for which no specific data are available, and what is the impact of DO boundary condition to the in-lagoon DO?

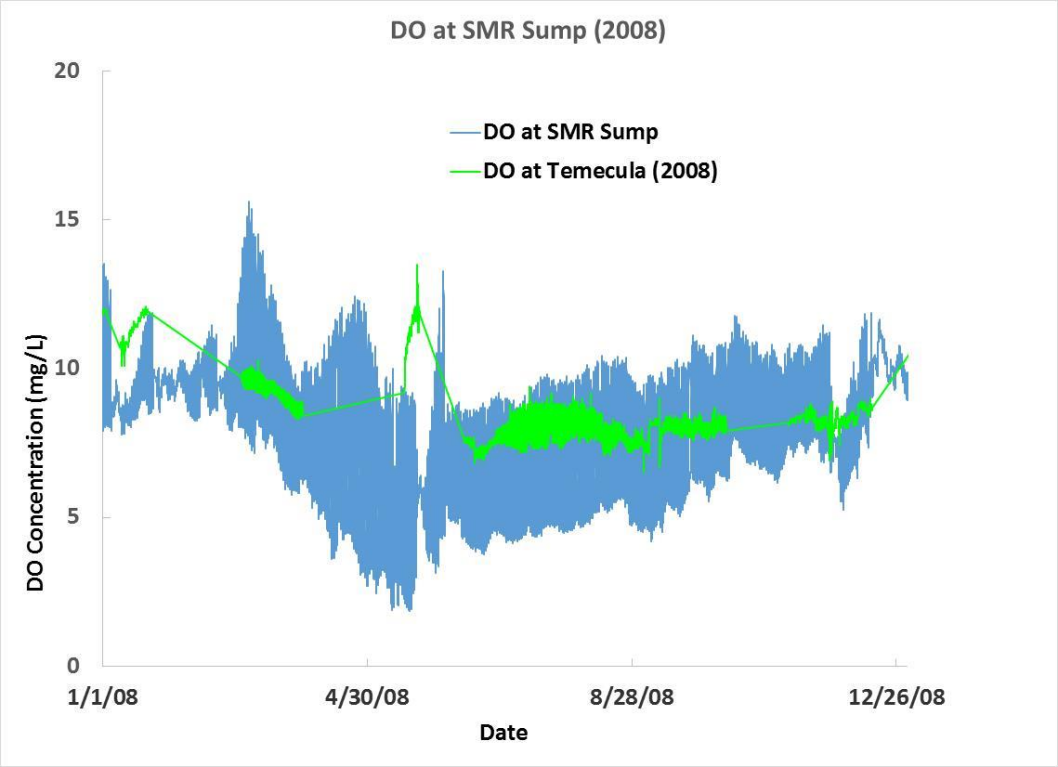

Figure 3-19. Dissolved oxygen concentrations measured at USGS station at Temecula and FPUD sump for 2008.

As part of the effort of knowing better about the eutrophic condition of the Santa Margarita estuaries, SCCWRP measured DO in the river during four periods from January to June 2015. In Figure 3-20, these data are plotted against the data measured at the USGS station at Temecula, which are plotted under the same 2015 date axis, knowing that data at Temecula are for 2008. Although each of the time series of the SCCWRP data are of short period, each ranging from 2 to 5 days, it shows that dissolved oxygen concentrations in the river were persistently lower than that of the USGS data at Temecula, by 1–8 mg/L. Meanwhile, dissolved oxygen concentrations at FPUD sump persistently exhibited diurnal oscillations with magnitudes ranging from 1–5 mg/L for the daily high/low, whereas the USGS data at Temecula exhibits little diurnal oscillation.

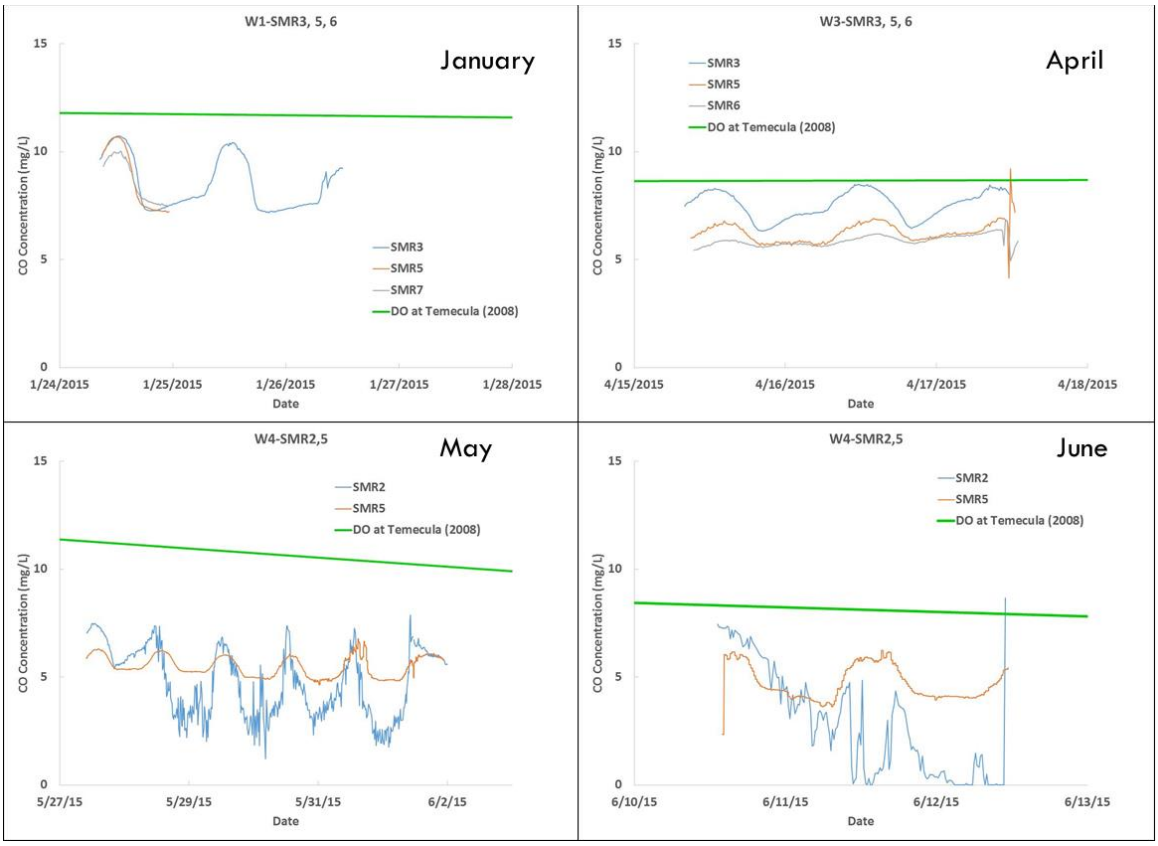

Figure 3-20. Comparison of measured dissolved oxygen concentrations in the Santa Margarita River during four periods of 2015 and comparison with DO data at USGS station at Temecula (2008).

With the knowledge that DO concentrations in the river were persistently lower than those measured at the USGS station at Temecula, we then investigated the most appropriate way of specifying the upstream boundary conditions of dissolved oxygen for the model and the impacts of the specified boundary conditions of DO to the dissolved oxygen dynamics in the lagoon. First we subtracted the USGS data at Temecula by 3 mg/L to reflect the difference of dissolved oxygen between the two stations. Then we superimposed diurnal oscillations with a magnitude of 4 mg/L to the processed DO data. We then conducted two model simulations, one with the diurnal oscillations and the other without as the boundary conditions for the dissolved oxygen. Figure 3-21 shows the time series of these two boundary conditions for 2009. Figure 3-22 shows the time series of simulated DO concentrations near the HWY 5 Bridge with the two different boundary conditions, and Figure 3-23 shows the corresponding cumulative probabilities of DO concentrations. Both figures show that difference in the simulated dissolved oxygen concentrations between these two boundary conditions is minimal. This result implies that, while the data of USGS at Temecula could not reflect the more eutrophic conditions in the Santa Margarita River, which exhibited DO with reduced concentrations and with more pronounced diurnal oscillations, dissolved oxygen in the lagoon is governed more by the eutrophic condition locally, much less affected by the upstream boundary condition. This finding is important, because, unlike nutrients in the lagoon that were governed by the watershed loads from the upstream boundary, in-lagoon DO concentration was primarily governed by the local eutrophic condition of the lagoon.

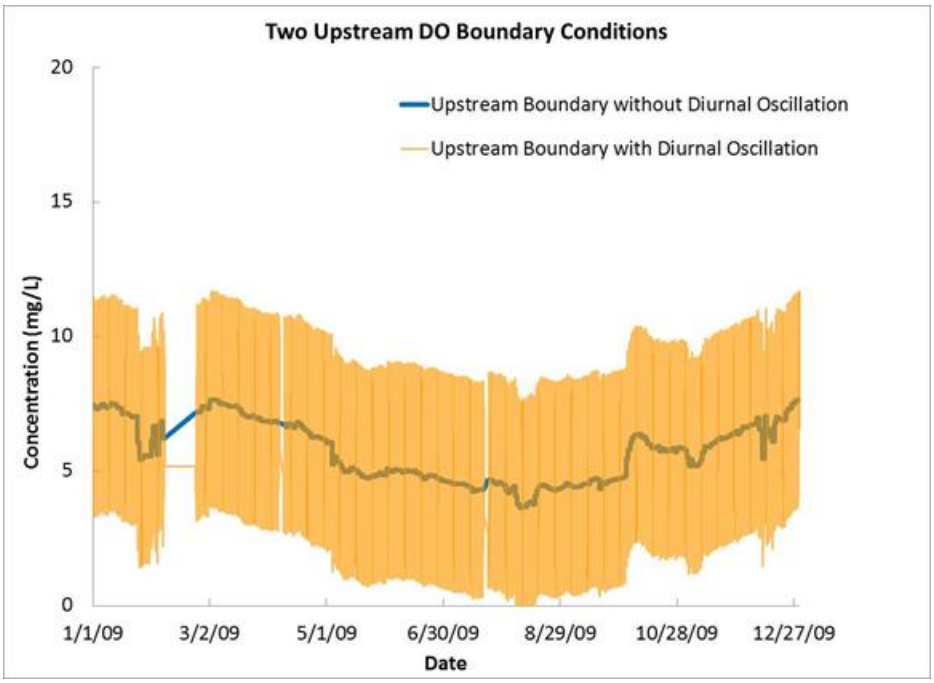

Figure 3-21. Two specified boundary conditions for dissolved oxygen with/without diurnal oscillations.

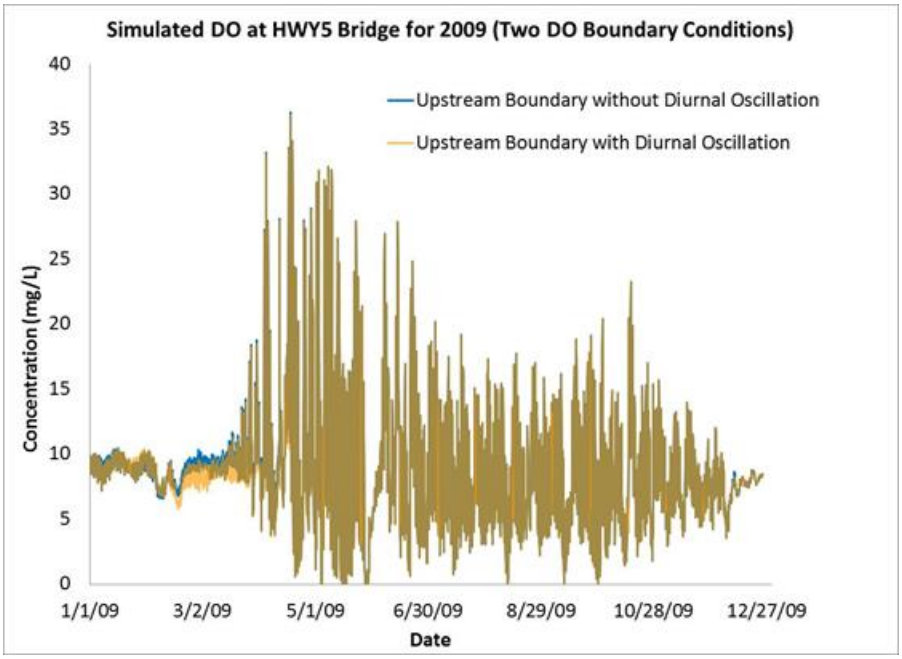

Figure 3-22. Simulated dissolved oxygen concentrations at Segment 1 (near HWY 5 Bridge) from the two boundary conditions (Figure 3-21).

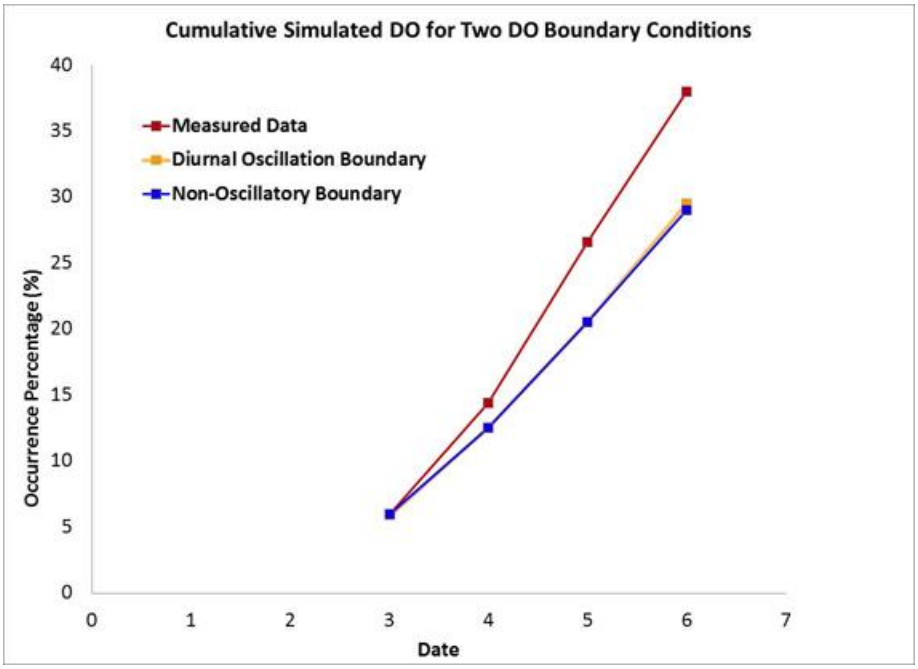

Figure 3-23. Simulated cumulative probabilities of occurrence for simulated and measured dissolved oxygen concentrations based on the two boundary conditions.

3.2.4 Macroalgae

Macroalgal biomass was measured at Segment 1 during 2008 and 2009, and at Segment 2 during 2008. Figure 3-24, Figure 3-25, and Table 3-11 show the model/data comparison of macroalgal biomass of Segment 1 for 2008 and 2009, and of Segment 2 for 2008. Overall, the model simulation results show that the model could capture the macroalgal bloom during the summer–fall period in magnitude at both locations though, with a difference in the timing of the peaks. The peak in the model results precede the peak observed in the data by about 1 to 2 months. The figures show that simulated biomass was positively correlated with water temperature as would be expected.

In addition to temperature, macroalgal growth is governed by availability of nutrients and light. These parameters are components of the model in the form of growth limiting factors or coefficients that are generated by the calibration. Figure 3-26 and Figure 3-27 show the macroalgal biomass growth limiting factors of nitrogen, phosphorous, and available light for Segment 1 and Segment 2, respectively. In general, macroalgae biomass production was more light-limited than nutrient-limited. During the peak of the summer in July and August, macroalgal biomass reached its peak values. However, self-shading of the macroalgae prevented the light from reaching to the lower part of the water column, limiting its growth. This reduction is proportional to the amount of algal biomass, Comparing simulated macroalgal biomass (Figure 3-24 and Figure 3-25) with the growth limiting factors (Figure 3-26 and Figure 3-27), it is observed that while more macroalgal biomass was predicted for Segment 1 (with peak values of 150–200 g-dw/m^2) than for Segment 2 (with peak values of 50–100 g-DW/m^2), the light-limiting factor at Segment 1 was slightly lower than that at Segment 2, which is a result of the self-shading effect. Light attenuation in the generally deeper water of Segment 2 also reduces the amount of sunlight reaching through the water column.

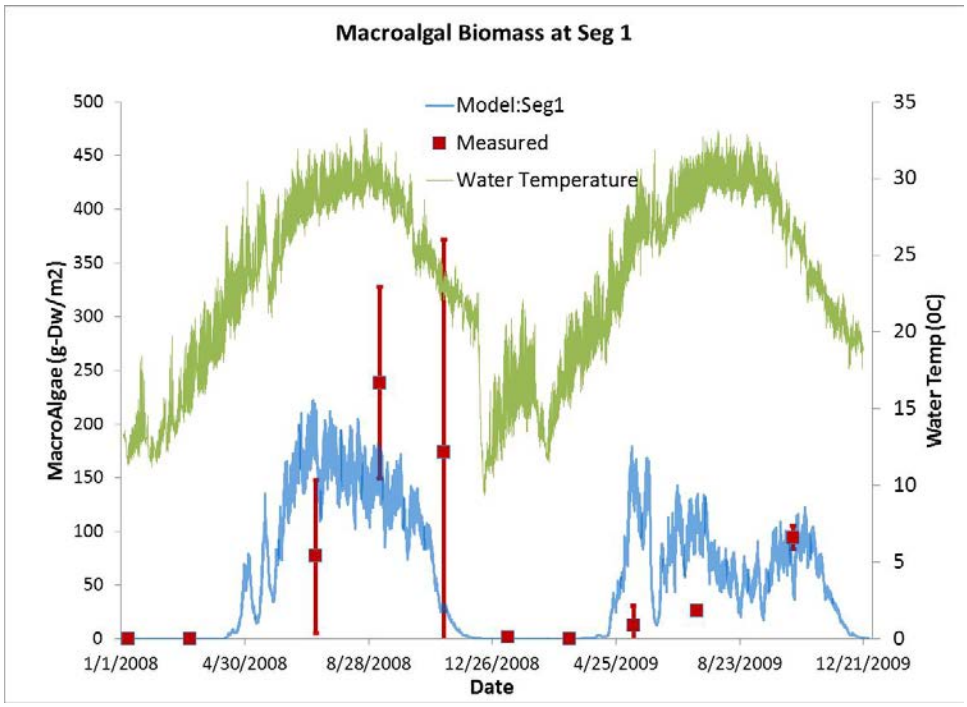

Figure 3-24. Simulated and measured macroalgal biomass at Segment 1 (Seg 1) during 2008–2009.

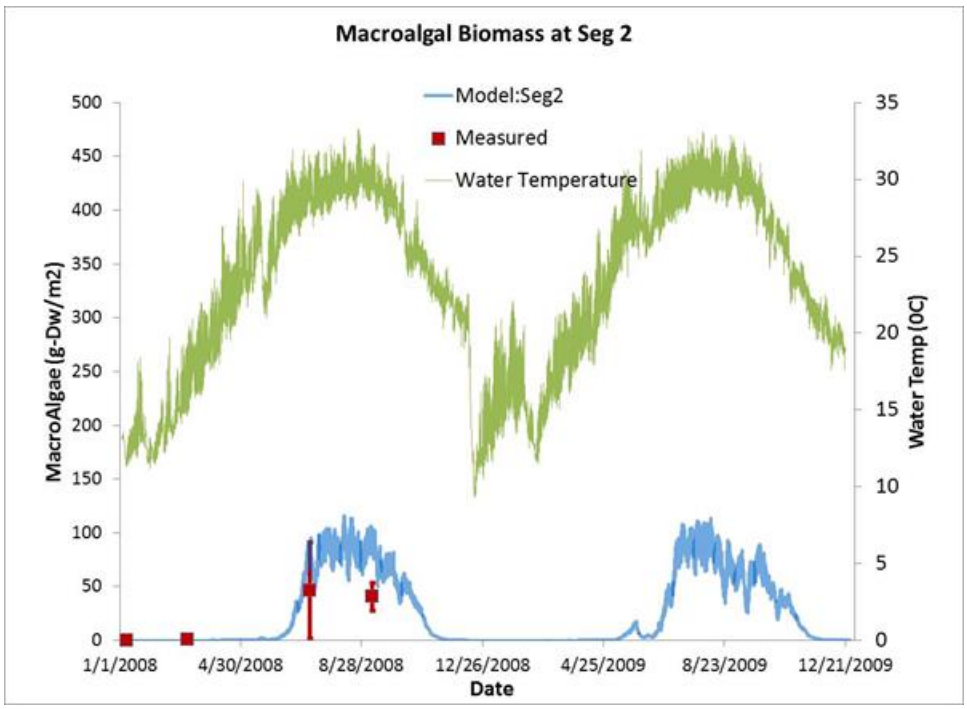

Figure 3-25. Simulated (2008–2009) and measured (2008) macroalgal biomass at Segment 2 (Seg 2).

Table 3-11. Modeldata comparison of macroalgal biomass.

Month/Year	Segment 1				Segment 2			
	Field Data (g-dw/m^2)		Model (g-dw/m^2)		Field Data (g-dw/m^2)		Model (g-dw/m^2)	
	Mean	Stdev	Mean	Stdev	Mean	Stdev	Mean	Stdev
Jan-2008	0	0	0.0	0.0	0	0	0.0	0.0
Mar-2008	0	0	0.1	0.1	0	0	0.0	0.0
Jul-2008	76.7	70.9	168.5	24.6	46.5	45.0	76.9	13.9
Sep-2008	238.4	89.2	130.1	19.9	40.8	13.0	68.5	13.4
Nov-2008	173.3	198.2	19.5	13.2	No data	No data	2.9	3.1
Jan-2009	1.5	1.3	0.1	0.1	No data	No data	0	0
Mar-2009	0.0	0.0	0.3	0.3	No data	No data	0	0
May-2009	12.6	17.9	109.2	38.0	No data	No data	5.7	4.8
Jul-2009	25.9	2.9	94.5	19.7	No data	No data	81.3	16.5
Oct-2009	94.4	10.9	82.0	16.1	No data	No data	40.1	11.9

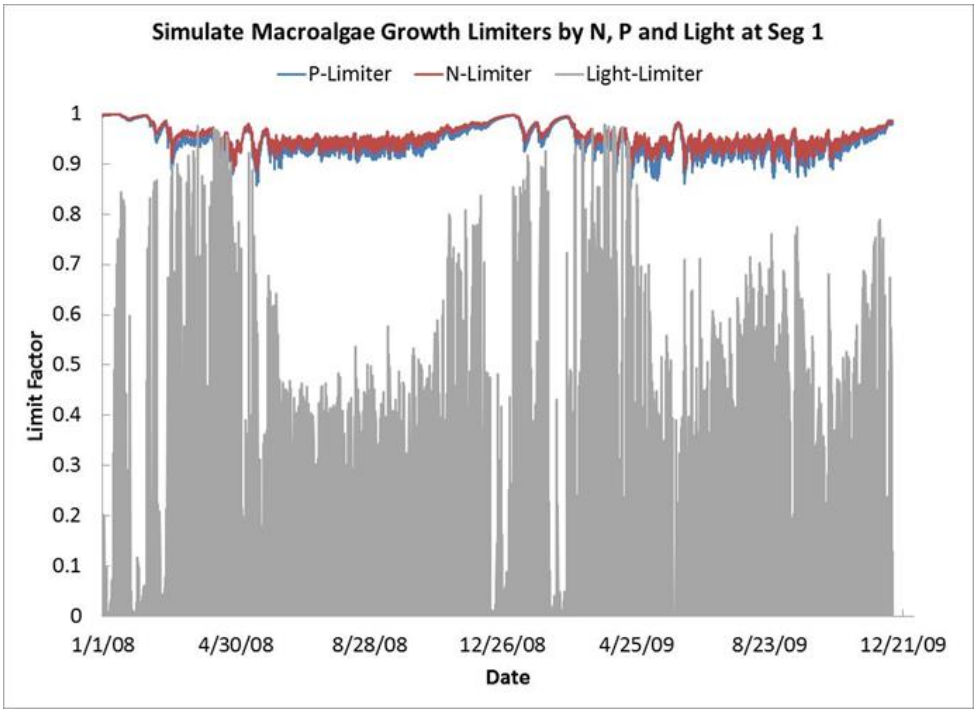

Figure 3-26. Simulated macroalgal biomass growth limiting factors of nitrogen, phosphorous, and light for Segment 1 (Seg 1) during 2008–2009.

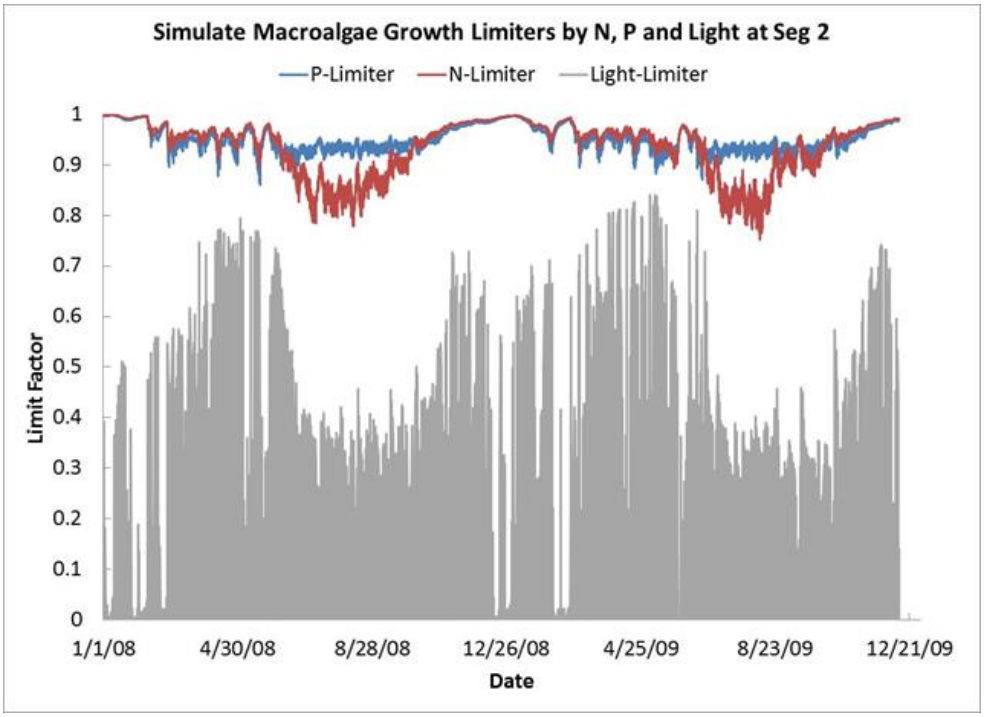

Figure 3-27. Simulated macroalgal biomass growth limiting factors of nitrogen, phosphorous and light for Segment 2 (Seg 2) during 2008–2009.

3.2.5 Sediment Fluxes of Nitrogen, Phosphorous, and Dissolved Oxygen

As part of the WASP 7.5X model, the sediment diagenesis module interacts with the eutrophication module for the water column. The model simulates the process of deposition of dead particulate organic matter after it settles and deposits to the bottom sediment bed as shown at the bottom of Figure 3-2. Once reaching the bottom, the organic material goes through biochemical reactions promoted by bacteria that re-mineralize and transform the organic material into its inorganic forms of nutrients and carbon. This respiration process utilizes oxygen, and the amount of change is referred to as sediment oxygen demand (SOD). Once in inorganic form, the nutrients as well as oxygen are available to flux back into the water column, depending on the concentration gradient between the sediment and overlying water.

Benthic flux measurements were made at two mid-channel stations in Segment 1 and Segment 2 by SCCWRP in 2008 (McLaughlin, 2013. The measurements included concentrations and fluxes of nitrogen (ammonia and nitrate), phosphorous (as phosphate), and oxygen collected during the four index periods. The field data were highly variable and were compared with the model results for the four index periods. The model output of sediment fluxes are compared to the summer and fall field measurements in Figures 3-28 through
3-30.

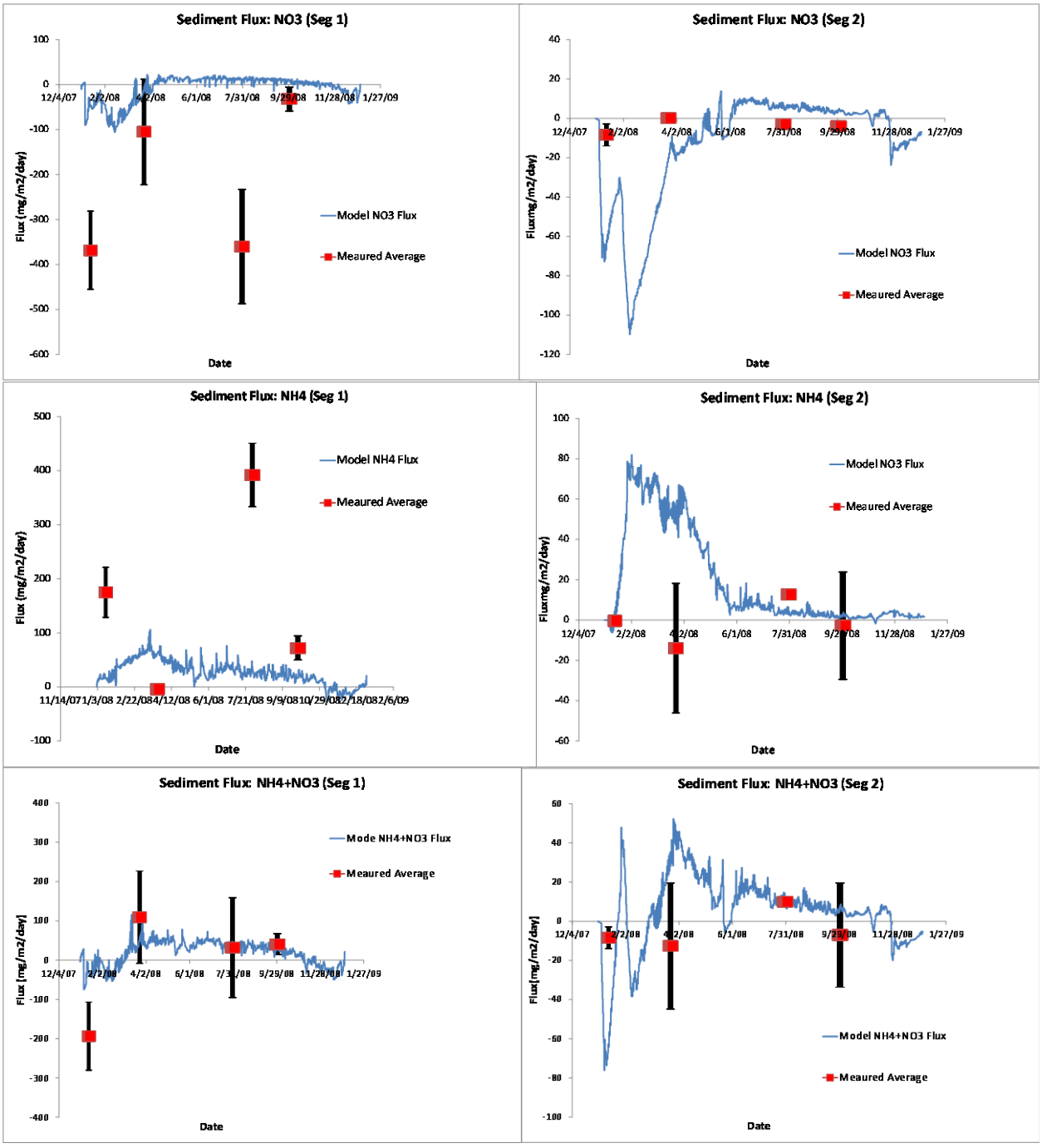

Figure 3-28. Simulated and measured sediment fluxes of nitrate-N (top), ammonia-N (middle) and inorganic-N (bottom) for Segment 1 (Seg 1) and Segment 2 (Seg 2) for 2008. The black bars show the range in the measured data values.

Overall, the model reasonably simulated the magnitude and direction of the sediment flux of nitrogen and phosphorus at both locations within the variability of the field data. Both the field data and model results showed nitrogen fluxes from the sediment to the water column for both periods in Segment 1. For Segment 2, measured nitrogen flux was positive for Period 3 and negative for Period

4. The field measured flux rates for Segment 1 averaged 32 and 40 mgN/m2-day for the two index periods, respectively, while the simulated fluxes averaged 35 mg and 25 mgN/m^2-day for the corresponding periods. The field measured flux rates for Segment 2 averaged 10 and -7 mgN/m2-day for the two index periods, respectively, while the simulated fluxes averaged 10.5 mg and 6.5 mgN/m^2-day for the corresponding periods. Figure 3-29 shows simulated and measured sediment fluxes of phosphorus for Segment 1 and Segment 2 for 2008. Both the simulated and measured fluxes were positive for both Segment 1 and Segment 2 for both periods. For Segment 1, the field measured flux rates for Segment 1 averaged 78 and 9 mgP/m^2-day for the two index periods, respectively, while the simulated fluxes averaged 20 mg and 11 mgP/m^2-day for the corresponding periods. For Segment 2, the field measured flux rates for Segment 1 averaged 12 mgP/m2-day for both index periods, while the simulated fluxes averaged 26 and 16 mgP/m^2-day for the corresponding periods. Field data exhibited large ranges for both Segment 1 and Segment 2.

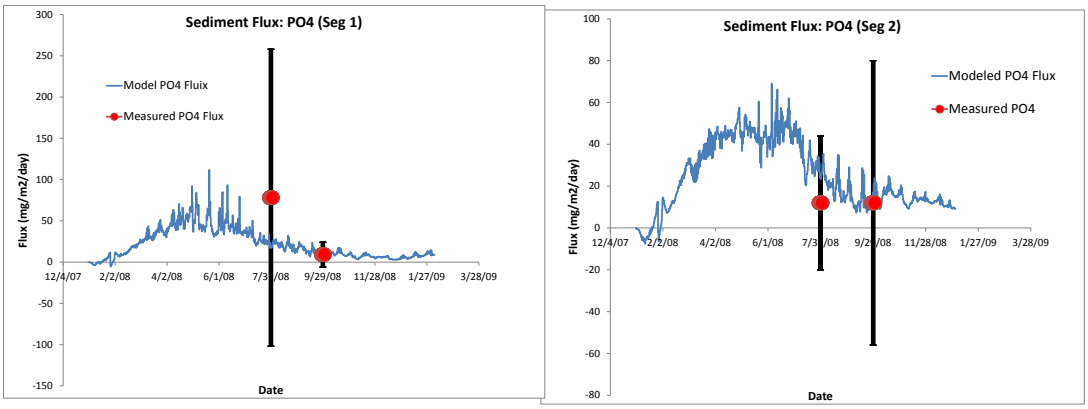

Figure 3-29. Simulate and measured sediment fluxes of phosphorous for Segment 1 (Seg 1) and Segment 2 (Seg 2) for 2008. The black bars show the range in the measured data values.

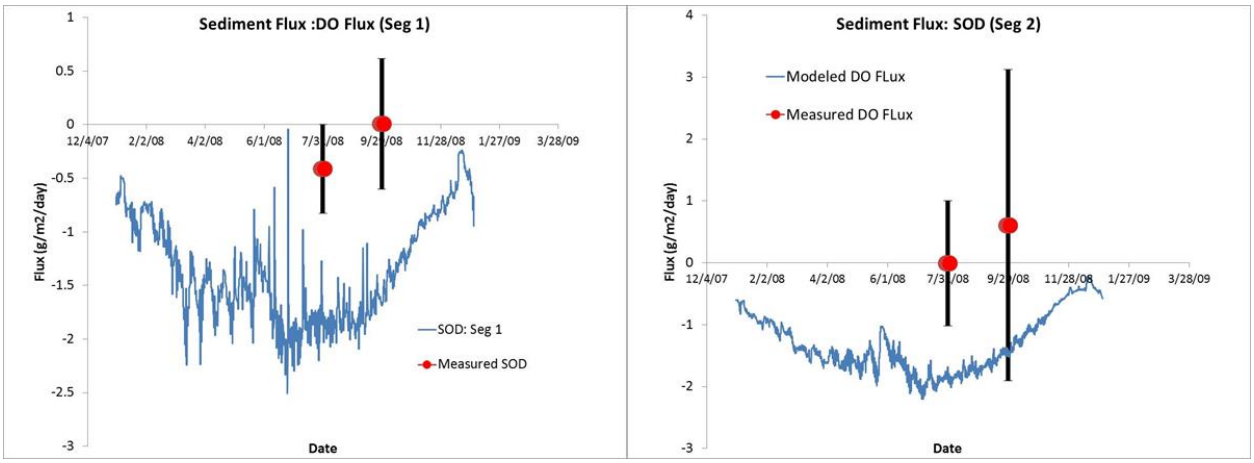

Figure 3-30. Simulated and measured sediment fluxes of dissolved oxygen for Segment 1 (Seg 1) and Segment 2 (Seg 2) for 2008. The black bars show the range in the measured data values.

3.2.6 Uncertainties in Eutrophication Modeling

3.2.6.1 Nutrient Loadings

Nutrient loads entered into the lagoon from multiple sources. Figure 3-31 shows the sources of nutrient loads. Although nutrient concentration data measured at the ME station were available in association with the watershed surface flow, loads from several other sources were estimated by calibration to best match with the in-lagoon measurements.

These nutrient loads estimated by calibration are listed below in the order of level of uncertainty and importance:

1. N and P loads from watershed groundwater (no available data)
2. P and N loads from Ag-field groundwater (measured data by SPAWAR since 2010) (data only available from 2010 onward)
3. Benthic fluxes of nutrients (highly variable)
4. Ocean boundary (well characterized)

While the model/data mismatch of nutrients at Segment 1 may be related to the uncertainty associated with the above sources, it is also quite likely that the mismatch is related to a difference between the spatial resolution of the model grid and the discrete field data sampling locations. In particular, the exceptionally high nutrient concentrations measured at Segment 1 were 1 to 2 orders of magnitude higher than those measured at any other stations. These values were clearly anomalous to any others measured since 2008 and appear related to a localized source that was likely tied to discharge of groundwater from the agricultural field either from advective flow directly into the estuary or directly from the surface discharge from the North County Transit District sump. The difference in the model/data spatial resolution would be sufficient to explain the observed differences or uncertainty in the results. An increase in the model grid resolution would like improve the model/data match.

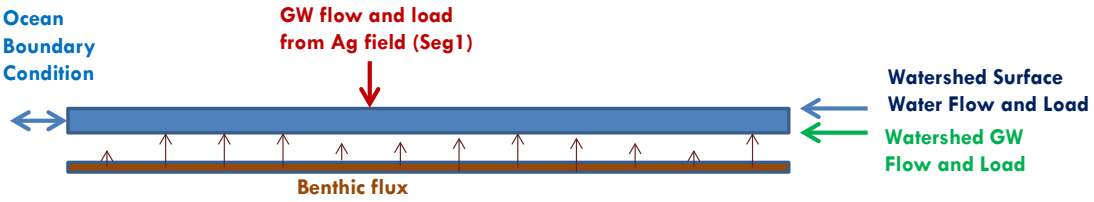

External Boundary	Data Sources
Bathymetry	Most updated survey by SPAWAR, Feb 2013
Watershed Surface Water Flow	USGS gage data at Ysidora
Surface Water Loads	Nutrient load from Mass Emission station
Watershed Groundwater Flow	Identified missing source when calibrating EFDC model.
Watershed Groundwater Load	No data, N and P load obtained from model calibration
Ag Field Flow and Load	N load measured by SPAWAR for 2010. P-load by calibration
Ocean Boundary Condition	Based on Scripps Data Measured at Del Mar
Benthic fluxes	Measured benthic fluxes with large variabilities

Figure 3-31. Nutrient load sources.

3.2.6.2 Dissolved Oxygen

The model calibration indicates that in-lagoon dissolved oxygen concentrations for the periods of 2008 and 2009 were governed by the local eutrophication condition and not significantly affected by the boundary conditions. This result is different from the result for nutrients that showed that in-lagoon concentrations were directly influenced by loading from the upstream boundary, particularly during wet weather.

In general, the model successfully simulated the critical level of dissolved oxygen concentration of 5 mg/L to within 6%. The observed discrepancy during winter concentrations is attributed to not implementing a baseline benthic algae production in the model (Martha Sutula, personal communication). Therefore, to fully describe and predict dissolved oxygen, benthic algae, phytoplankton, and macroalgae, all must be included in the model simulations.

3.2.6.3 Macroalgae

The model reasonably matched the field data in Segment 2, but under-predicted concentrations in Segment 1 during the summer condition. It is clearly challenging to compare model prediction based on a model grid resolution of 2700 m^2 with discrete intertidal sampling that represent e, an intertidal shoreline area of about 30 m^2 (Figures 3 through 32). Like the nutrient data in Segment 1, the differences in model/data spatial resolution would be sufficient to explain the observed differences or uncertainty in the results. It is important for both modeling purposes as well as understanding the spatial nature of algal biomass in the lagoon that sampling of macroalgal biomass should include both intertidal and subtidal regions.

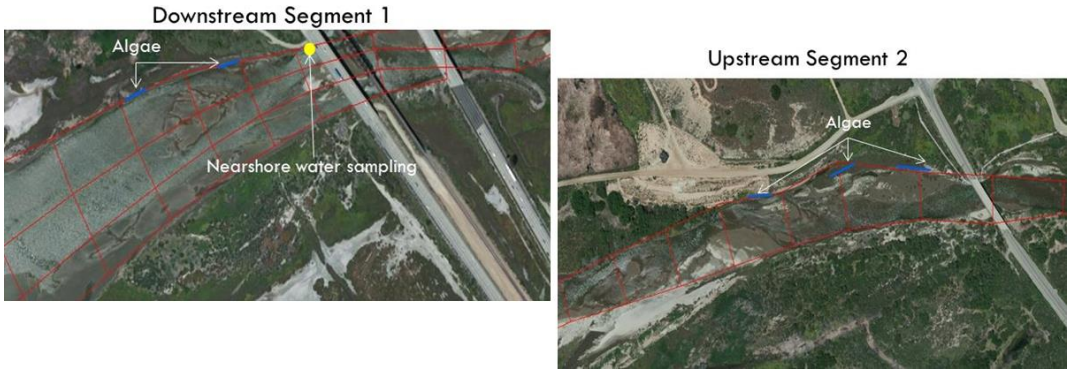

Figure 3-32. Model grids and transect locations for macroalgal biomass sampling.

3.2.6.4 Benthic Flux

The model/data comparison of benthic flux was hampered by the high variability in the benthic flux data and use of only two index period data (Martha Sutula, personal communication). While the general flux direction was matched, the average magnitudes were difficult to match (Figures 3-28 and 3-29 for nutrients and Figure 3-30 for dissolved oxygen). Validation of the flux data would be needed for a better understanding of the source of the model/data mismatch. Another level of uncertainly was introduced into the model, the assumption of constant organic matter deposition rate throughout the lagoon when there may be variation in deposition and/or scouring occurring at various times throughout the year. This assumption also needs further validation. In reality, the lagoon is a highly dynamic estuarine system with complex hydrological and biochemical processes. While the dataset collected in the lagoon was considerable, the model calibration effort identified many processes and data sources that would need further collection and evaluation to improve the model/data evaluation.

4. SUMMARY AND DISCUSSION

4.1 ESTUARY HYDRODYNAMIC MODEL

The initial calibration did not accurately simulate the measured water surface elevation and salinity data measured during the period. Two key elements were iteratively altered to improve the initial calibration to these critical parameters. The first included an adjustment for the height of the sand berm at the mouth as it changed over time, a function of freshwater flows and varying ocean tides. The second iterative adjustment was to add an additional source of freshwater flow to the lagoon that occurs as a result of groundwater coming in from the watershed and is not captured by the USGS gage data used to measure surface flow.

Evaluation of the water surface measurement datasets showed daily low water depths in the lagoon were increasing at a rate of ~0.5 m from the winter into the summer and fall, resulting from the increasing berm height during the period. This change was accounted for in the model by applying an empirical change to the depth of the grid cell at the mouth to match the daily low water depth dataset for both 2008 and 2009. Field data from 2008 were used for model calibration. Once calibrated, the model was used to simulate the 2009 event and model results were compared with field data of 2009 for model validation. The model calibration using the empirical berm height change resulted in a highly accurate simulation in water surface elevation, agreeing within 8 cm of all observations. The model was compared to the mean daily minimum, mean daily mean, and mean daily maximum elevations. Simulation of water surface elevation illustrated that the hydrodynamic model was working well during wet weather, winter dry weather (when the mouth was open), and summer dry weather (when the Lagoon mouth was partially closed). Differences between predicted and observed mean WSE were 1 and 3 cm for 2008 and 2009, respectively, indicating a less than 1% error rate. The good performance of the hydrodynamic model provided a measure of confidence that it was ready to use for water quality modeling.

The magnitude of the changing semidiurnal salinity signal, particularly for low salinity in the lagoon, could not be initially matched by the model, which implied that there must be an additional amount of freshwater coming into the lagoon that was unmeasured at the USGS gauge. An evaluation of simulated freshwater inflow from a watershed model developed by Tetra Tech, Inc. for the regional board could not account for the additional freshwater. The stakeholder technical group was aware that groundwater upstream of the lagoon domain was a potential source of freshwater that might explain both the model-lagoon data mismatch and the lack of observation of the flow made at the USGS gage. The output of a groundwater model developed for Camp Pendleton by Stetson Engineers, Inc. was added as a source of freshwater to the lagoon. The calibration was optimized by adding this groundwater flow only between November and April, presumably when infiltration is highest. The optimization improved the accuracy of the model such that the model versus observed salinity data matched the daily minimum and maximum range 88.6% of the time in 2008 and 90.2% of the time in 2009.

Groundwater flow, although small in magnitude compared with the freshwater inflow from the watershed during the wet weather, constitutes an important source of freshwater source during the dry season. Watershed groundwater flow was considerably larger in magnitude than the local agricultural field groundwater flow, though the associated nutrient concentrations for the agricultural field was considerably larger than the upstream groundwater source. The result is that loading from both groundwater sources were equally important to the lagoon during summer dry weather.

The final hydrodynamic model calibration metric for calibration was for lagoon temperature, which was simulated by including solar radiation as an additional source of heat for the entire lagoon

water. The model output under-predicted the measured daily mean temperature of the lagoon by about 10%.

Overall, the three key hydrodynamic parameters, including water surface elevation, salinity, and temperature, were simulated by the EFDC model with adequate accuracy. The calibration highlighted and revealed that key physical processes were not originally implemented in the standard EFDC model, and were not necessarily understood at the start of the effort. Specifically, the requirement of freshwater from an upper watershed groundwater source to the lagoon had considerable implications for the water quality calibration process.

4.2 LINKED WASP-EUTRO CALIBRATION

Calibration of WASP-Eutro, like EFDC, was conducted by iteratively applying known inputs, evaluating results with known data, and then adjusting parameters using best professional judgement to provide simulation outcomes that best matched the measured datasets. Similar to the approach for the hydrodynamic modeling study, field water quality data of 2008 were used for model calibration. Once calibrated, the model was used to simulate the 2009 event and model results were compared with field data of 2009 for model validation. The field datasets included a suite of measurements of nutrients and macroalgae collected by CDM Federal Programs Corporation for the stakeholders and by SCCWRP through the 2008 and 2009. Not all measurements were collected concurrently, resulting in calibration of the model only for specific periods of the 2 years. In addition, total dissolved nitrogen data collected by CDM had an unquantifiable level of uncertainty, and therefore, were not used for model calibration.

The measurements included the collection of water column nutrients during four seasonal month-long index periods in 2008 at a fixed site near the Railroad Bridge and at a set of 13 sites along an axial transect from the mouth (including the ocean inlet) to the Stuart Mesa Bridge. The measurements at the fixed location were made at high and low water once a week during the index period, while the axial measurements were made once per index period. Index period measurements of macroalgae biomass and cover were made along three intertidal transects along the northern shoreline near to the HWY 5 and Stuart Mesa Bridges and at a site roughly halfway between them bimonthly during 2008–2009. Benthic flux and sediment nutrient and oxygen measurements were collected at two sites representing the lower lagoon near the HWY 5 Bridge (Segment 1) and the upper lagoon near the Stuart Mesa Bridge (Segment 2) during 2008 by SCCWRP. Dissolved oxygen, salinity, and temperature were also measured continuously during 2009 by SCCWRP near to the fixed sampling location at the HWY 5 Bridge. Additionally, event mean storm water nutrient concentrations were collected during three storm events in 2008 by CDM at a site ~9 kilometer upstream of the lagoon. This site was also sampled for nutrients during the four index periods during non-storm conditions.

As described earlier, the hydrodynamic model calibration process, particularly the need to introduce a watershed groundwater source of freshwater to balance salt in the lagoon, highlighted limitations in our knowledge of the lagoon system**.** The calibration of the water quality model exposed additional gaps in our knowledge, which required more iterations and professional judgement adjustments to optimize the model-measurement comparisons. The calibration process was also challenged by the lack of fully concurrent field data, and in some cases, their high variability. Specifically, a localized groundwater source from the historic agricultural fields above the northern shore by the HWY 5 Bridge was found entering the lagoon and quantified between 2010 and 2014. This source, measured outside the model time domain, was found to be a potentially important source of nutrients to the lower lagoon**.** A nutrient load from the groundwater source entering in from the upper watershed also had to be assigned by calibration. The nutrient loads

assigned from the upper watershed groundwater source were obtained by model calibration. However, since no field data was available to validate the assumption, the calibrated nutrient load could be attributed to other sources, such as benthic flux between the upstream boundary and the Stuart Mesa Bridge.

Another gap identified by the calibration process was found when attempting to match discrete field measurements of macroalgal biomass made along the intertidal shoreline with a model that did not allow for the development of an intertidal condition (generation of tide flats) and one that had a grid spatial resolution that was considerably larger than the size of these discretized and heterogeneous measurements. The grid size also appeared to play a role in a mismatch between water column nutrients measured in the very shallow shoreline near to the groundwater entry point from the agricultural field with model results. These issues were painstakingly evaluated and iteratively adjusted to provide an optimized model calibration output that best matched observations.

Water column nutrient model results were evaluated against field measurements at the HWY 5 and Stuart Mesa Bridge locations, the axial transect sites, and at the mouth. The main adjustments to the model input parameters included assigning a nitrogen and phosphorous load from the upper watershed groundwater source and load from the local groundwater source from the agricultural field near to the HWY 5 Bridge. The loads were developed using the flow rates developed in the hydrodynamic model and fixing a nutrient concentration that balanced the other loads derived from the surface water coming in from upper watershed and with the load tidally exchanged at the mouth. The model was iteratively run to balance the loads to best match the average lagoon concentration data and specifically at the comparison sites.

On average, total nitrogen, inorganic nitrogen, and nitrate predicted by the model were within 8% (over prediction) of the field dataset. The model also simulated the temporal trends observed in the lagoon, decreasing from relatively high levels in winter to considerably lower levels in summer and fall during the dry season. The concentration data were well matched to the upper lagoon location and to the transect data (within 10%), but was poorly matched to the concentrations measured at the HWY 5 Bridge location (Segment 1). The model under-predicted the measured concentrations of inorganic nitrogen by over a factor of 10: 2.7 mg/L (model) vs. 27 to 37 mg/L (measurement). As mentioned previously, the mismatch at this location appeared to be explained by the localized groundwater flowing in near the site, the shallow water sampling in the vicinity of that input, and the potential that there was an unmeasured but previously observed surface water flow to the lagoon at the same location by the North County Transit District.

On average, total and inorganic phosphorous predicted by the model were within 15% of the field dataset**.** The model also simulated the temporal trends observed in the lagoon, increasing from winter into summer and fall (opposite to the trend in nitrogen). The model also simulated the increasing spatial trend in the data showing a relatively even distribution over the lagoon in winter and then an increasing trend up the lagoon in summer and fall. Unlike the nitrogen results, the model phosphorous concentration data were well matched to all three observation points to within 15%. The better match of the model to the observed data at the HWY 5 location suggest that the groundwater sources of phosphorous there were relatively low.

Water column dissolved oxygen model results were evaluated against the continuous field measurements made in 2009 at the HWY 5 Bridge. Overall, the model could only match the mean and daily minimum nighttime concentrations in the lagoon, with 26.6% and 20.5% for the dissolved oxygen less than 5 mg/L for the model prediction and field data, respectively. The model could capture the diurnal variation but overpredicted the peak daytime concentrations, a result of the model not accounting for oxygen flux across the seawater surface interface. Considerable effort was applied

to calibrating the model to meet the observed oxygen data, including adjusting the boundary conditions and the feedback mechanisms of the interaction of macroalgae growth, death, and benthic flux. The final model calibration, while not able to simulate the peak values correctly, did provide a good match to the low nighttime dissolved oxygen values that are a potential key metric under consideration for assessing impairment of the lagoon.

The benthic flux of nutrients and oxygen generated in the calibrated model were evaluated against the field measurements made at two field locations. The field data were highly variable and were compared with the model results for the four index periods. The model correctly simulated the flux direction (into or out of the sediments) for both inorganic nitrogen and phosphorous during both periods. The model over predicted the nitrogen flux by a factor of 4 and the phosphorous flux by a factor of 58, noting that large variances were associated with the field data with magnitudes larger or equivalent to the difference of mean model and field data. The benthic dissolved oxygen field data were even more variable than the nutrient data. The model was also able to match the oxygen flux direction but over-predicted the magnitude by a factor of 4.

The calibrated model results for macroalgal biomass were evaluated against average conditions throughout the estuary and specifically at the two field measurement locations at the HWY 5 and Stuart Mesa Bridge locations. The model correctly simulated the growth of macroalgae from the zero values observed in the winter months to peaks of macroalgal biomass observed during late summer, though the model generated peak production about one to two months earlier than observations. The model generated an average biomass in the estuary of 82 g-dw/m^2 compared to the measured value 72 g-dw/m^2, during the period of April to November for 2008 and 2009. The comparison at the lower lagoon site near the HWY 5 Bridge generally showed agreement with observation except during the late summer when the model result (179 g-dw/m^2) was under-predicted compared with the observed value of 238 g-dw/m^2 algae. The mismatch at this site is comparable to the mismatch observed in the nutrients and can be potentially explained by growth stimulated by the localized groundwater source flowing in near the site, and that the model grid size is 90 times larger than the spatial extent of the discrete measurement along the shoreline. The model/data comparison for the macroalgal biomass at the upper lagoon location (Segment 2) was within 27%, with averaged values of 60.2 g-dw/m^2 and 44.3 g-dw/m^2 for the model and field data, respectively, during the period of June 1 to November 3 for 2008 and 2009.

The model matched well in magnitude with the measured macroalgal biomass at both locations, Segment 1 and Segment 2, during 2008–2009. The timing of the peaks of predicted macroalgal biomass peaks were about 1 month ahead of that of measured data. The limited amount of light in the lagoon affected the growth of macroalgae, accounting for a 50% reduction in growth during the peak of the summer. Growth was slightly limited by nitrogen for Segment 2 only during the short period of summertime, and phosphorous was not limiting throughout the periods. The timing of predicted biomass was consistent with the water temperature trends, thus the lag between predicted and measured macroalgal biomass need further investigation.

Predicted sediment fluxes of nitrogen and phosphorous were in agreement with the measured fluxes for both direction of the flux and magnitude, considering the large variances associated with the measured data. Model assumed uniform deposition of organic matters throughout the lagoon during 2008–2009. In reality, We suspect that different deposition patterns may exist during the wet and dry weather and among different parts of the lagoon. The above discussion reveals that model results were consistent with the assumption of uniform deposition and field data was consistent with the hypothesis of non-uniform deposition. This issue should be further studied by including the study of sediment transport with the dynamics of deposition in the lagoon.

Macroalgae biomass is under consideration as a key metric for assessing impairment of the lagoon. Because of this, considerable efforts were made to assess the processes of macroalgal growth that might provide insight into the factors for the mismatch. We discovered that light limitation, particularly along the intertidal shoreline, was a key process that controls production. The adjustment of light, shelf-shading of plants, and the model minimum water depth set at the shoreline were all adjusted to provide the best match to the observed data. A higher spatial resolution grid, allowing drying of the intertidal zone at low tide, and/or providing measures of subtidal macroalgae biomass would all potentially lead to a better model simulation result compared to the macroalgal datasets.

In general, model calibration should be conducted with the external loads that are well defined and assigned. However, for this study we have identified multiple sources of uncertainties and data gaps. Given the uncertainties and data gaps discussed, the eutrophication model, WASP-EURO, we had to assign loads (e.g., P-load from watershed groundwater) that could only be obtained by calibration. The calibrated loads could be attributed to the uncertainty associated with watershed groundwater load or benthic flux (or other sources) between the Stuart Mesa Bridge and the model upstream boundary. However, no existing data could support either assumed sources. Therefore, these loads, obtained by calibration, need to be further validated for their sources and quantities, before further model calibration/ validation can be conducted.

Despite of these uncertainties in the data and the model, the overall calibration of the linked EFDC WASP-Eutro models provided a sufficiently reasonable match to field datasets collected between 2008 and 2009. The model should be able to simulate and compare the relative water quality responses among different scenarios, such as load reduction and effect of different benthic flux scenarios and others. To fully characterize and evaluate model performance, a sensitivity analysis should be conducted. In this analysis, key processes that govern the dynamics of the water quality parameters can be identified, which should help design and plan load management scenarios.

REFERENCES/BIBLIOGRAPHY

California Regional Water Quality Control Board Los Angeles Region (CRWQCB) and U.S. Environmental Protection Agency Region 9. 2011. "Dominguez Channel and Greater Los Angeles and Long Beach Harbor Waters Toxic Pollutants Total Maximum Daily Loads." Los Angeles, CA.

CDM Federal Programs Corporation. 2009. "Water Quality Field Data for Santa Margarita Lagoon." Data file provided by Southern California Coastal Water Research Project (SCCWRP) Costa Mesa, CA.

California Irrigation Management Information System (CIMIS). Information available online at http://www.cimis.water.ca.gov/). Accessed June 15, 2016.

DiToro, D. M., P. R. Paquin, K. Subburamu, and D. A. Gruber. 1990. "Sediment Oxygen Demand Model: Methane and Ammonia Oxidation," *Journal of Environmental Engineering 116* (5):945–986.

McLaughlin, K., M. Sutula, J. Cable, and P. Fong. 2013. "Eutrophication and Nutrient Cycling in Santa Margarita River Estuary: A Summary of Baseline Studies for Monitoring Order R9-2006-0076." SCCWRP Technical Report 635. Southern California Coastal Water Research Project, Costa Mesa, CA.

NOAA Quality Controlled Local Climatological Data (QCLCD) Archive. Information available online at https://www.ncdc.noaa.gov/data-access/land-based-station-data/land-based-datasets/quality-controlled-local-climatological-data-qclcd). Accessed June 15, 2015.

Tetra Tech, Inc. 2002. "Hydrodynamic and Transport Extension to the EFDC Model." A report to the U.S. Environmental Protection Agency, Fairfax, VA.

USEPA. 1997. "Compendium of Tools for Watershed Assessment and TMDL Development." EPA 841-B-97-006. Office of Water (4503F), Washington, DC. Available online at http://uncw.edu/cms/aelab/LCFRP/TMDL/EPA's%20Compendium%20of%20Tools....pdf. Accessed June 16, 2016.

USGS Station #11044000
Information available online at http://nwis.waterdata.usgs.gov/nwis/inventory/?site_no=11044000&agency_cd=USGS. Accessed June 15, 2016.

USGS Station #11046000
Information available online at http://nwis.waterdata.usgs.gov/nwis/inventory/?site_no=11046000&agency_cd=USGS. Accessed June 15, 2016.

Wang, P-F, M. Sutula, B. Chadwick, and W. Choi. 2013. "Watershed Loading, Hydrodynamic, and Water Quality Modeling in Support of the Loma Alta Slough Bacteria and Nutrient TMDL." SCCWRP Technical Report 666. Southern California Coastal Water Research Project, Costa Mesa, CA.

APPENDIX A

Table A-1. Data Sources for 2008–2009.

	Data Sources	Parameters Used	Note
1	USGS Gauge at Ysidora (11046000)	Freshwater Discharge	For upstream boundary condition: USGS discharge
2	USGS Gauge at Temecula (11044000)	Water conductivity, temperature, pH, dissolved oxygen	For upstream boundary condition: Salinity and Temperature and dissolved oxygen
3	Scripps Inst. of Oceanography at nearshore/Del Mar sites	Salinity, temperature and Dissolved oxygen	For model boundary conditions at the ocean
4	Meteorological Data at USGS CIMIS Station at Temecula	Air Pressure, temperature, relative humidity, rainfall, cloud cover, wind speed/direction	For water/air interface boundary
5	Meteorological Data from MCAS Camp Pendleton Airport	Evapotranspiration, solar radiation	For water/air interface boundary
6	USGS Gauge at Railroad Bridge (11046050)	Water depth, conductivity and temperature	For model/data comparison
7	SCCWRP water sampling data at Railroad Bridge	Water depth, temperature, conductivity, turbidity, pH, Chlorophyll-*α*, DO	Salinity and temperature used for model/data comparison
8	SSC Pacific's Groundwater seepage for 2010 and 2012 (April–May, both west seasons)	See page flow rate and nitrogen concentration from egg field	To be used as a groundwater source of freshwater flow and nutrient (not used for this hydrodynamic model study)

REPORT DOCUMENTATION PAGE

Form Approved
OMB No. 0704-01-0188

PLEASE DO NOT RETURN YOUR FORM TO THE ABOVE ADDRESS.

1. REPORT DATE *(DD-MM-YYYY)*	2. REPORT TYPE	3. DATES COVERED *(From - To)*
July 2016	Final	

4. TITLE AND SUBTITLE

Calibration of Linked Hydrodynamic and Water Quality Model for Santa Margarita Lagoon

5a. CONTRACT NUMBER

5b. GRANT NUMBER

5c. PROGRAM ELEMENT NUMBER

6. AUTHORS

Pei-Fang Wang
Chuck Katz
Ripan Barua
SSC Pacific

James Martin
Mississippi State University

Tim Wool
U.S. EPA Region 4
Water Management Division

5d. PROJECT NUMBER

5e. TASK NUMBER

5f. WORK UNIT NUMBER

7. PERFORMING ORGANIZATION NAME(S) AND ADDRESS(ES)

SSC Pacific
53560 Hull Street
San Diego, CA 92152–5001

Mississippi State Univ.
222 Walker Engineering Building
Dept. of Civil and Environmental Eng.
Mississippi State, MS 39762-9546

U.S. EPA. Region 4
Water Management Division
Atlanta Federal Center
61 Forsyth Street
Atlanta, GA 30303

8. PERFORMING ORGANIZATION REPORT NUMBER

TR 3015

9. SPONSORING/MONITORING AGENCY NAME(S) AND ADDRESS(ES)

Environmental Security
Resource Enforcement and Compliance
P.O. Box 555008
Camp Pendleton, CA 92055-5008

10. SPONSOR/MONITOR'S ACRONYM(S)

11. SPONSOR/MONITOR'S REPORT NUMBER(S)

12. DISTRIBUTION/AVAILABILITY STATEMENT

Approved for public release.

13. SUPPLEMENTARY NOTES

14. ABSTRACT

The Santa Margarita Lagoon (SML) is a water body that forms where the Santa Margarita River and its tributaries meet the Pacific Ocean. The lagoon and lower part of the river are within Marine Corps Base Camp Pendleton (Camp Pendleton). The Regional Water Quality Control Board, San Diego listed the lagoon as an impaired waterbody for eutrophication with excessive nutrients and issued an Investigative Order (R9-2006-076) in 2007 to evaluate the extent of impairment. A watershed stakeholder group, including Camp Pendleton, was established to develop and implement a water quality monitoring effort to evaluate the impairment in 2008. Those data along with measurements made by the Southern California Coastal Water Research Project (SCCWRP) in 2009 provided the first relatively comprehensive evaluation of water quality in the lagoon.

For this study, we have identified multiple sources of uncertainties and data gaps. For example, the p-load obtained by calibration could be attributed to the uncertainty associated with watershed groundwater load or benthic flux (or other sources) between the Stuart Mesa Bridge and the model upstream boundary. However, no existing data could support either assumed sources. Despite these uncertainties in the data and the model, the overall calibration of the linked Environmental Fluid Dynamics Code (EFDC) hydrodynamic model was selected and linked with the Water Quality Analysis Simulation Program–Eutrophication (WASP-Eutro) models provided a sufficiently reasonable match to field datasets collected between 2008 and 2009. The model should be able to simulate and compare the relative water quality responses among different scenarios, such as load reduction and effect of different benthic flux scenarios and others. To fully characterize and evaluate model performance, a sensitivity analysis should be conducted. In this analysis, key processes that govern the dynamics of the water quality parameters can be identified, which should help design and plan load management scenarios.

15. SUBJECT TERMS

Mission Area: Environmental Science
Santa Margarita Lagoon; model calibration and verification; water quality; hydrodynamic model; estuary-eutrophication model; linked WASP-Eutro calibration

16. SECURITY CLASSIFICATION OF:			17. LIMITATION OF ABSTRACT	18. NUMBER OF PAGES	19a. NAME OF RESPONSIBLE PERSON
a. REPORT	b. ABSTRACT	c. THIS PAGE			Pei-Fang Wang
U	U	U	U	98	19B. TELEPHONE NUMBER *(Include area code)* (619) 553-9192

INITIAL DISTRIBUTION

84300	Library	(2)
71750	P. F. Wang	(1)
71750	C. N. Katz	(26)
71760	R. Barua	(1)

Defense Technical Information Center
Fort Belvoir, VA 22060–6218 (1)

Approved for public release.

SSC Pacific
San Diego, CA 92152-5001